In presenting the dissertation as a partial fulfillment of the requirements for an advanced degree from the Georgia Institute of Technology, I agree that the Library of the Institute shall make it available for inspection and circulation in accordance with its regulations governing materials of this type. I agree that permission to copy from, or to publish from, this dissertation may be granted by the professor under whose direction it was written, or, in his absence, by the Dean of the Graduate Division when such copying or publication is solely for scholarly purposes and does not involve potential financial gain. It is understood that any copying from, or publication of, this dissertation which involves potential financial gain will not be allowed without written permission.

3/17/65
b

ATMOSPHERIC TIDAL MOTION IN THE 90 TO 120 KILOMETER HEIGHT REGION

A THESIS

Presented to

The Faculty of the Graduate Division

by

Arthur Woodrum

In Partial Fulfillment

of the Requirements for the Degree

Doctor of Philosophy in the School of Physics

Georgia Institute of Technology

June , 1968

ATMOSPHERIC TIDAL MOTION IN THE 90 TO 120

KILOMETER HEIGHT REGION

Approved:

Date approved by Chairman: 5/20/68

Dedicated to those whose patience and encouragement

were beyond value:

My wife, Mary Alice;

and my parents,

Mr. and Mrs. W. G. Woodrum, Sr.

ACKNOWLEDGMENTS

The author wishes to express his appreciation to his thesis advisor, Dr. H. D. Edwards, whose advice and guidance have been invaluable. A great deal of gratitude is also extended to Dr. C. G. Justus of the School of Aerospace Engineering for his interest, suggestions and enlightening discussions in the field of the author's research. The helpful discussions and suggestions of W. B. Moseley, fellow physics graduate student and friend of the author, and Dr. R. G. Roper, formerly a visiting professor to Georgia Institute of Technology from Australia, are also acknowledged.

Thanks also go to the many people working with Dr. Edwards in the field and in the laboratory who have contributed to the gathering and reduction of the data on which the analysis of this thesis is based. Special thanks go to Miss Doris Lunsford for her diligent typing of the manuscript.

Funds for this work were provided by the National Aeronautics and Space Administration through Grant NsG-304-63, the United States Air Force through Contract AF 19(628) - 4781, and the Atmospheric Sciences Section, National Sciences Foundation, NSF Grant GP 3876.

TABLE OF CONTENTS

Table of Contents (Cont'd.)

LIST OF TABLES

LIST OF ILLUSTRATIONS

List of Illustrations (Cont'd.)

List of Illustrations (Cont'd.)

SUMMARY

Atmospheric tides produce small, regular, world-wide air pressure oscillations which occur with periods of $1/\lambda$ times a solar or lunar day, where $\lambda = 1,2,3, \ldots$ The generating forces of these tides are either the gravitational forces of the sun and moon or the thermal forces of the sun caused by the periodic absorption and emission of solar heat by the atmosphere.

In the lower atmosphere, these pressure variations are almost totally masked by pressure variations associated with normal weather conditions. The systematic variations show up most prominently in the equatorial regions. By harmonic analysis, these variations were extracted and it was shown that the solar semidiurnal oscillations were by far the strongest. This situation puzzled the early scientists very much because it was known that the diurnal temperature variations were stronger than the semidiurnal temperature variations. Why, therefore, should the diurnal pressure variation not be the strongest?

Several theories were developed to answer this question, the most notable of which is the so-called "resonance" theory. However, it was only recently that the question seems to have been answered in terms of propagating waves and a semidiurnal thermal drive region in the stratosphere.

Recent measurements in the upper atmosphere (around the 100 km altitude) have shown, contrary to the ground measurements, that the diurnal oscillations are dominant or at least equal to the semidiurnal

oscillations. Hence, there has been a recent increase in interest in the development of tidal theory for diurnal oscillations in the height region.

It has been very difficult to analyze existing winds measurements near the 100 km altitude region in terms of the tidal harmonic motion because of the intermittency of the data. There are enough data from meteor trails to perform a harmonic analysis, but the meteor wind data only extend from about 80 to 100 km. Also, the resolution of the meteor wind data has not been very good until recently. As a result, immediately above 100 km wind data from chemiluminous clouds ejected from rockets must be used. The expense and manner by which the wind data are obtained from rockets makes it impossible to get a large amount of data closely spaced together. Modifications of the Fourier analysis must be found in order to analyze the data in terms of the tidal components. By making use of the physical behavior of the prevailing, diurnal and semidiurnal winds, a geometrical method of analysis was developed in which these three components were resolved. This analysis is very similar to the procedure developed by Hines [1966] in which he separated the diurnal component only.

In addition, the rocket wind data were analyzed by using a procedure developed by Groves [1959]. According to Groves, his procedure alleviates somewhat the problem of intermittency in the data with respect to time and height distribution. His procedure is a generalization of the least-squares procedure.

The results of the two analyses agree very well with each other and reasonably well with the predictions of the linearized tidal theory.

Both analyses computed a prevailing wind which had a wavelike nature with height. The vertical wavelength and phase difference between the northward and eastward velocity components associated with this wavelike motion were 26 km and 102° to 123°.

The computed vertical wavelengths of the propagating diurnal tide were 19 and 25 km by the geometrical and Groves analyses respectively. Tidal theory predicts a vertical wavelength of 20 km for the (1,3) mode of oscillation. This value agrees well with the geometrical method: but if any viscous dissipation of the diurnal energy takes place, then the vertical wavelength is expected to be lengthened to become more in agreement with the Groves analysis. The computed velocity amplitudes for the diurnal tide were found to be 19 and 23 m/sec. These values are well below the theoretical value and hence show that strong dissipation forces are acting on the wind just above 100 km. The phase differences between the component velocities were calculated to be 100° to 120°, which are significantly larger than the value of 90° predicted by the linearized tidal theory.

The semidiurnal tide was found to be smaller than the diurnal and prevailing winds. This tide was so small in the case of the geometrical analysis as compared to the error that very little information could be obtained about it. However, the Groves analysis calculated a velocity amplitude of about 20 m/sec and a vertical wavelength of 36 km. This calculated vertical wavelength agrees very well with the (2,4) mode of oscillation. The phase difference between the component velocities was calculated to be 107°; which again is significantly larger than the theoretically predicted value of 90°.

In all cases, the winds were observed to be rotating clockwise with increasing height and to have a downward phase propagation in agreement with theory.

Energy analysis of the tidal winds showed that energy dissipation was definitely occurring immediately above 100 km. This dissipation of the energy may be attributed to viscous forces and to the effects of nonlinear velocity terms, which were neglected in the tidal theory.

Velocity differences of wind profiles, which had launch times differing by integral multiples of a day, were also found for 1 to 15 day separations. These velocity differences were attributed chiefly to the effects of gravity waves. The results agreed very well with the results of Kochanski [1964].

CHAPTER I

EARLY HISTORY

Introduction

For many years man has been familiar with the systematic changes of the tides in the ocean, with a maximum and minimum tide occurring twice a day. These tides could easily be explained as a result of the gravitational forces exerted on the earth by the sun and moon. Also, due to the fact that the sun is much farther from the earth than the moon, the influence of the moon on the tides is about twice the influence of the sun.

The early scientists also knew that these same gravitational forces were acting on the earth's atmosphere. Thus they concluded that there should also be some systematic tidal motion of the air in the atmosphere. With the use of the barometer it was natural for the scientists to start looking for tidal variations in the atmospheric pressure. At first no such systematic variations could be detected, especially at moderate latitudes. Then late in the eighteenth century, barometric measurements were carried out in the tropics which showed distinct solar 12 hour variations if the variations were plotted for a few days.

These early observations puzzled the scientists. The gravitational force of the moon is twice as great as the sun's force, and the lunar atmospheric tides should therefore certainly be as great

as or greater than the solar tides if gravitational forces only were considered. At about this time, P. S. Laplace of Paris, France developed the first dynamical theories of oceanic and atmospheric tides. In his work he postulated that the solar barometric oscillations are mainly due to the thermal action of the sun rather than to the gravitational action.

Beginning of Resonance Theory

This explanation of the solar oscillations was also a puzzle because it was a known fact that the diurnal term in the temperature variation was much larger than the semidiurnal variation. However, Lord Kelvin in 1882 presented a way out of this dilemma. His theory postulated that if the whole atmosphere were regarded as an oscillating system, then the semidiurnal pressure oscillation could be enhanced by the atmosphere through a process of resonance.

The first test of the validity of this theory would be to investigate the period of free oscillations of an atmosphere covering a spherical earth to check if the atmosphere could support resonance of the 12 hour periodic oscillation. Laplace was the first to develop tidal theory. His theory was developed in 1823 and was applied to ocean tides. He made a calculation of the free oscillation of a spherical ocean of uniform depth h in the presence of the gravitational field of the earth which is assumed to cause a constant vertical acceleration g. The spherical ocean of uniform depth can be considered as a two dimensional resonator if only waves of much greater length than the depth of the ocean are considered. The velocity of these

long waves was shown to be $\sqrt{gh}$. Thus it is natural to expect the resonant frequencies to depend on the depth of the ocean as well as the period of oscillation.

Then Laplace tried to apply his theory to atmospheric tides by assuming that the atmosphere was isothermal and that oscillations in the atmosphere took place isothermally. From these assumptions he was able to show that the resonant periods of the atmosphere were the same as those of an ocean with a depth equal to the scale height of the atmosphere. The scale height of the atmosphere is defined as

$$H = \frac{RT_o}{Mg} \qquad \text{(I-1)}$$

where R is the universal gas constant, M is the mean molecular weight of air and T_o is the undisturbed temperature.

Development of Notation. Before further development of the history is carried out, some additional nomenclature should be given.

Let S_λ represent the solar pressure oscillation with a period of $24/\lambda$ hours. The amplitudes and phases of S_λ will be dependent on both the longitude and latitude. It is possible to resolve S_λ into terms of S_λ^s ($s = 0, 1, 2, \ldots$) where the amplitudes and phases will now depend on the colatitude only. Here S_λ^s is called a wave family. A still further reduction may be obtained by expanding S_λ^s in terms of a set of spherical harmonics called Hough's Functions. Hough [1898] developed these functions for the specific purpose of solving Laplace's tidal wave equation. Each term of these expansions has constant

amplitude and constant phase and is called a wave type and is denoted by $S^{s}_{\lambda,n}(n = 1, 2, 3 \ldots)$. As was suggested above, the appropriate resonance parameter is the quantity h, which is called the "equivalent depth" when applied to atmospheric tides. The quantity h depends on all three of the parameters λ, s, n so that each wave type has its own particular equivalent depth. From theoretical formulism it follows that free oscillations of the atmosphere may occur only at one or more values of h which are called eigenvalues of the atmosphere and denoted as $\hat{h}$. These eigenvalues will depend on the structure of the atmosphere under consideration. The closer a value of h is to an eigenvalue $\hat{h}$, the higher the resonance magnification will be.

It was found that the wave type most responsible for the semi-diurnal solar pressure oscillation was the $S^{2}_{2,2}$ term, which has an equivalent depth of h = 7.85 km. For purposes of convenience, the wave types $S^{s}_{\lambda,n}$ are many times abbreviated to (s,n) modes, i.e. $S^{2}_{2,2}$ is called the (2,2) mode.

Atmosphere in Adiabatic Equilibrium. In 1910, Lamb [1924] showed that Laplace was not justified in considering the atmosphere as isothermal. Lamb assumed that the atmosphere was in adiabatic equilibrium and that oscillations in the atmosphere took place adiabatically. From this he showed that the conclusions of Laplace were valid only if the depth of the "equivalent ocean" was taken to be $\hat{h} = H_o$ where H_o is the scale height of the atmosphere at ground level. The value of H_o varies from about 7.3 km at the poles to 8.7 km at the equator with a mean value of 8.4 km. This agrees well with equivalent depth of the

(2,2) mode, so resonant magnification of the 12 hour period would be expected.

Lamb also showed that if dissipative forces were small the resonance could be very sharp, so that, if the semidiurnal oscillation were to be amplified appreciatively, the period of the free oscillation would have to be within a few minutes of 12 hours. He also pointed out that if this sharp resonance were the case, then the solar semidiurnal oscillation could be greatly magnified without the lunar semidiurnal oscillation being magnified. The period of the lunar semidiurnal oscillation is about 12 hours 25.2 minutes. This result would mean that the relative importance of the gravitational and thermal tide-producing forces should be reconsidered because the solar semidiurnal oscillation could now be produced from either generating force, gravitational or thermal. This question was not solved until much later.

Two-layer Temperature Model. Resonance theory seemed to be well established. However as time went on, knowledge of the earth's atmosphere was increased. The structure of the atmosphere turned out to be a more complicated one than at first considered. New calculations of the free oscillations of the atmosphere were made by using a two-layer model of the atmosphere. This model consisted of a constant temperature gradient in the lower layer, the troposphere, and uniform temperature in the upper layer, the stratosphere. The eigenvalue that was calculated from this model was $\hat{h} = 10$ km which corresponds to a free period of about 10.5 hours. Taylor [1936] showed

that this calculated eigenvalue was in very good agreement with data that was obtained from the Krakatau volcano eruption in 1883. According to Laplace's theory, the wave disturbance caused by the eruption should propagate at a velocity given by $V^2 = g\hat{h}$. Pressure measurements at different points on the earth showed that the velocity of the disturbing wave was about 319 m/sec. This velocity would correspond to a value of $\hat{h} = 10.4$ km in agreement with the above eigenvalue.

Five-layer Temperature Model. If the two-layer model were correct in its prediction of a free period of oscillation of 10.5 hours, then resonance theory would be completely destroyed. This possibility led Taylor to show that model atmospheres could exist with more than one eigenvalue. Pekeris [1937] extended Taylor's investigation by calculating two eigenvalues of the atmosphere, $\hat{h} = 10$ km and $\hat{h} = 8$ km. Pekeris assumed a five-layer model of the atmosphere which took into account the temperature maximum near the height of 50 km which was deduced from studies of the anomalous propagation of sound and from the existence of noctilucent clouds. In his paper Pekeris also brought the mathematical treatment of the problem, restricted to gravitational excitation, into final form.

Thus resonance theory again gained good standing. However, all the work that had been considered up to this time had been done for essentially one purpose: to explain the large semidiurnal solar oscillation. Pressure oscillations with other periodicities, such as 24 hour and a small 8 hour and 6 hour, had also been observed but they were more or less ignored in the development of the theory.

Breakdown of the Resonance Theory. Siebert and Kertz separately extended the theoretical developments to include all the oscillations that had been observed before 1957. Their conclusion was that the resonance magnification of the (2,2) mode of oscillation is of the same order of magnitude as that of the other oscillations. Hence, the semidiurnal oscillation could not be favored by resonance. Also, with the advent of new data on the upper atmosphere obtained by rockets, the temperature maximum at about 50 km altitude, needed for the calculation of the eigenvalue $\hat{h} = 8$ km, was observed to be too small. The temperature maximum was observed to be less than 300° K. A temperature maximum of at least 350° K was needed to obtain an eigenvalue of $\hat{h} = 8$ km.

Thus these considerations and other empirical facts suggested abandonment of the resonance theory. However, this would mean that the semidiurnal oscillation and the other oscillations would have to be caused solely by thermal effects. Therefore additional sources of thermal excitation were investigated. It was found by Siebert [1961] and by Small and Butler [1961] that absorption of solar energy by water vapor in the troposphere and ozone in the stratosphere can act as sources of the thermal oscillations. Their theories agree rather well with observations.

In addition to the new theories on the sources and driving forces of the atmospheric oscillations, recent rocket and meteor data have shown that, even though the semidiurnal oscillations appear as the strongest oscillations at ground level, the diurnal oscillations

appear to be dominant, or at least equal to the semidiurnal oscillations, in the mesospheric and thermospheric regions.

To conclude the historical development, Figure 1 shows the temperature models of the atmosphere which were used in the development of the theory. Compared with these models is the current temperature model which was obtained from the U. S. Standard Atmosphere [1962].

A more thorough bibliography of the historical development of atmospheric tidal theory is given in Siebert [1961].

Purpose of Further Research

Present theories consider only a non-resonant atmosphere. A further understanding of the structure of the atmosphere, such as temperature and density profiles, is being sought in an effort to explain atmospheric oscillations and eventually to predict these oscillations over short periods of time.

Further research in the general area of upper atmosphere physics is greatly needed for many reasons, some of which will be discussed here. One problem under consideration deals with communciations. Research is being done on the possibility of using artificial clouds of ions, deposited in the atmosphere by rockets, to reflect signals so that communication can be continued between different points on the earth even during ionic storms. Also, Rosenberg, Edwards, and Wright [1964] have shown a distinct correlation between wind shears and the sporadic E. Other people are investigating the possible correlation of winds with other atmospheric parameters.

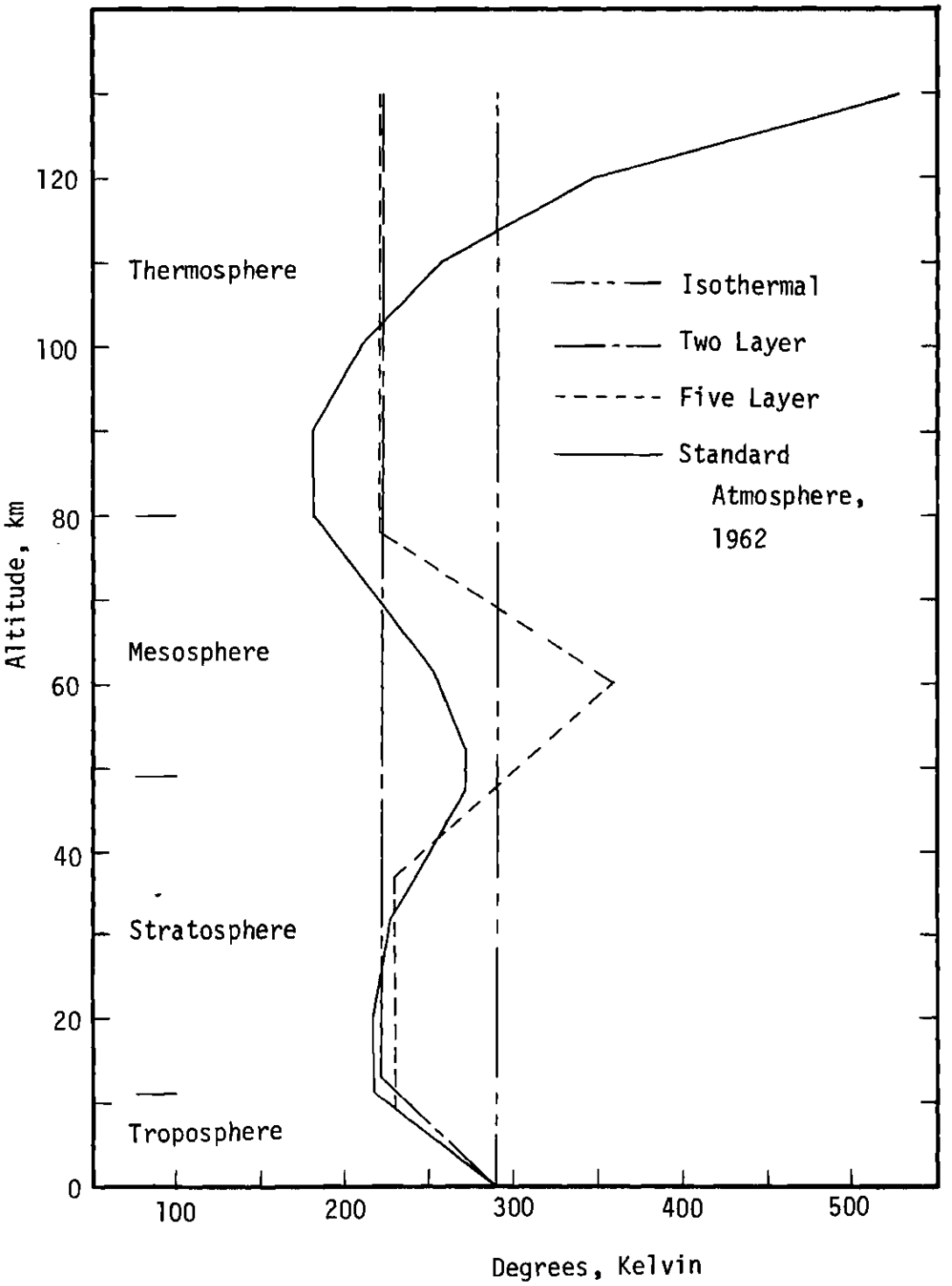

Figure 1. Temperature Models of the Atmosphere.

Another problem deals with the determination of the forces that the atmosphere exerts on rockets and space vehicles as they pass through the atmosphere. These forces present problems with trajectory calculations because the density profile and density fluctuations of the atmosphere are not known accurately enough.

Yet another problem deals with radioactive fall-out. Better understanding of the upper atmospheric circulation is needed in order to predict the paths of radioactive materials in the atmosphere.

The purpose of the present study is to present additional information on some of the parameters of the tidal winds, such as wavelength, phase and velocity amplitudes of different modes, in the height region around 100 km. This is the height region which is too high for balloon and meteor research and too low for satellites. Hence rockets which released chemi-luminous clouds into the atmosphere were used. This height region is also important because it is the region where viscous forces begin to play an important role in the dissipation of atmospheric energy.

CHAPTER II

THEORY

Until recent times atmospheric tidal theory dealt almost exclusively with the semidiurnal oscillation. This situation was brought about by the dominance of the semidiurnal oscillations in the atmospheric winds and pressure variations at or near ground level. However with the development of better techniques of obtaining data in recent years, such as improved rocket techniques and improved radar observations of meteor trails, the diurnal oscillations seem to be dominant in the mesopheric winds. As a result, the atmospheric theory for the diurnal oscillations has gained a great deal of interest. In the following development of the theory, main emphasis will be given to the recent developments on the diurnal oscillations.

Tidal Equations

A summary of the atmospheric tidal theory developed prior to the 1960's is given by Siebert [1961]. An expansion of his work in mathematical detail is given in Appendix A. The basic theoretical equation is Laplace's Tidal Equation which is given for a longitudinal wave number s and a frequency of oscillation σ (See equation A-95).

$$\frac{\partial}{\partial \mu}\left(\frac{1-\mu^2}{f^2-\mu^2}\,\frac{\partial\,\Theta^s_{\lambda,n}}{\partial\,\mu}\right) - \frac{1}{f^2-\mu^2}\left(\frac{s}{f}\,\frac{f^2+\mu^2}{f^2-\mu^2} + \frac{s^2}{1-\mu^2}\right)\Theta^s_{\lambda,n}$$

$$+ \frac{4\,a^2\,\omega^2}{g h_n} \quad \Theta^s_{\lambda,n} = 0 \qquad \text{(II-1)}$$

where μ = $\cos\theta$

θ = colatitude

$f = \frac{\sigma}{2\omega}$

a = radius of the earth

ω = earth's rotation rate

g = constant acceleration of gravity

h_n = equivalent depth

$\Theta^s_{\lambda,n}$ = Hough Functions

This equation gives the latitude dependence for the atmosphere of the quantity

$$\chi - \frac{\kappa J}{g h} \qquad \text{(II-2)}$$

where χ is the divergence of the wind velocity, $\kappa = \frac{\gamma - 1}{\gamma}$, H is the scale height as defined by equation I-1 and J is the heat added per unit mass per unit time. The altitude dependence of the quantity II-2 is given by equation A-68.

$$\frac{\partial^2 y_n(x)}{\partial x^2} - \frac{1}{4}\left[1 - \frac{4}{h_n}\left(\kappa H(x) + \frac{\partial H}{\partial x}\right)\right] y_n(x) = \frac{\kappa}{g\gamma h_n} J_n(x) e^{-x/2} \qquad \text{(II-3)}$$

where $x = \int_0^z \frac{d\xi}{H(\xi)}$

z = altitude

$$y_n(x)e^{x/2} = \chi_n(z) - \frac{\kappa J_n(z)}{g H(z)}$$

$$\gamma = \frac{c_p}{c_v} = 1.4 \text{ (ratio of specific heats)}$$

Then the tidal fields can be expressed in terms of $y_n(x)$ and $\Theta^s_{\lambda,n}(\mu)$ as (See equations A-121 thru A-125):

$$u_n = \frac{\gamma g h_n e^{x/2}}{4 a \omega^2 (f^2 - \cos^2\theta)} \left(\frac{\partial y_n}{\partial x} - \frac{1}{2} y_n \right) \left(\frac{\partial}{\partial \theta} - \frac{i \cot\theta}{f} \frac{\partial}{\partial \phi} \right) \Theta^s_{\lambda,n} e^{i(\sigma t + s\phi)} \qquad \text{(II-4)}$$

$$v_n = \frac{i \gamma g h_n e^{x/2}}{4 a\omega^2 (f^2 - \cos^2\theta)} \left(\frac{\partial y_n}{\partial x} - \frac{1}{2} y_n \right) \left(\frac{\cos\theta}{f} \frac{\partial}{\partial \theta} - \frac{i}{\sin\theta} \frac{\partial}{\partial \phi} \right) \Theta^s_{\lambda,n} e^{i(\sigma t + s\phi)} \qquad \text{(II-5)}$$

$$w_n = -\frac{i\sigma}{g} \Omega_n + \gamma h_n e^{x/2} \left[\frac{\partial y_n}{\partial x} + \left(\frac{H}{h_n} \right. \right.$$

$$- \frac{1}{2} \Big) \; y_n \Big] \; \Theta^s_{\lambda,n} \, e^{\,i(\sigma t + s\phi)} \tag{II-6}$$

$$\delta p_n = \frac{p_o(0)}{H} \left[- \frac{\Omega_n}{g} \, e^{-x} + \frac{\gamma h_n}{i\sigma} \, e^{-x/2} \left(\frac{\partial y_n}{\partial x} \right.\right.$$

$$\left.\left. - \frac{1}{2} \, y_n \right) \right] \; \Theta^s_{\lambda,n} \, e^{\,i(\sigma t + s\phi)} \tag{II-7}$$

$$\delta T_n = \frac{M}{R} \left\{ \frac{\Omega_n}{H} \frac{\partial H}{\partial x} - \frac{\gamma g h_n}{i\sigma} \, e^{x/2} \left[\frac{\kappa H}{h_n} + \frac{1}{H} \frac{\partial H}{\partial x} \left(\frac{\partial}{\partial x} \right.\right.\right.$$

$$\left.\left.\left. + \frac{H}{h_n} - \frac{1}{2} \right) \right] \; y_n + \frac{\kappa J_n}{i\sigma} \right\} \; \Theta^s_{\lambda,n} e^{\,i(\sigma t + s\phi)} \tag{II-8}$$

where u_n, v_n, w_n, δp_n and δT_n are components of the southward, eastward, and vertical velocities, pressure variation and temperature variation respectively. The total southward velocity is given by

$$u = \sum_{n=1}^{\infty} u_n$$

The total eastward and vertical velocities, the total pressure and temperature variations are also defined similarly.

Since the Hough Functions are incomplete for diurnal oscillations, as explained by Lindzen [1966], the additional equations A-126 through

A-130 must be added to equations II-4 through II-8 whenever diurnal oscillations are considered.

Boundary Conditions

In order to solve the differential equation II-3, certain boundary conditions must be imposed. Wilkes [1949] discusses the boundary conditions in detail.

Lower Boundary. One boundary condition imposed on the solutions is that the vertical velocity component (and, hence, each of its eigenfunctions) be zero at the surface of the earth, or $w_n(0) = 0$. From equation II-6, this implies that

$$\left[\frac{\partial y_n}{\partial x} + \left(\frac{H}{h_n} - \frac{1}{2}\right) y_n\right]_{x=0} = \frac{i\sigma}{\gamma g h_n} \Omega_n(0) \qquad \text{(II-9)}$$

Upper Boundary. The second boundary condition is concerned with the behavior of the solutions as x approaches infinity. To find the nature of this boundary condition we must consider the flow of energy in the different directions. Wilkes [1949] gives the rate at which energy is flowing across a unit area (flux of energy) as

$$E = \frac{1}{2} R\,(p\ v^*) \qquad \text{(II-10)}$$

where v and p denote the velocity and changes in pressure in the direction of concern. R denotes the real part of the quantity in parenthesis.

An examination of equation II-7 shows that if we assume that

$\frac{\partial y_n}{\partial x} - \frac{1}{2} y_n$ does not decrease rapidly with height, then for large x, the term in Ω can be neglected. The assumption about $\frac{\partial y_n}{\partial x} - \frac{1}{2} y_n$ was proved to be valid by Wilkes [1949]. Further examination of this pressure equation and equation II-4 shows that the pressure oscillations and the north-south wind oscillations are 90° out of phase for large x. Hence, there is essentially no flow of energy towards the poles.

The rate of energy flow in the east-west direction can be obtained from equations II-10, II-5 and II-7. It is

$$E = \frac{\gamma^2 g h_n^2}{8 a\omega^2} \frac{p_o(0)}{H} \left| \frac{\partial y_n}{\partial x} - \frac{1}{2} Y_n \right|^2 \frac{\Theta^s_{\lambda,n}}{f^2 - \cos^2\theta} \left(\frac{\cos\theta}{f} \frac{\partial \Theta^s_{\lambda,n}}{\partial \theta} - \frac{s}{\sin\theta} \Theta^s_{\lambda,n} \right) \qquad \text{(II-11)}$$

The expression is independent of the longitude ϕ. Thus the amount of energy entering a volume of air horizontally from an easterly direction is exactly equal to amount of energy flowing out of the volume of air horizontally in the westerly direction. Hence, in the study of energy balance, the horizontal flow of energy can be ignored.

The vertical flow of energy is given by the equations II-10, II-6 and II-7.

$$w_n^* = \gamma h_n e^{x/2} \left[\frac{\partial y_n}{\partial x} + \left(\frac{H}{h_n} - \frac{1}{2} \right) y_n^* \right] \Theta^s_{\lambda,n} e^{-i(\sigma t + s\phi)}$$

where the term in Ω is neglected.

$$\delta p_n \, w_n^* = \frac{p_o(0)\gamma^2 \, h_n^2}{i \, \sigma \, H} \left(\Theta^s_{\lambda,n}\right)^2 \left[\left(\frac{\partial y_n}{\partial x} - \frac{1}{2} y_n\right)^2 + \frac{H}{h_n} \frac{\partial y_n}{\partial x} y_n^* - \frac{H}{2h_n} y_n^2\right]$$

Thus

$$E = \frac{p_o(0) \, \gamma^2 h_n}{2 \, \sigma} \left(\Theta^s_{\lambda,n}\right)^2 \, I\left(\frac{\partial y_n}{\partial x} \, y_n^*\right) \qquad \text{(II-12)}$$

where I denotes the imaginary part of the quantity in brackets.

Now we can consider the boundary condition for equation II-3 as x becomes very large. For convenience, let us consider the case where the scale height is independent of altitude. Then equation II-3 becomes, for large x

$$\frac{\partial^2 y_n}{\partial x^2} + \left(\frac{\kappa H}{h_n} - \frac{1}{4}\right) y_n = 0 \qquad \text{(II-13)}$$

For solutions of this equation, two cases must be considered.

Case I:

$$\frac{\kappa H}{h_n} - \frac{1}{4} = -k^2 < 0$$

Then the solutions are

$$y_n(x) = A \, e^{kx} + B \, e^{-kx}$$

When equation II-14 is substituted into equation II-12, then we get that the rate of flow of energy across a horizontal plane is zero for this case. Physically this means that for any mode of atmospheric motion whose altitude dependence is given by equation II-14, then the energy contained in this mode is trapped at the altitude where the energy source is located.

Case II:

$$\frac{\kappa H}{h_n} - \frac{1}{4} = \mu^2 > 0$$

Then solutions of equation II-13 become

$$y_n(x) = A\, e^{i\mu x} + B\, e^{-i\mu x} \qquad \text{(II-15)}$$

In this case, $y_n(x)$ remains finite in both cases, $A \neq 0$ and $B \neq 0$. In order to choose between the two solutions, we must note that the energy sources of atmospheric oscillations are located in the lower atmosphere, i.e. below about 50 km altitude. The reason for this is that most of the solar energy is absorbed by the atmosphere where the air density is greatest. So at a sufficiently high altitude, energy will be propagated upwards only. This condition corresponds to the condition that

$$I\left(\frac{\partial y_n}{\partial x}\; y_n^*\right) > 0 \qquad \text{(II-16)}$$

from equation II-12. By substituting equation II-15 into this relation, we get that

$$B = 0$$

So

$$y_n(x) = A\, e^{i\mu x} \qquad \text{(II-17)}$$

Therefore, energy contained in any mode of oscillation whose altitude dependence is governed by equation II-17 will propagate upward from its source region. It might be noted here that since the region of concern in the present paper is sufficiently above the source region, then the results of the present paper should show an upward flow of energy. It will be shown later in this chapter that this corresponds to a downward propagation of the phase.

Wavelength

By analogy with the second order differential equation for the propagation of electromagnetic waves, Weekes and Wilkes [1947] showed that equation II-3 could be considered as a wave travelling in a medium having a refractive index μ given by

$$\mu^2 = \frac{H(x)}{h_n}\left(\kappa + \frac{\partial H}{\partial x}\right) - \frac{1}{4} \qquad \text{(II-18)}$$

In the case here, μ would correspondingly be the wave number from which the theoretical vertical wavelengths for the different modes of oscillation can be derived. If λ is taken to be the vertical wavelength, then we have

$$\mu^2 = \left[\frac{2\pi}{\lambda(x)}\right]^2$$

$$\lambda(x) = \frac{2\pi}{\left[\frac{H}{h_n}\left(\kappa + \frac{1}{H}\frac{\partial H}{\partial x}\right) - \frac{1}{4}\right]^{1/2}}$$

To transform from the scale height corrected altitudes x to the geometric altitude z, we get from the definition of x

$$H(z)\, dx = dz$$

Also

$$\lambda(x) = \frac{\partial x}{\partial z}\,\lambda(z) = \frac{1}{H(z)}\,\lambda(z)$$

Then

$$\lambda(z) = \frac{2\pi H(z)}{\left[\frac{H(z)}{h_n}\left(\kappa + \frac{\partial H}{\partial z}\right) - \frac{1}{4}\right]^{1/2}} \qquad \text{(II-19)}$$

The wavelengths for particular modes of oscillations are given by specifying the values of the equivalent depths h_n. Figure 2 shows the theoretical vertical wavelengths for the (1,3) mode, the (2,2) and (2,4) modes. These modes have been observed to be the main contributors to the experimentally determined diurnal and semidiurnal oscillations in the lower atmosphere. The equivalent depths for these modes were obtained from equations A-142, A-132, and A-134 respectively. The height dependence of the scale height H was obtained from The U. S.

Standard Atmosphere [1962]. This figure shows that the wavelengths of the (1,3) and (2,4) modes are approximately constant over the 90 to 120 km height range. The theoretical wavelength of the (2,2) mode varies rapidly in this altitude region, approaching infinity at an altitude near 90 km. In the region immediately below 90 km, the (2,2) mode wavelength becomes imaginary. This is the case when the altitude dependence of the (2,2) mode is exponential as shown by equation II-14. One of the consequences of an imaginary wavelength is that the energy contained in this mode is trapped at this particular height region and will decay exponentially with increasing height. Another consequence is that if there were a propagating wave for this mode below the height region where the wavelength is imaginary, then the height region of the imaginary wavelength would act as a partial barrier to the propagating wave which would then be reflected downward from the height region. This process could set up a standing wave and it was the basis of the resonance theory. The strength of the reflection depends on the width of the height region for which the wavelength is imaginary.

Hough Functions for Diurnal Oscillations

The solution of Laplace's Equation II-1 was obtained by Hough [1898]. He developed a set of spherical functions $\Theta^{s}_{\lambda,n}(\theta)$, which together with $P^{1}_{2}(\theta)$ (Associated Legendre Function) form a complete set for the tidal wave functions. Until recently, it was felt that the value of n must be positive because negative n leads to negative equivalent depths. The idea of a negative equivalent depth may seem unreasonable, but in fact, the name - equivalent depth - is misleading. The meaning of the equivalent depth can be seen from equations II-4,

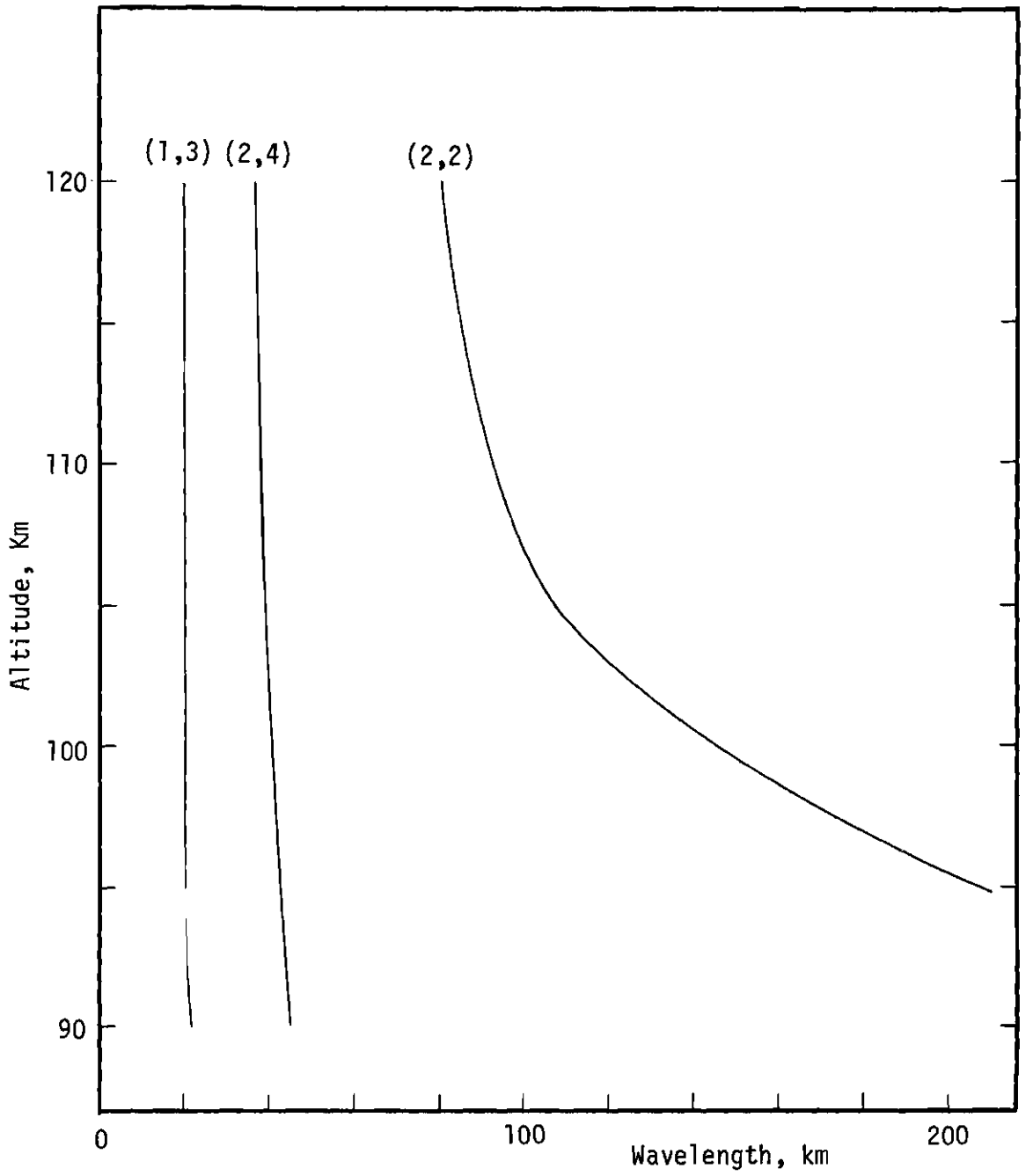

Figure 2. Theoretical Wavelengths for the (1,3), (2,4) and (2,2) Modes of Oscillation.

II-5, II-6 and the boundary conditions on equation II-3. For positive h_n's, case II of the boundary conditions prevails and the quantities u_n, v_n, and w_n are seen to increase with altitude as $e^{x/2}$. For negative h_n's, case I of the boundary conditions of equation II-3 prevails and the quantities u_n, v_n and w_n decrease with altitude. Lindzen [1966] and Kato [1966] independently showed that the existence of negative equivalent depths should be taken into account. As a consequence, the diurnal oscillations can now be represented latitudinally by a complete set of Hough Functions rather than half of a complete set.

A plot of the most important symmetric Hough Functions for the diurnal tide and the most important antisymmetric function ($P_2^1(\theta) = \cos\theta \sin\theta$) was given by Lindzen [1966] and is shown here as Figure 3. It should be noted that for positive n, the Hough Functions are concentrated between the latitudes of $\pm$ 30°, whereas for negative n, the maximum value of the Hough Functions occur between 30° latitude and the poles.

An expansion of the more important Hough Functions for the semidiurnal and diurnal oscillations in terms of the Associated Legendre Polynomials is given in Appendix A.

Energy Sources

The main sources of the thermal drive for the tidal winds are the direct absorption of solar energy by the water vapor in the troposphere and by ozone in the stratosphere. A model for the diurnal thermal drive was developed by Siebert [1961] and was expressed in terms of normalized Hough Functions by Lindzen [1967]. It is

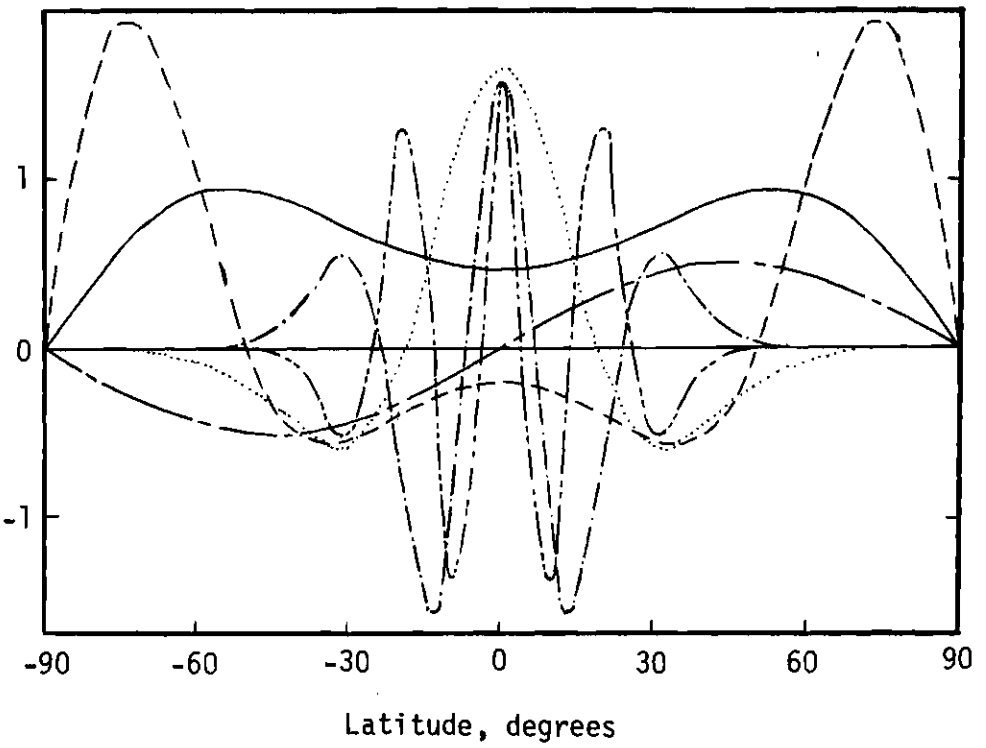

sin θ cos θ

$\Theta^1_{1,-1}$

$\Theta^1_{1,-3}$

$\Theta^1_{1,3}$

$\Theta^1_{1,5}$

$\Theta^1_{1,7}$

Figure 3. Symmetric Hough Functions for Diurnal Tide. Also Shown is sin θ cos θ, the Most Important Odd Mode (After Lindzen [1967]).

$$J_{\text{water vapor}} = \frac{i\,\sigma\,R}{\kappa}\, e^{-x/3}\, e^{i(\sigma t + \phi)}$$

$$\times \left[0.157\ \Theta^1_{1,\,-1} - 0.055\ \Theta^1_{1,\,-3} \right.$$

$$+ \quad 0.062\ \Theta^1_{1,3} \quad - 0.016\ \Theta^1_{1,5}$$

$$+ 0.008\ \Theta^1_{1,7}$$

$$+ \quad 0.0848\ g\ (\text{season})\ \sin\theta\ \cos\theta$$

$$+ \quad \left. \ldots \right] \qquad \text{(II-20)}$$

Leavy in 1964 gave a model for the diurnal thermal drive due to ozone absorption and it was expanded in terms of the normalized Hough Functions by Lindzen [1967] as follows:

$$J_{\text{ozone}} = \frac{i\,\sigma\,R}{\kappa}\ \exp\left[0.0116\ (z-z_1)\right]\ \sin\frac{\pi}{60}\ (z-z_1)\ e^{i(\sigma t + \phi)}$$

$$\times \left[1.6308\ \Theta^1_{1,-1} \ - \ 0.5128\ \Theta^1_{1,-3} \ + \ 0.5447\ \Theta^1_{1,3} \right.$$

$$- \quad 0.1411\ \Theta^1_{1,5} \quad + 0.0723\ \Theta^1_{1,7}$$

$$+ 0.1869\ g\ (\text{season})\ \sin\theta\ \cos\theta + \ldots .\Big] \qquad \text{(II-21)}$$

for $z_1 \leq z \leq z_2$

and $J_{ozone} = 0$

for $z \leq z_1, \quad z \geq z_2$

where $z_1 = 18$ km

$z_2 = 78$ km

For both equations II-20 and II-21, the numerical coefficients have units of degrees Kelvin and the quantity

$$g\ (\text{season}) = +1 \text{ for summer}$$
$$= -1 \text{ for winter}$$
$$= 0 \text{ for equinoxes}$$

Since the Hough Functions in equations II-20 and II-21 are normalized, then the coefficients are measures of the thermal drive for the different diurnal modes. It is noted that about 80% of the energy input goes into modes with negative equivalent depths. Hence this energy is trapped in modes of oscillations which decay exponentially with height.

Numerical Theoretical Predictions

To get numerical values for the velocities u, v, and w in equations II-4, II-5 and II-6, the sum of the equations II-20 and II-21 must be used in equation II-3 in order to solve for the quantity

$y_n(x)$. However, equation II-3 is a second order, inhomogeneous, differential equation with variable coefficients. Lindzen [1967] showed that for diurnal oscillations, an isothermal model would not be a bad assumption because the equivalent depths for the diurnal modes are either very small or negative. As a result of these small equivalent depths, the quantity μ^2 in equation II-18 (which is the coefficient of equation II-3) is sufficiently far from zero so that the effect of varying H(x) with height is of relatively small importance.

Hence, if the isothermal atmosphere is assumed, then equation II-3 becomes an ordinary, inhomogeneous, constant coefficient, second order, linear differential equation which can be solved for $y_n(x)$. And with the Hough Functions given as solutions of Laplace's Tidal Equation II-1, then it is a matter of mathematical computations to solve numerically for the velocities u, v and w. Lindzen [1967] has done these computations and his results will be presented here.

Horizontal Velocity Amplitudes and Phases. The southward velocity u is given by summing equation II-4 over all n. For a latitude of 30°, the amplitude and phase of u are given in Figures 4 and 5.

Figures 4 and 5 also show the amplitude and phase of the eastward velocity v.

Note that Figure 5 shows that there is a downward propagation of phase with a 360° cycle of phase about every 20 to 30 km displacement of height. This means that the diurnal wind will be observed to change direction with increasing height and time in the clockwise direction and will rotate through 360° at a particular height every

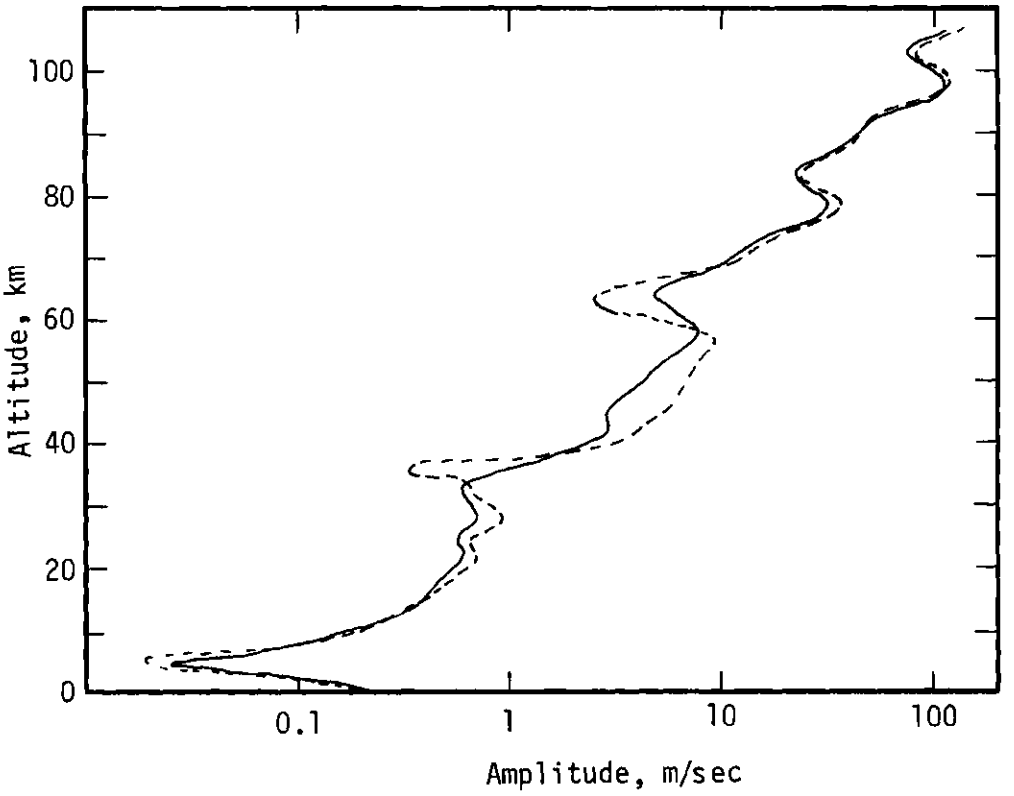

Figure 4. Theoretical Velocity Amplitudes for the Southward Component (Dotted Curve) and Eastward Component (Solid Curve) at 30° Latitude and Under Equinoctal Conditions (After Lindzen [1967]).

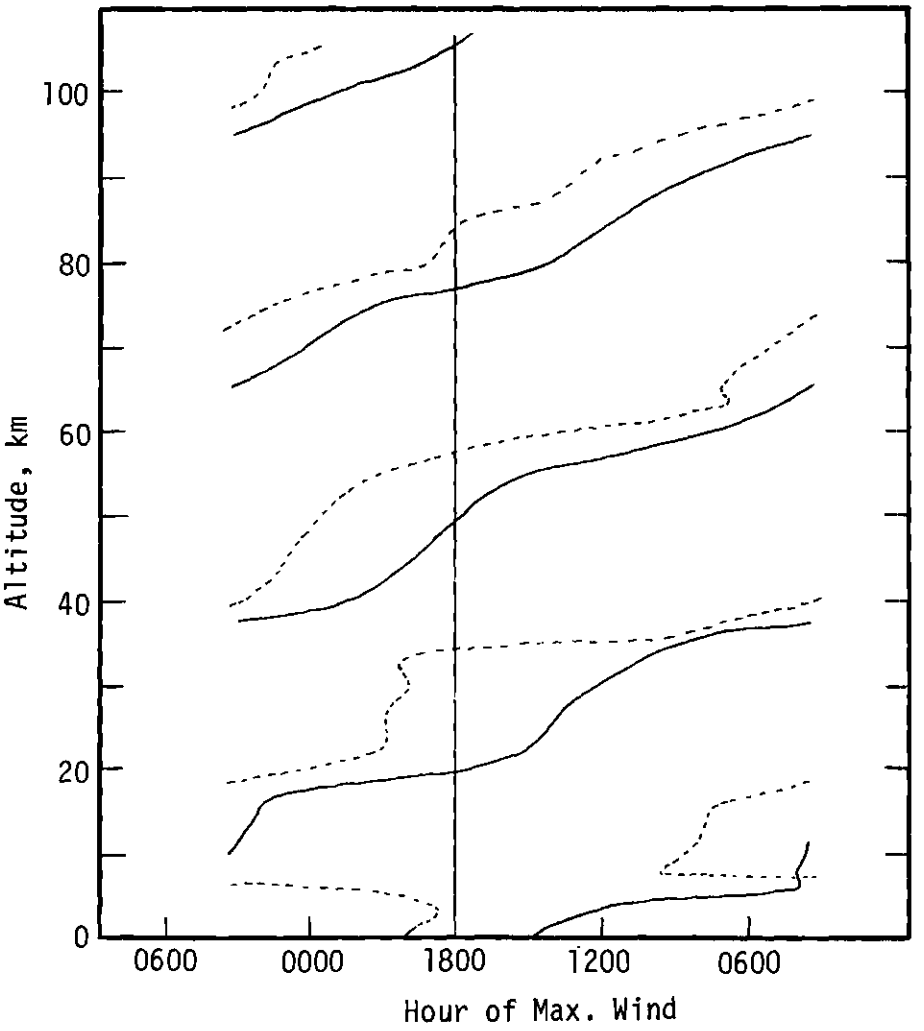

Figure 5. Phase Distribution of Diurnal Tide for Southward (Dotted Curve) and Eastward (Solid Curve) Components at 30° Latitude and Under Equinoctial Conditions (After Lindzen [1967]).

24 hours. Similar results show that the semidiurnal oscillations have a downward phase propagation and the wind vector rotates clockwise with increasing height and time.

Also by Figure 5, the eastward winds are observed to be approximately 6 hours ahead of the southward winds. This would correspond to the eastward wind being approximately 90° out of phase with the southward wind. The reason for this can be seen from equation II-4 and II-5 of the linearized Euler equations of motion. For a single mode of oscillation, these equations show that the southward and eastward velocities are 90° out of phase. Figure 5 shows the phase of a superposition of many modes of oscillations, but the phase difference is still observed to be near 90°, but not exactly 90°, at the higher altitudes.

Figure 4 shows that the southward and eastward velocities have approximately equal amplitudes for 30° north latitude. This is not true for lower latitudes but is true for 30° and higher latitudes.

The predicted value of the vertical velocity was less than 1 m/sec at about 85 km altitude.

Surface Pressure. From equations II-6 and II-7 and the condition that $w(0) = 0$, we get for the surface pressure variation

$$\delta p_n(0) = \frac{i\gamma}{\sigma} p_o(0)\, y_n(0)\, \Theta^{1}_{1,n}\, e^{i(\sigma t + \phi)} \qquad \text{(II-22)}$$

if we neglect the term in Ω_n. It is interesting to see the contribution of the water vapor absorption and ozone heating to $\delta p(0)$ separately.

From Lindzen [1967],

$$\delta p_{\text{water vapor}}(0) = [137\,\Theta^{1}_{1,-1} - 68.2\,\Theta^{1}_{1,-3} + 117e^{56i}\,\Theta^{1}_{1,3} - 13.0e^{75.3\,i}\,\Theta^{1}_{1,5} + 4.11\,e^{80.5\,i}\,\Theta^{1}_{1,7} + \ldots]\,e^{i(\sigma t + \phi)}\ \mu b \qquad \text{(II-23)}$$

and

$$\delta p_{\text{ozone}}(0) = [44.1\,\Theta^{1}_{1,-1} - 3.4\,\Theta^{1}_{1,-3} + 94.1e^{12.75i}\,\Theta^{1}_{1,3} - 3.75\,e^{16.1\,i}\,\Theta^{1}_{1,5} + 0.754\,e^{-6.57\,i}\,\Theta^{1}_{1,7} + \ldots]\,e^{i(\sigma t + \phi)}\ \mu b \qquad \text{(II-24)}$$

Comparing these two equations, we see that the largest contributions to the surface diurnal pressure variation is from the water vapor. However, Small and Butler [1961] and Siebert [1961] have shown that the semidiurnal pressure oscillation can be satisfactorily accounted for by thermal drives resulting mainly from ozone absorption of solar energy.

Equation II-23 also shows that the source energy for the diurnal pressure oscillations has mainly been put into modes of oscillations with

negative equivalent depths. Hence, the energy is trapped in the troposphere and does not propagate to the ground. This may be an explanation of the observed weak diurnal pressure oscillations at ground level and the observed strong semidiurnal oscillations. A further check on this could be made by observing how the two energy sources affect the horizontal velocity, say the southward velocity. Figure 6 gives an altitude distribution of the amplitude of u at 30° latitude and for equinoctial conditions resulting from (a) drive due to ozone absorption alone, and (b) drive due to both ozone and water vapor absorption. This figure shows that below about 75 km the amplitude due to ozone alone is greater than 0.5, and often greater than 0.75, of that due to both ozone and water vapor absorption. Furthermore, at ground level the ozone alone accounts for practically all of the amplitude. Since it has been shown that the ozone absorption gives rise mainly to semidiurnal pressure oscillations, then this is in very good agreement with observations at ground level.

Above 75 km altitude, the amplitude due to ozone absorption alone falls to less than 25% of the ozone and water vapor absorption. Hence this would again agree with observations because the water vapor absorption supposedly gives rise mainly to a diurnal oscillation.

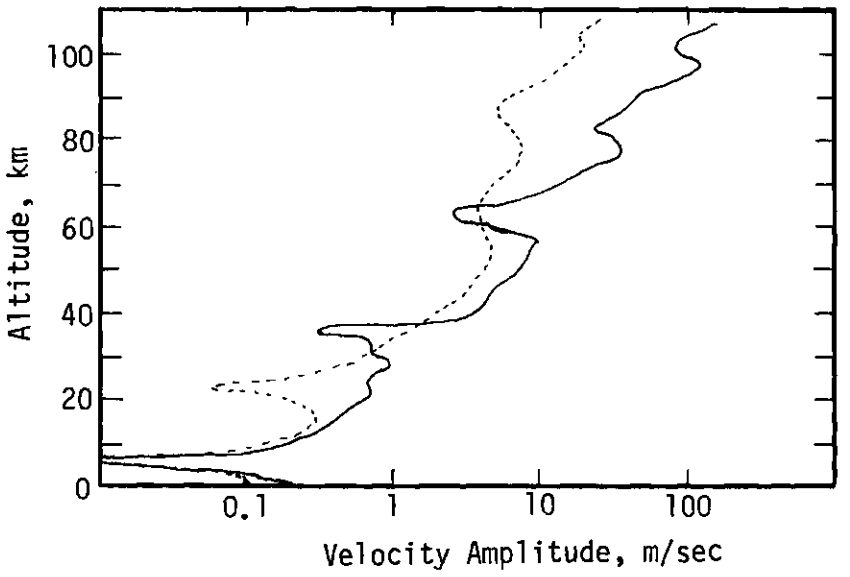

Figure 6. Southward Velocity Amplitude Distribution at 30° Latitude and For Equinoctial Conditions Resulting From (a) Drive Due to Ozone Absorption Alone (Dotted Curve), and (b) Drive Due to Both Ozone and Water Vapour Absorption (Solid Curve) (After Lindzen [1967]).

CHAPTER III

EXPERIMENTAL MEASUREMENTS

Radar observations of meteor trails in the 80 to 105 km region have shown the existence of both systematic and irregular winds in this height range. The systematic winds consist of a slowly varying prevailing component, diurnal and semidiurnal tidal oscillations, and a small terdiurnal component. (For a bibliography of the meteor trail tidal observations see Hines [1966].) As expected from tidal theory presented in Chapter II, the diurnal and semidiurnal components exhibit clockwise rotation of the wind vector in the northern hemisphere.

With the use of rockets, a large number of chemical release experiments have now been performed in the northern hemisphere, primarily in the 80 to 140 km region and at morning or evening twilight. The use of Trimethyl Aluminum (TMA) releases has recently provided nighttime wind data, primarily in the 90 to 140 km region. Most of the wind profiles obtained by photographic tracking of these chemical release trails show a clockwise rotation of the total wind vector with increasing height. These observations indicate that tidal components may make a large contribution to the total winds observed by this method. However, a method of extracting tidal components from individual wind profiles has not been found, and to date, there have not been large numbers of chemical releases sufficiently closely spaced in time on which to perform an harmonic analysis similar to that employed on the meteor trail winds.

Geometrical Method of Analysis

Hines [1966] has developed and employed a method of extracting tidal components from the mean winds obtained from large numbers of chemical releases. This method uses only dawn and dusk wind data and resolves the averaged winds at a given altitude into diurnal and prevailing plus semidiurnal components. The resultant components represent some form of average of the tidal winds over the period of observation (four years, for the data which Hines used). Hines confirms the clockwise rotation of the diurnal wind vector and determines the wave length of the diurnal tide to be 20 ± 3 km in the 100 to 120 km height region. This is in agreement with the theoretical wave length of the (1,3) tidal mode, as shown by Figure 2.

The Analysis Procedure

The following geometrical method of analyzing the wind data is an extension of the method developed by Hines. This analysis makes use of winds obtained near midnight, as well as dawn and dusk wind data. The method is designed to separately resolve the semidiurnal and prevailing components in addition to the diurnal component.

Method of Analysis. The wind data used here were obtained from chemical releases fired from Eglin AFB, Florida (30° N, 87° W) during the period from October 1962 through November 1965. Chemilumious clouds were ejected from rockets. As the winds in the atmosphere distorted the cloud, photographs from three separate tracking stations on the ground were taken of the cloud as a sequence of time. The atmospheric winds were determined from the photographs by a method of triangulation which is described by Justus, Edwards and Fuller [1964 a, b].

These data include several wind profiles obtained at various times throughout the night by use of TMA trails. The wind data were divided into dawn (or A.M.), dusk (or P.M.) and midnight groups. The P.M., midnight and A.M. groups contained 12, 11, and 15 releases, respectively. A seasonal breakdown of the wind data shows that 82 per cent were obtained in the fall (launch dates 23 September through 14 December), and 69 per cent of all wind data came from the early and mid-fall period (launch dates 23 September through 18 November).

At each altitude (1 km intervals) the wind data in each of these groups were averaged by the method used by Hines [1966]. Thus, for each altitude and time group one can determine a mean wind and its corresponding "variance" and "probable error." The "variance" s is defined by

$$s = \left[\frac{1}{n} \sum \left(s_E^2 + s_N^2 \right) \right]^{1/2} \qquad \text{(III-1)}$$

and the "probable error" p is given by

$$p = \frac{0.6745\ s}{(n-1)^{1/2}} \qquad \text{(III-2)}$$

Here n is the number of releases in the group and s_E and s_N are respectively the eastward and northward components of the individual wind deviations from the mean. Other formulas for the probable error may also be applicable to the data considered here. However, since the results of the present analysis will be compared mainly with the

results of Hines [1966], it was desirable to use the same formulas for the "variance" and "probable error" as he did. Formula III-2 gives the probable error of the mean and should be accepted as only indicative of the actual error.

The method of extracting the assumed prevailing, diurnal, and semidiurnal components from these average winds is illustrated in Figure 7. Here the origin (the zero wind vector) is at point 0, and the observed average wind vectors at dusk, midnight, and dawn are represented by the points P, M, and A, respectively. The observed average winds are presumed to be made up of a prevailing OI, a diurnal component which at dusk, midnight, and dawn is given by the lines ID_P, ID_M, and ID_A, plus a semidiurnal component which at dusk, midnight, and dawn is given by D_PP, D_MM, and D_AA. These components can be determined by the following procedure: (1) Construct point C_1 as the midpoint of PA. (2) Construct line C_1R equal in length to C_1P and rotated clockwise 90° from the line C_1P. (3) Construct point C_2 as the midpoint of RM. Geometrical analysis of Figure 7 shows that the diurnal component at dusk, midnight, and dawn is equal to C_1P, C_1R, and C_1A, respectively; the semidiurnal component at dawn and dusk is equal to C_2R and at midnight is equal to C_2M; and point I may be found by parallel displacement of line C_1R to the position IC_2.

Assumptions of the Method. Consider a model for a tidal component such that the northward and eastward directed tidal wind components are given by

$$V_n = A \sin (kz + \phi_n) \qquad \text{(III-3)}$$

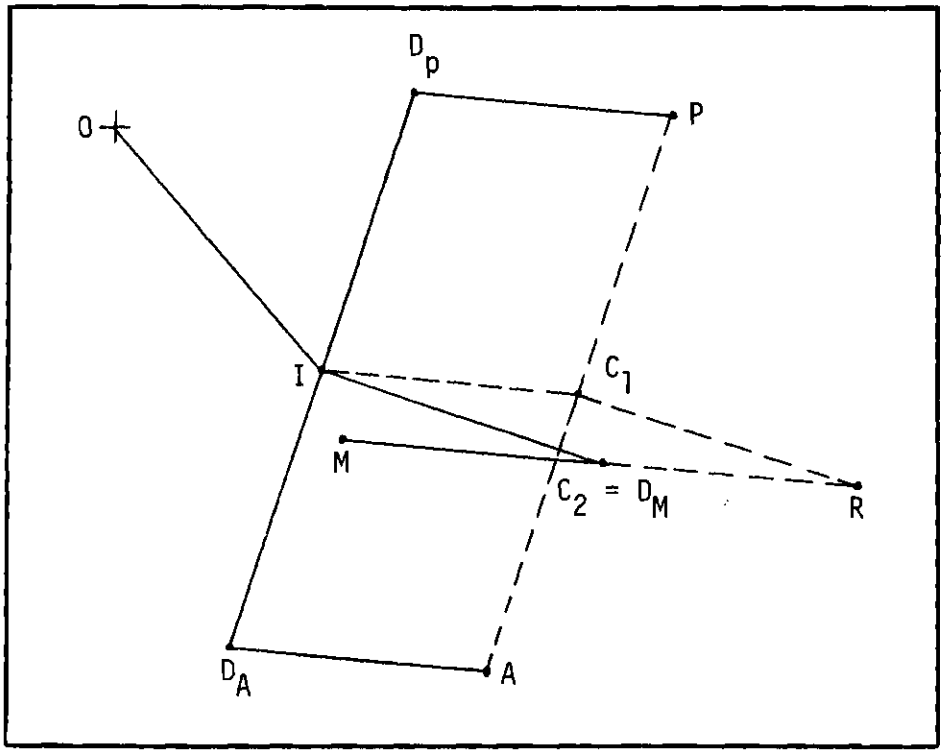

Figure 7. Method of Analysis

$$V_e = B \sin (kz + \phi_e) \qquad \text{(III-4)}$$

where z is the altitude, A and B are the amplitudes, k is the wave number (2π/wave length) and ϕ_n and ϕ_e are the phase angles. The tidal wind speed $V = (V_n^2 + V_e^2)^{1/2}$ as a function of altitude is shown in Appendix D to be

$$V^2 = \frac{A^2 + B^2}{2} - C \cos (2kz + \phi_n + \phi_e + \beta) \qquad \text{(III-5)}$$

where the angle β is determined by

$$\tan \beta = \frac{A^2 - B^2}{B^2 + A^2} \tan \phi \qquad \text{(III-6)}$$

and the factor C is given by

$$C = AB \left[\cos^2 \phi + \frac{1}{4} \left(\frac{A}{B} - \frac{B}{A} \right)^2 \right]^{1/2} \qquad \text{(III-7)}$$

where ϕ is the phase difference $\phi_n - \phi_e$.

If A, B, k, and ϕ vary slowly with altitude, then relation III-5 represents a slowly varying mean speed squared curve modulated by a cosine function with an amplitude C and a wave length equal to one-half the tidal component wave length. The amplitude C is zero only if A = B and $\phi = \pm 90°$.

The tidal component wind speed as a function of the tidal component wind heading θ ($\tan \theta = V_e/V_n$) is shown in Appendix E to be

$$V^2 = \frac{a^2 b^2}{a^2 \sin^2(\theta - \alpha) + b^2 \cos^2(\theta - \alpha)} \qquad \text{(III-8)}$$

where a and b are given by

$$\left.\begin{matrix} a^2 \\ b^2 \end{matrix}\right\} = \frac{A^2 + B^2}{2} \pm \frac{1}{2} (A^4 + B^4 + 2A^2B^2 \cos 2\phi)^{1/2} \qquad \text{(III-9)}$$

where the positive sign of the second term goes with a^2 and the negative sign with b^2. The angle α is determined by

$$\tan 2\alpha = \frac{2AB \cos \phi}{A^2 - B^2} \qquad \text{(III-10)}$$

If A, B, k, and ϕ vary slowly with altitude, then relation III-8 represents an ellipse with semi-axes a and b rotated by an angle α from the north-south and east-west coordinate axes. Angle α is zero only for $\phi = \pm 90°$. Relation III-8 reduces to a circle (a = b) only when $\phi = \pm 90°$, and A = B.

The time variation of a tidal component at a given altitude is sinusoidal and is represented by equations analogous to III-3 and III-4. Therefore, the tidal component wind speed, at a given height, as a function of the time varying tidal component wind heading at that altitude is given by an equation corresponding to III-8. The geometrical method of tidal extraction presented above assumes clockwise

circular rotation of the diurnal component wind vector with increasing time. The discussion in Chapter II concerning Figure 5 shows that the clockwise rotation is predicted by tidal theory with phase propagating downward and tidal energy propagating upward. The assumption of circular rotation requires the assumptions that the magnitudes, A and B, of the northward and eastward diurnal components are equal and that their phase difference $\phi = \phi_n - \phi_e$ is 90°. This assumption essentially makes the value of C in equation III-7 zero. Note that Figure 4 in Chapter II shows that the quantities A and B are predicted to be equal by the linearized tidal theory at 30° latitude. Also the phase difference ϕ between the eastward and northward component velocities for a single mode of oscillation is predicted to be 90°. However for actual cases, these conditions probably will not be met; hence, an indication of the probable error caused by these assumptions for the data here should be given. First, it should be noted that only the dawn and dusk averaged winds are needed to evaluate the diurnal component at dawn or dusk. Therefore, the above assumptions do not affect the evaluation of the diurnal component at these two times. The assumptions, however, will affect the evaluation of the diurnal component at midnight, and hence, the semidiurnal tide and the prevailing wind also. Now if the clockwise circular rotation of the diurnal component is assumed correct, then a probable error from this circular rotation can be calculated by use of equation III-5. This probable error is shown in Appendix F to be

$$\delta = \frac{C}{2(A^2 + B^2)^{1/2}} \qquad \text{(III-11)}$$

To calculate δ, one needs to know A, B and the phase difference, ϕ. The value of ϕ can be obtained from Table 2 to be 120°. The value of A and B can be found by least squares fitting a function of the form $Y(z) = \text{constant} + D \sin(kz + \theta)$ to the components of the diurnal tide. Here z is height, θ is a phase term, D is the amplitude and k is $2\pi/\lambda$ where λ is the vertical wave length as obtained from Table 1. In this manner, A and B were found to be 17 and 19 m/sec, respectively. Then the probable error in the determination of the diurnal tide at midnight due to the assumption of circular rotation is calculated from equations III-7 and III-11 to be 3 m/sec.

Note that no assumptions about the phase difference or rotational nature of the semidiurnal tide and prevailing wind have been made. So the probable error of 3 m/sec is also the probable error in the semidiurnal and prevailing wind due to the assumption of circular rotation of the diurnal component.

Different values for the calculated semidiurnal component would also result from the assumption of counterclockwise rotation of the diurnal component. However, the results presented later in this chapter confirm that the diurnal component does, in fact, rotate clockwise near the 100 km region. Thus, only computed semidiurnal component values resulting from the method which assumes clockwise rotation will be presented here.

Another assumption of the geometrical method presented here is that the appropriate mean times for the P.M., midnight, and A.M. groups are 18:00, 00:00, and 06:00, respectively. The mean launch times (CST) actually obtained for the P.M., midnight, and A.M. groups were 18:16, 23:55 and 5:10. To calculate the errors due to these time differences, consider Figure 8. If the assumption of circular clockwise rotation of the diurnal wind vector is made, then from Figure 8 the magnitude of the diurnal component at dawn or dusk can be represented as A. However, if the time difference between dusk and dawn time groups is not exactly 720 minutes, then one will not measure a value A for the diurnal magnitude but will measure a value of x as shown. The error in the measurement will just be A-x. Then by geometry, the error in the calculation of the diurnal tide at dawn or dusk due to the separation time being 654 minutes is about 0.3 m/sec. Also, if a time error is considered only, this quantity will also be the error in the magnitude of the diurnal component at midnight.

A calculation similar to the above can be done for the error in the semidiurnal magnitude due to the fact that the time separation of the midnight group from either of the other groups was only 327 minutes instead of 360 minutes. This error was found to be about 0.2 m/sec. Therefore, the total error in the semidiurnal magnitude due to the assumed time differences would be the sum of the above two values, that is, 0.5 m/sec. This would also be the error in the prevailing wind magnitude due to the assumed time differences.

Some caution must be used in comparing the theoretical predictions and the experimental calculations because of the coordinate systems

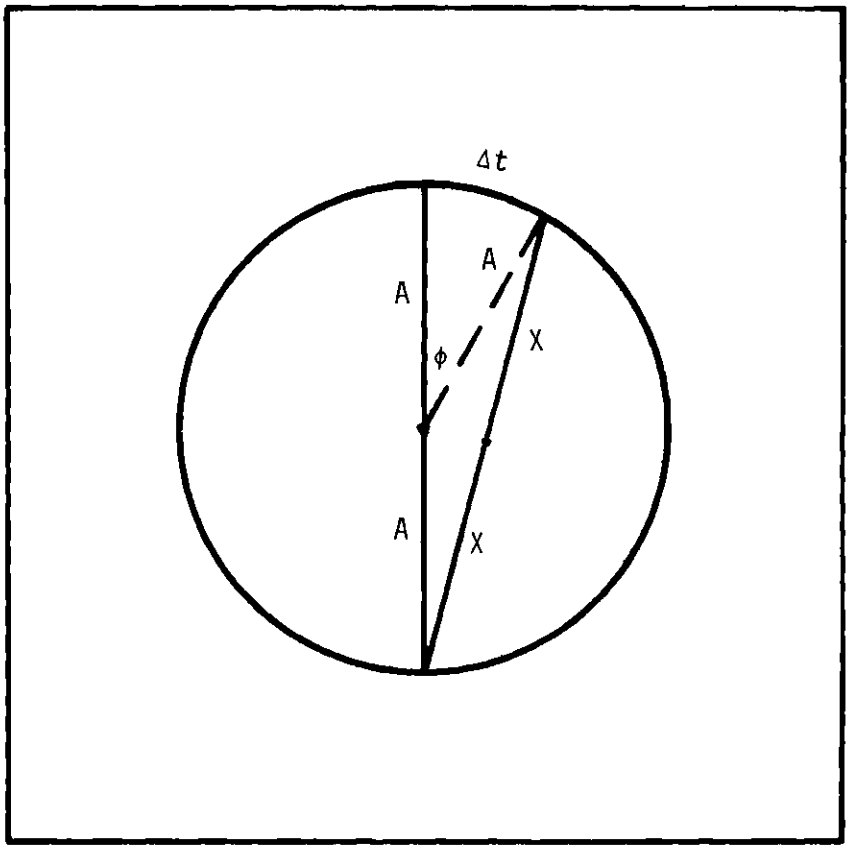

Figure 8. Time Circle For Diurnal Tide

that were used. The coordinate system used for the theoretical calculations had positive directions as eastward, southward, and vertically upward. However, it has become conventional in recent times to display the experimental data in a coordinate system which is positive in the northward, eastward, and vertically upward directions. The latter coordinate system has been rotated 90° in a counterclockwise direction about the vertical axis as compared with the former coordinate system. No difficulty will arise in applying the theoretical predictions to the experimental data if one will remember that the theoretical predictions derived for the eastward and southward wind components are to be applied to the northward and eastward wind components, respectively, of the experimental data.

One other source of error is the spread of the wind values before averaging. This error is given by equation III-2. The mean probable errors calculated from this equation were 16, 17, and 12 m/sec for the dusk, midnight and dawn groups, respectively. The overall average probable error was 15 m/sec. The total probable errors in the magnitudes of the tidal and prevailing winds are just the sum of these individual errors. The probable error in the diurnal component at dusk or dawn is about 15 m/sec. The probable error in the diurnal component at midnight, the semidiurnal component and the prevailing wind is about 19 m/sec. The mean values, calculated from the geometrical procedure described above, of the diurnal tide, the semidiurnal tide and the prevailing wind were found to be 25, 15, and 23 m/sec. Therefore, it is seen that the probable errors are nearly as large as the mean values of the winds; however, some information should be able to be gathered

about the diurnal tide and the prevailing winds.

Results of Analysis

Averaged Winds. The wind data in the P.M., midnight, and A.M. groups were averaged at one km intervals over the height range 90 to 120 km. The resultant averaged wind components are shown in Figure 9. Correlation analysis of the averaged wind profiles showed that the predominant wave length is 23 ± 3 km for all three time groups. Cross correlation of the northward and eastward components showed that their phase difference ($\phi_n - \phi_e$) is 147°, 87° and 84° for the P.M., midnight, and A.M. groups, respectively. Thus, the average phase difference for the three time groups is 106° ± 35°. An explanation of the correlation and cross correlation analysis is given in Appendix C. Figure 9 shows also that the averaged wind profiles moved downward an average of 5 ± 2 km during the period from dusk to dawn. This motion corresponds to a mean downward phase progression of 78° ± 25° from dusk to dawn.

Rosenberg and Justus [1966] have observed a downward phase progression on two sets of four wind profiles obtained from chemical releases launched throughout the nights of 3 December 1962 and 17-18 May 1963. However, the phase progression for these profiles was determined to be 310° ± 50° during the 12-hour period from dusk to dawn, and the mean phase difference between northward and eastward components was 70° ± 30°. From the observed phase progression it was assumed that the semidiurnal tidal component predominated the wind profiles during these two nights.

The small phase progression determined from the averaged winds of Figure 9 would seem to indicate that the semidiurnal component

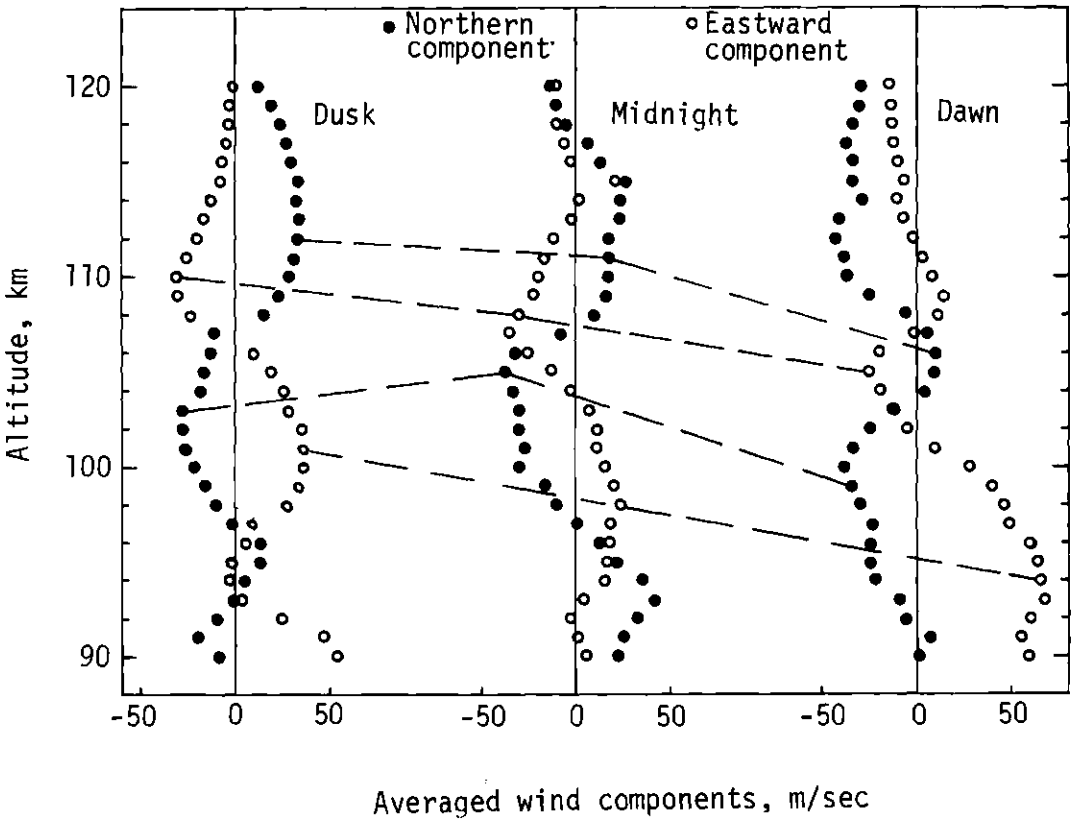

Figure 9. The Northward and Eastward Components of the Averaged Winds Versus Height at Dusk, Midnight, and Dawn. The Dashed Lines Show the Downward Phase Progression of Wind Profile Features.

plays only a small part in the determination of these averaged winds and that the diurnal and/or prevailing winds make a major contribution to the averaged winds. This conclusion is borne out by the results of the tidal component analysis presented in the following sections.

Variance. The "variance" was calculated for each altitude and time group by relation III-1. Figure 10 shows the computed variance for each time group as a function of altitude. The "variance" will be discussed more extensively in a later section of this chapter.

Prevailing and Tidal Winds. The geometrical method used here is designed to yield the prevailing wind and the diurnal and semidiurnal tidal winds. According to the predictions of the tidal theory in Chapter II, the computed tidal winds should rotate clockwise with increasing altitude and have vertical wavelengths given by equation II-19.

The geometrical analysis has been applied at one km height intervals between 90 and 120 km. Figure 11 shows the computed values for the prevailing winds, the diurnal tide in its dawn phase, and the semidiurnal tide in its dawn or dusk phase. This figure shows that the computed prevailing and diurnal components exhibit a significant systematic variation over much of the altitude region under consideration. There is no significance to the variation of the computed semidiurnal tide because its error is too large in comparison to the possible amplitude for this component. Figure 12 shows the diurnal component at dawn as computed by Hines [1966]. Figure 11 shows that the computed diurnal tide does rotate clockwise with altitude over most of the altitude range under investigation.

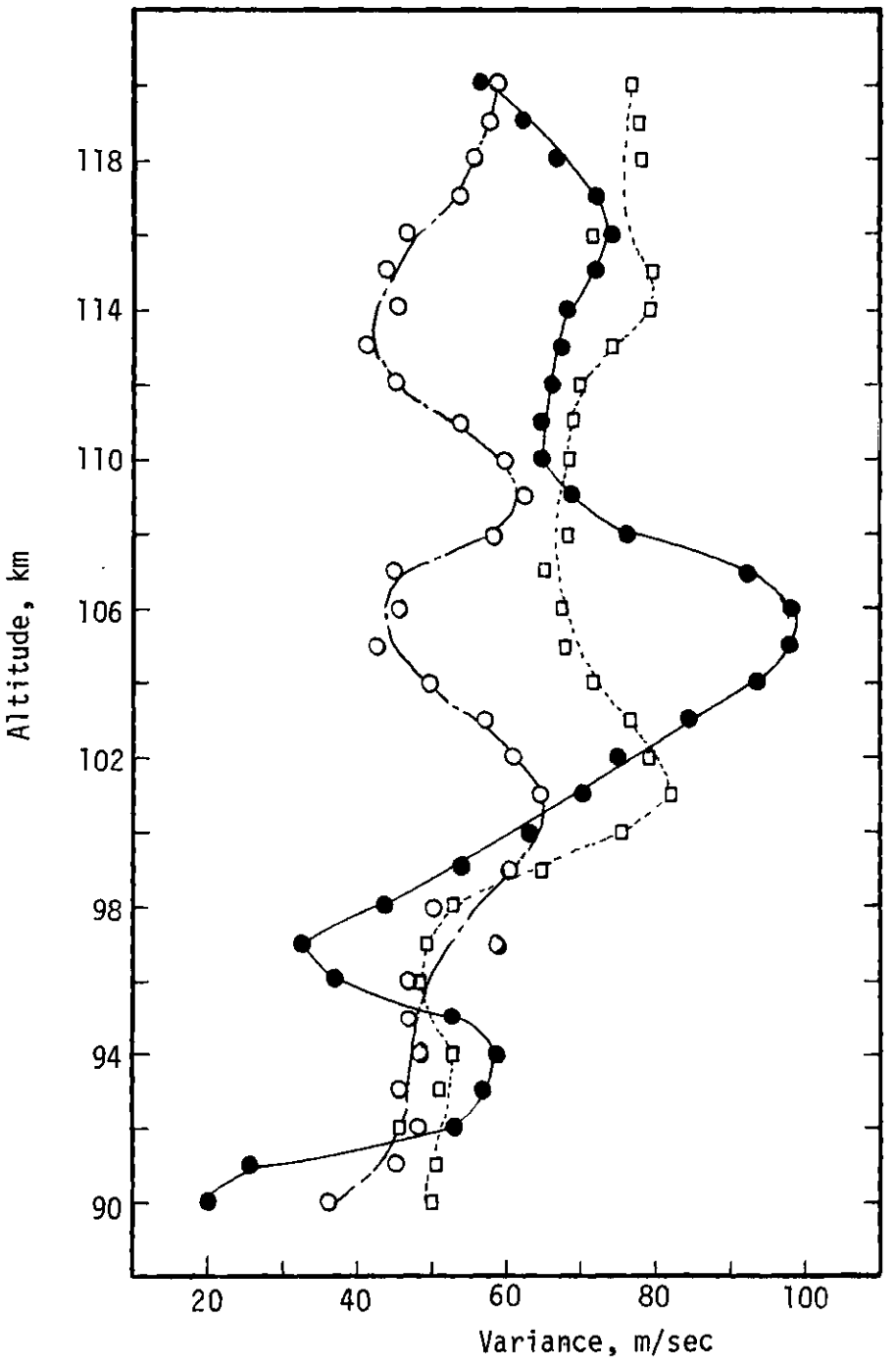

Figure 10. The Variance of the Averaged Winds at Dusk (Solid Dot), Midnight (Square), and Dawn (Open Circle).

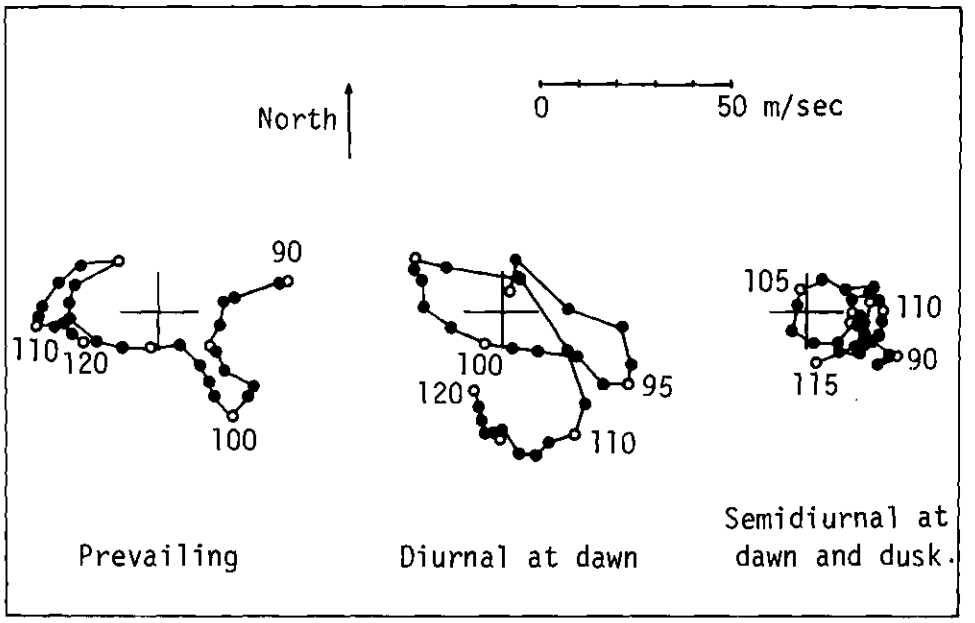

Figure 11. The Computed Prevailing Wind, Diurnal Tide at Dawn, and Semidiurnal Tide at Dawn or Dusk. The Magnitude and Direction of the Wind Vectors are Represented by Lines Drawn from the Crosses in Each Figure to the Individual Dots.

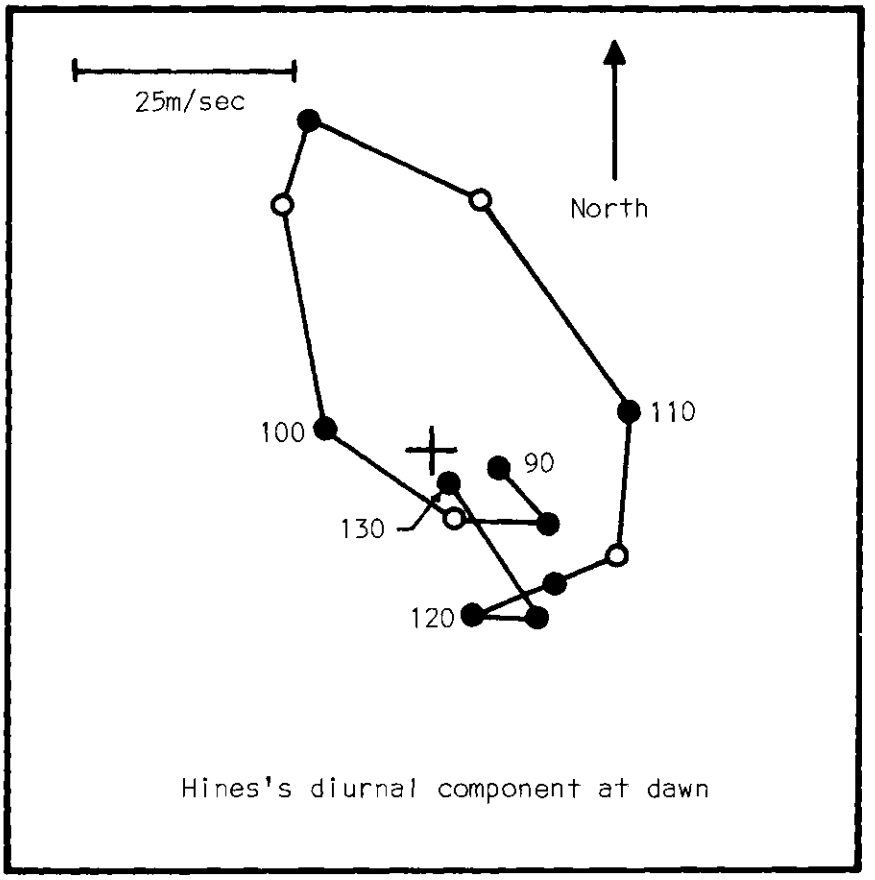

Figure 12. The Diurnal Tide at Dawn, as Computed by Hines [1966].

For calculations of the wave length, the winds can be plotted in more convenient form than that used in Figure 11. Figure 13 shows the wind heading versus height for the computed prevailing and diurnal tide, and Figure 14 shows the computed northward and eastward components of the winds. Note that in Figures 13 and 14 the diurnal tide is represented in its dusk phase rather than the dawn phase shown in Figure 11. The result represented by equation III-5 shows that the wave length may also be estimated from a graph of the wind speed squared versus altitude. Figure 15 gives such a graph for the calculated prevailing and tidal winds. A discussion of the results presented in Figures 11 through 15 will be given in the following section.

Discussion of Results

Prevailing Wind. The observed values of the deduced prevailing wind could perhaps be explained by the assumption that this wind is in geostrophic balance. This assumption would lead to assumed pressure and temperature gradients directed in a similar fashion to those discussed by Hines [1966]. However, the appearance of the graphs of the deduced prevailing wind, especially as shown in Figure 14, indicates that these observations can most easily be explained in terms of some wave phenomenon. Unfortunately, since the exact source of the assumed wave motion is not known, no comparison between computed and theoretical wave length can be made for the prevailing wind. Further study of the possible oscillation should be made before any explanation is attempted. Recently, a similar oscillation with a vertical wave length of about 26 to 28 km has been observed in the prevailing

component of meteor winds [Roper, private communication].

The wave length of the assumed wave phenomenon responsible for the computed prevailing wind can be estimated by a subjective analysis of the component plot of Figure 14 and the speed squared graph of Figure 15 (by the use of equation III-5). This wave length can be determined more objectively from the observed change of prevailing wind heading with altitude shown in Figure 13 and from a correlation analysis of the components plotted in Figure 14. Table 1 gives the wave length values computed by these four methods. The average prevailing wind wave length is seen to be 27 km ± 5 km rms. It will be seen later that this wave length is not significantly different from the vertical wave length obtained for the dominant propagating diurnal mode. Due to the errors brought about by the former assumptions, one may suggest that this oscillatory motion of the prevailing wind is actually not real but is just part of the diurnal wind that has been extracted as the prevailing wind. An analysis of this hypothesis will be made later in the section on the diurnal mode.

Figure 15 shows that the magnitude of the prevailing wind decreases with altitude. This decrease may be the result of viscous damping of the wave phenomenon responsible for the observed prevailing winds.

The phase difference between the northward and eastward prevailing components can be determined from a subjective analysis of Figure 14 and, more objectively, by cross correlation of the computed values of these components. The phase difference can also be estimated from the magnitude of the oscillations in the speed squared graph of Figure 15

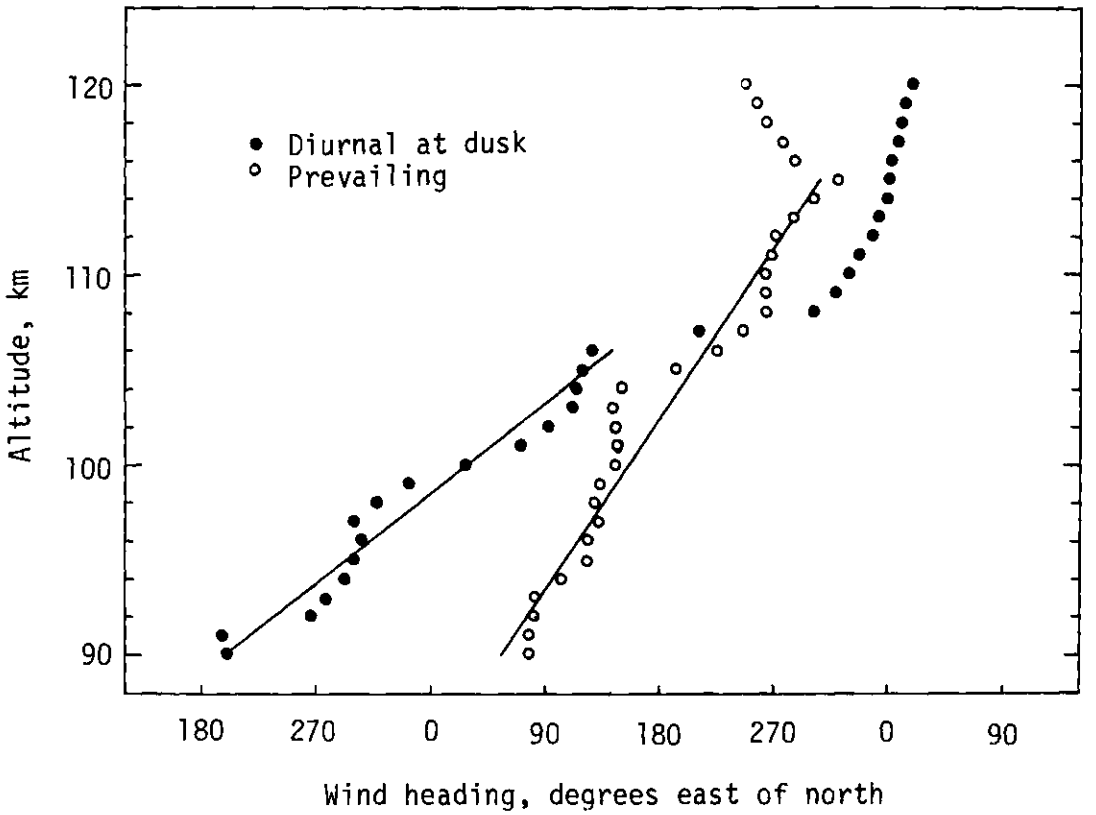

Figure 13. Heading Versus Altitude for the Computed Prevailing and Diurnal Winds. The Straight Lines are Least-squares Fit of Data Over Indicated Altitudes.

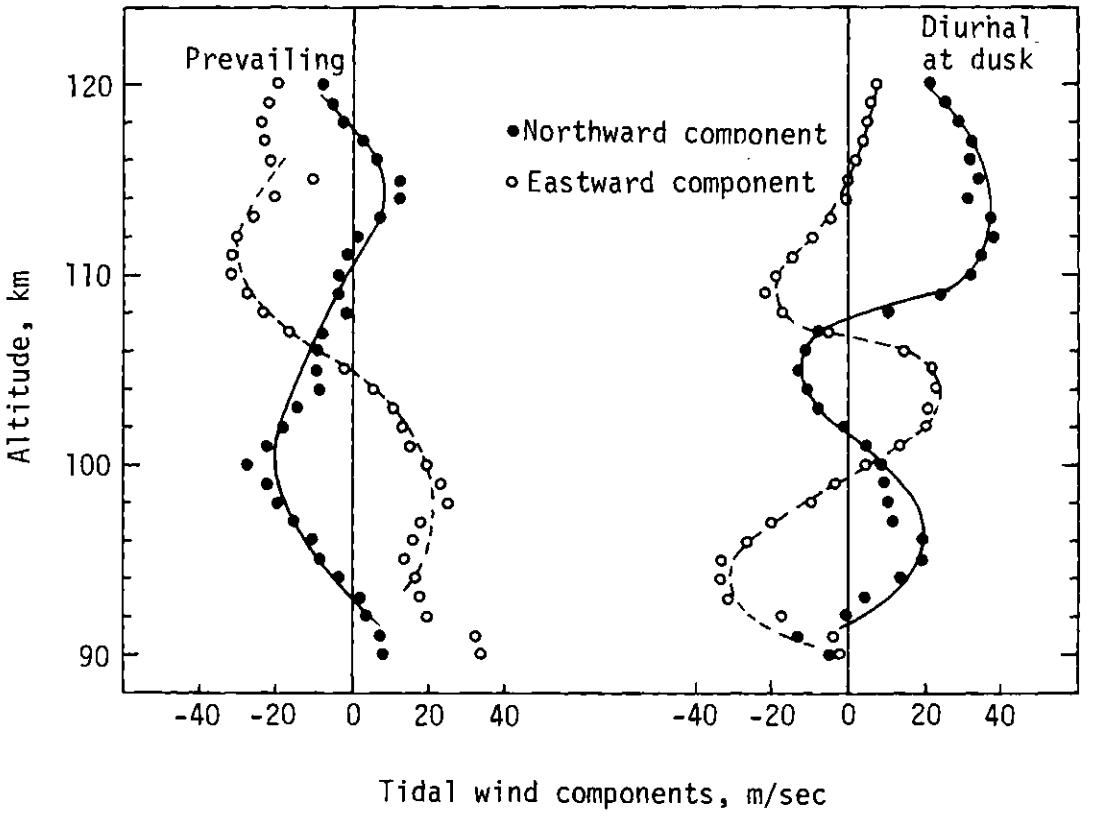

Figure 14. Northward and Eastward Components of the Calculated Prevailing Wind and Diurnal Tide at Dusk. The Curves Represent Subjective Fits of Approximately Sinusoidal Functions to the Wind Component Data.

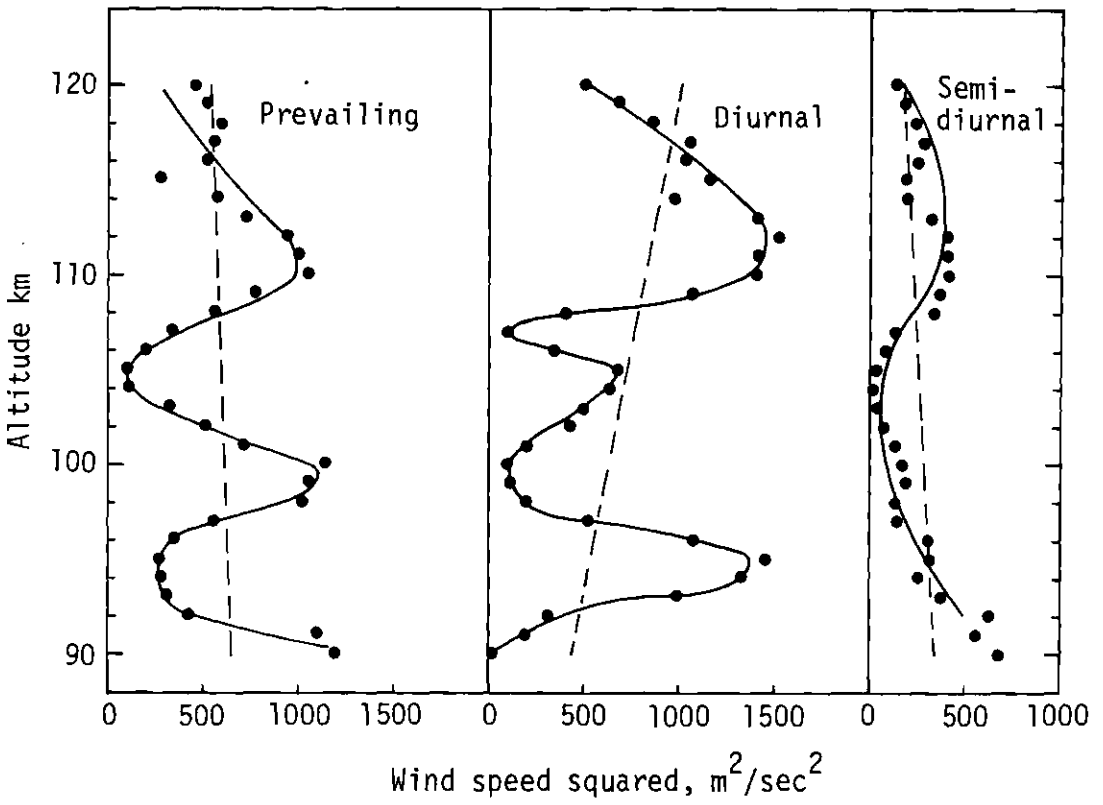

Figure 15. The Wind Speed Squared as Computed for the Prevailing, Diurnal and Semidiurnal Tidal Winds.

Table 1. Wave Lengths of the Prevailing and Diurnal Winds in the 90 to 120 km Region.

Wave Length Determined From	Prevailing Wave Length, km	Diurnal Wave Length, km
Heading	32	19
Components	27	18
Correlation	30	19
Speed Squared	20	18
Average	27	19

by the use of equations III-5 and III-7. Table 2 gives values of the prevailing component phase difference as computed by these three methods. The average phase difference is seen to be 123° ±8° rms. Figure 13 shows that the prevailing wind has a clockwise rotation with altitude between 90 and 115 km.

Diurnal Tide. The computed diurnal tide provides the least ambiguous results of the analysis because the calculated magnitude is large enough to be significant with respect to the computed probable errors and the deduced wave length may be compared with both tidal theory and the value previously determined by Hines [1966]. The computed diurnal wave length can be determined by the same methods discussed in the previous section. Table 1 gives the calculated diurnal wave length. The average value is 19 ± 1 km rms. This value is in agreement with Hines' value of 20 ± 3 km and the theoretical value for the (1,3) tidal mode in the 90 to 120 km regions, as shown in Figure 2.

Hines has mentioned that meteor measurements of the diurnal tide do not show a change of phase with height in the 80 to 105 km altitude range. This was true only for early meteor work which had poor height resolution. More recent meteor results do show a phase progression for the diurnal tide in the 80 to 105 km region which is comparable to that shown in Figure 12 [Roper, private communication]. Figure 13 shows an almost linear increase of the diurnal wind heading between 90 and 107 km.

At altitude 107 km, a sharp phase shift is observed and afterwards the phase remains almost constant. Figure 12 shows that the diurnal tide data of Hines also exhibits a near constant phase in the

Table 2. Phase Difference $\phi = \phi_n - \phi_e$ Between the Northward and Eastward Components of the Prevailing and Diurnal Winds in the 90 to 120 km Region.

Phase Difference Determined From	Prevailing Phase Difference, degrees	Diurnal Phase Difference, degrees
Components	126	123
Cross-correlation	112	110
Speed Squared	131	126
Average	123	120

115 to 130 km region. These constant phases might be explained, as Hines pointed out, by a severe damping of the diurnal tidal energy at these altitudes.

Figure 15 shows that the magnitude of the diurnal tide increases only slightly in the 90 to 120 km region. The theory of atmospheric tides requires that if the kinetic energy of the wind motion remains constant with height, then the rate of increase of tidal wind speed with height should be governed by the relation ρu^2 = constant, where u is the wind speed and ρ is the atmospheric density. As the height increases from 90 to 120 km, ρ falls by a factor of 140 [U. S. Standard Atmosphere, 1962]. However, the increase of the speed squared over the same height interval is only about twofold. This slow increase of the diurnal speed magnitude may be attributed to viscous damping of the tidal energy and supports the significance of the observed constant diurnal phase above about 110 km.

As mentioned before, the computed diurnal vertical wave length is not significantly different from the computed vertical wave length of the prevailing wind. Thus, the possibility should be examined that the oscillations in the prevailing wind are not real and have been transferred from the diurnal tide by means of the errors involved. The largest error in the data is caused by the actual averaging of individual wind profiles into the different time groups. However, it is very doubtful that this error will contribute very much to the oscillatory motion of the prevailing wind because the

process of averaging the wind profiles would tend to average out the oscillatory errors. Then the errors caused by the assumptions of the analysis (time difference, circular and clockwise motion of the diurnal components, etc.) should be the most probable cause of the possible transfer of oscillatory motion. However, the sum of all these errors amounts to only about 4 m/sec. In comparison, the amplitude of the prevailing wind oscillation is about 19 m/sec. Therefore, the observed oscillation in the prevailing wind appears to be valid.

The phase difference between the northward and eastward diurnal components may be measured by the same methods discussed in the previous section. Table 2 shows the measured values of this phase difference. The average value is 120° ± 7° rms. This shows that the observed phase difference is apparently significantly different from the value of 90° predicted for a single mode of oscillation by tidal theory. This result indicates that the diurnal wind may be composed of a superposition of two or more modes of oscillations. However, this conclusion cannot be final because the effects of viscous damping and the nonlinear velocity terms, which were neglected in the linearized tidal theory, may tend to increase the phase difference also.

Figures 11 and 12 provide a comparison between the diurnal tidal measurements of Hines [1966] and those presented here. These data have a number of similarities in addition to the comparable wave lengths already discussed. Both figures show that the diurnal wind pattern is approximately elliptical over much of the 90 to 120 km altitude region, with the semi-major and semi-minor axes of the ellipse being about 30 and 15 m/sec in both cases. The elliptical pattern of

both figures appears to be tilted with respect to the coordinate axes (indicating a component phase difference of something other than 90°). However, there are also differences between Hines' diurnal tide data and that presented here. Hines' computed diurnal wind headings are consistently larger than those presented here, by about 45°, over the 90 to 107 km region. Also, there is an abrupt change in phase at altitude 107 km in Figure 11; whereas the phase varies smoothly throughout the height range 90 to 120 km in Figure 12. Some of these differences may be due to the different latitudes involved and/or a different seasonal bias in the average winds used to compute the tides. It should also be noted that if the probable error circles were included in Figures 11 and 12, it would be possible to fit quite different ellipses (or even circles) to the data in these figures.

Semidiurnal Tide. Unfortunately, the computed magnitude of the semidiurnal component is approximately equal to the "probable error." Therefore, values of the semidiurnal vertical wave length and phase difference are incalculable. The only safe deduction that can be drawn from present analysis about the semidiurnal component is that the magnitude is small compared to diurnal and prevailing wind (less than 18 m/sec) in this altitude range. It must also be kept in mind that the data used in this analysis are heavily biased toward the fall. Hence, the small computed magnitude of the semidiurnal component may only indicate that it is small during this season. This result agrees well with the suggested seasonal variation of the diurnal and semi-diurnal wind by Roper [1966] (maximum diurnal tide in Fall and Spring and minimum diurnal tide in Winter and Summer, the reverse for the

semidiurnal tide).

If, by chance, the probable errors were estimated too large and one attempted a determination of the vertical wave length from the present data, then from Figure 15 it can be seen that the wave length would be estimated to be about 60 km. This value lies between the expected wave lengths of the (2,2) and (2,4) modes.

Summary of Geometrical Analysis

Table 3 shows a summary of the experimental results of the geometrical analysis and their comparisons with the theoretical predictions of Chapter II. It is seen that the sense of rotation of the wind vector and the vertical wavelengths agree very well with theory. The phase difference of diurnal component velocities is observed to be significantly larger experimentally than that predicted for a single mode of oscillation by theory. Also, the velocity amplitude of the diurnal and semidiurnal oscillation is observed to be very much less than the value predicted by theory. However these discrepancies may be attributed to the effects of viscous damping and the nonlinear velocity terms. Both processes, which were neglected, would tend to reduce the energy content of the atmospheric oscillations and hence would decrease the velocity amplitudes.

Groves Analysis

One of the main difficulties with the geometrical method of analysis is that it averages the wind data into time groups and then uses a mean time for all the wind data. It would be much better to use the actual time of each wind datum if possible. Also another problem

Table 3. Summary of the Geometrical Analysis

Oscillation	Sense of Rotation	Wavelength	Phase Difference	Velocity Amplitude
Prevailing				
a) Experimental	Clockwise	27 ± 5 km	123° ± 8°	23 m/sec
Diurnal				
a) Theoretical	Clockwise	20 km	≃ 90°	100 m/sec
b) Experimental	Clockwise	19 ± 1 km	120° ± 7°	19 m/sec
Semidiurnal				
a) Theoretical	Clockwise	40 km [(2,4) Mode] or 100 km [(2,2) Mode] at 110 km altitude	≃ 90°	≃ 100 m/sec
b) Experimental	Clockwise	≃ 60 km	- -	15 m/sec

is the small amount of data available.

G. V. Groves [1959] has developed a method of analysis which seems to have alleviated both of these problems. His method is described briefly in Appendix B. It is a generalization of the least-squares procedure and refers the actual times of the wind data to a time period equal to the period of investigation.

The Groves analysis has been successfully applied to meteor wind data obtained at Adelaide, Australia by Roper and Elford [1965]. Roper and Elford collected data for each month in 1961 and applied the Groves analysis to each month's data. No one has yet published a Fourier analysis of wind data obtained from the chemical releases from rockets using the Groves analysis. For this purpose a variation of the Groves analysis was adapted to analyze the chemical release wind data and was applied to essentially the same wind data that was used for the geometrical method of analysis.

Energy Spectrum

In addition to calculating the velocity amplitudes and phases of the 24 hour harmonics, the Groves analysis also permits the calculation of an energy spectrum function over a large range of periods. Velocities for each hour of the day and velocity amplitudes for winds with periodicities of 6 to 46 hours were calculated. These quantities were calculated for a height range from 90 to 140 km. Computed amplitudes with calculated errors of more than about 10 m/sec were considered unreliable. Thus usable data were obtained only for the height range 95 to 135 km.

The distribution of the wind energy with the period of the wind

motion is shown by plotting graphs of the sum of the squares of the amplitudes of the zonal and meridional velocity components of the periodic wind versus periodicity for each altitude. A sample graph for altitudes 95 km and 115 km is shown in Figure 16. The ordinate of this graph has units of velocity squared or energy per unit mass. The graphs for the other altitudes appear in Appendix G.

Table 4 shows the significant energy bearing periods obtained from these energy spectrum graphs. It is seen from this table that, as expected, the 24-hour tidal harmonics carry a large portion of the energy. However from this analysis, there is also a disturbingly large amount of energy carried by periods near 20 and 33 hours. Roper and Elford [1965] also observed a strong peak near the 20 hour period in their analysis of the month of September, 1961. They mentioned that this period was close to the value for the period of inertial oscillations in the atmosphere at the latitude of Adelaide (35°S). However, the value for the period of inertial oscillations at the latitude of Eglin AFB, Florida is about 24 hours and thus these oscillations would be indistinguishable from the 24 hour tide.

Possible explanations for the nonharmonic oscillations may be: (1) the oscillations are true atmospheric oscillations which are independent of the 24 hour harmonic oscillations, (2) the oscillations are caused by effects of the nonlinear velocity terms acting on the 24 hour harmonic oscillations, or (3) the oscillations are caused mathematically by a process known as aliasing.

As to the first possibility, atmospheric theory has not presented any reason to suspect any atmospheric motion other than the 24 hour

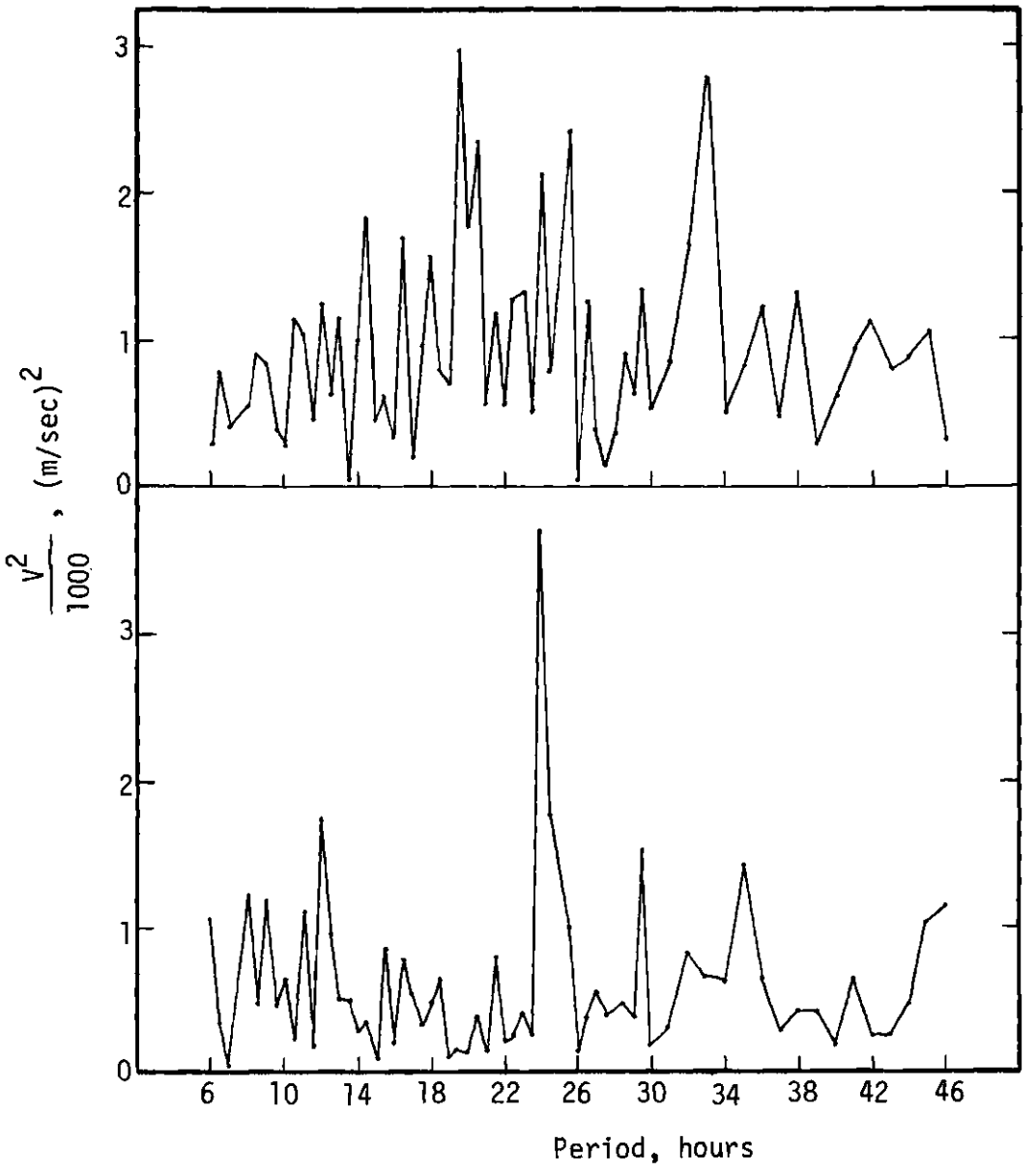

Figure 16. Energy Spectrum of Periodic Motions at 95 km (Lower) and 115 km (Upper).

Table 4. Significant Energy-bearing Periods. The Significant Periods Are Taken as Those Peaks in the Energy Spectrum Graphs in Which the Energy is Greater Than the Average Energy Plus One and a Half Standard Deviations. The Columns Designated as "Number" Shows the Number of Height Levels for Which an Energy Peak at the Corresponding Period was Significant.

Period (hours)	Number	Period (hours)	Number
8	2	24	4
12	1	25.5	3
13	1	27.5	1
16	1	29.5	1
16.5	1	33	6
19.5	8	36	3
20.5	4	40	2
23	3	41	1
23.5	2		

hour harmonics unless the motion had very large periods (planetary waves with periods of a few days and seasonal variations) or very small periods (turbulence and gravity waves). One expects to find the 24 hour harmonic motions because of the action of the systematic thermal and gravitational forces of the sun and moon on the atmosphere. So, the first possibility seems unlikely as an explanation of the nonharmonic motions.

Explanation number two presents some interesting possibilities but the mathematics of nonlinear systems prevent the full understanding of the effects of the nonlinear terms. Shiren [1965] presents a simplified theory of traveling-wave ultrasonic nonlinear interactions in which he hypothesized that nonharmonic motion could be obtained by the effects of nonlinear terms if proper resonance requirements were met. For an example, suppose in our case that there was a very small, but not zero, atmospheric oscillation with a period of 48 hours. Then under proper resonance conditions, the 24 hour period and the 48 hour period could interact through the nonlinear velocity terms to form the 16 hour periodic oscillation by the addition of the two frequencies. The 16 hour motion happens to be one of the periodic motions given in Table 4. The other nonharmonic motions in Table 4 could conceivably be formed in a similar manner. Although explanation two is an interesting possibility and has far-reaching effects if it were true, further theoretical study must be made before any conclusive results about it can be drawn.

If the nonlinear velocity terms were responsible for the nonharmonic motions, then by Figure 30 in Appendix A the nonharmonic motions

would be expected to become appreciable at about 100 km altitude and to increase in importance above this height. Figure 17 shows the speed squared curve versus height for the 20 and 33 hour periods. The motion for these two periods appear small below a height of 105 to 110 km and then rapidly increases in magnitude above this altitude. Data for the 16 and 36 hour periods show similar results and hence supports the possibility of the influence of the nonlinear terms.

Explanation number three also presents a very likely possibility. The process of aliasing is a mathematical error which is brought about by too few data points. If one is trying to Fourier analyze too few data points, then extraneous periodic motions can be fitted to the data which are correct mathematically but are entirely wrong physically. The amount of data which were used in the present analysis (about 50 wind profiles) would seem to be enough to prevent the process of aliasing. However, a true test would be if the results of analysis are changed significantly as more wind profiles are added to the analysis.

It is interesting to note that practically all of the non-harmonic motion displayed in Table 4 can be accounted for by addition or subtraction of the harmonic periods. This seems peculiar because one would expect addition and subtraction of frequencies rather than the periods.

The remainder of the explanation of the results of the Groves analysis will be concerned only with tidal harmonics.

Tidal Winds

The variation of the square of the velocity amplitudes is shown

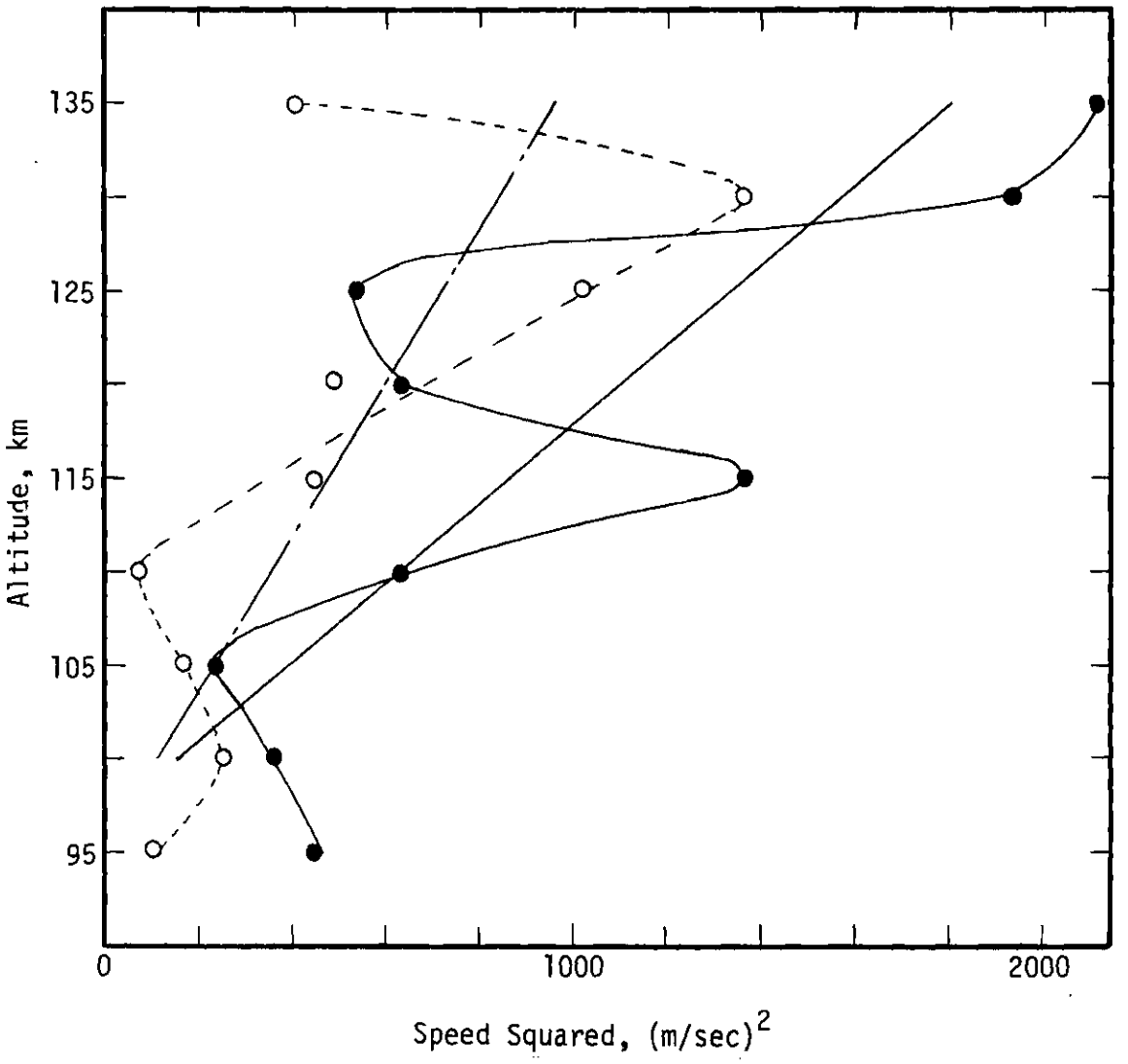

Figure 17. The Speed Squared Versus Height for the 33 (Solid Dots) and 20 (Open Circles) Hour Periods. The Straight Lines are Least Squares Fit of the Curves Over the Shown Height Range.

in Figures 18, 19 and 20 for the 24, 12 and 8 hour periods respectively. One must remember that data presented here were computed from wind data collected over a period of about three years and thus these results represent some sort of an average over this time period. Furthermore, the data presented here are heavily biased toward the early and mid-fall period with 69% of all the wind data coming from times between the dates September 23 and November 18. Thus the results presented here would be expected to agree relatively well with the September, October and November data of Roper and Elford [1965] as is shown.

It should be noted that the Roper and Elford data show rather well the seasonal variation of the 24 hour and 12 hour period suggested by Roper [1966] (i.e. maximum amplitudes of the 24 hour tide in fall and spring, maximum amplitudes of the 12 hour tide in summer and winter). The data presented here show that the 24 hour period is stronger than the 12 hour period. Since the data are biased toward late September and October, this would seem to uphold the suggested seasonal variation of the two tidal components.

Figures 18 and 19 show that the velocity squared values stay rather constant with altitude from 100 km to 135 km for the 24 hour and 12 hour periods. Since the density is decreasing rapidly, this shows that energy is being dissipated from these tidal components. However, Figure 20 shows that the velocity squared values for the 8 hour period have a definite increase. Figure 21 shows a semi-log plot of ρV^2 versus height for the 24, 12 and 8 hour periods, where ρ is the density obtained from the U. S. Standard Atmosphere Supplements, [1966] tables for 30° N latitude in July. Kochanski [1964] suggested a variation of

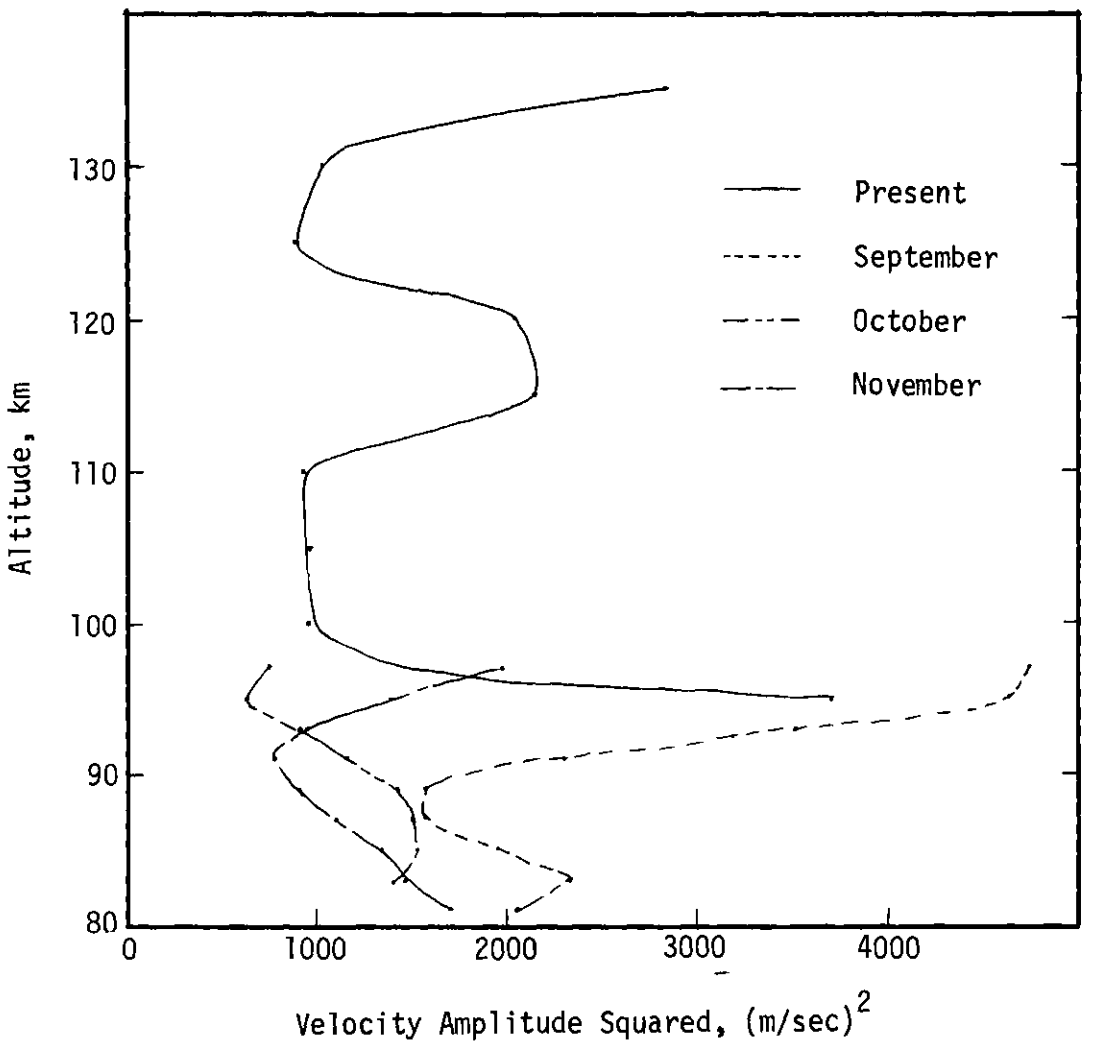

Figure 18. The Square of Velocity Amplitude Versus Height For the 24 Hour Period. Data For the Months of September, October and November of 1961 by Roper and Elford [1965] are Shown for Comparison.

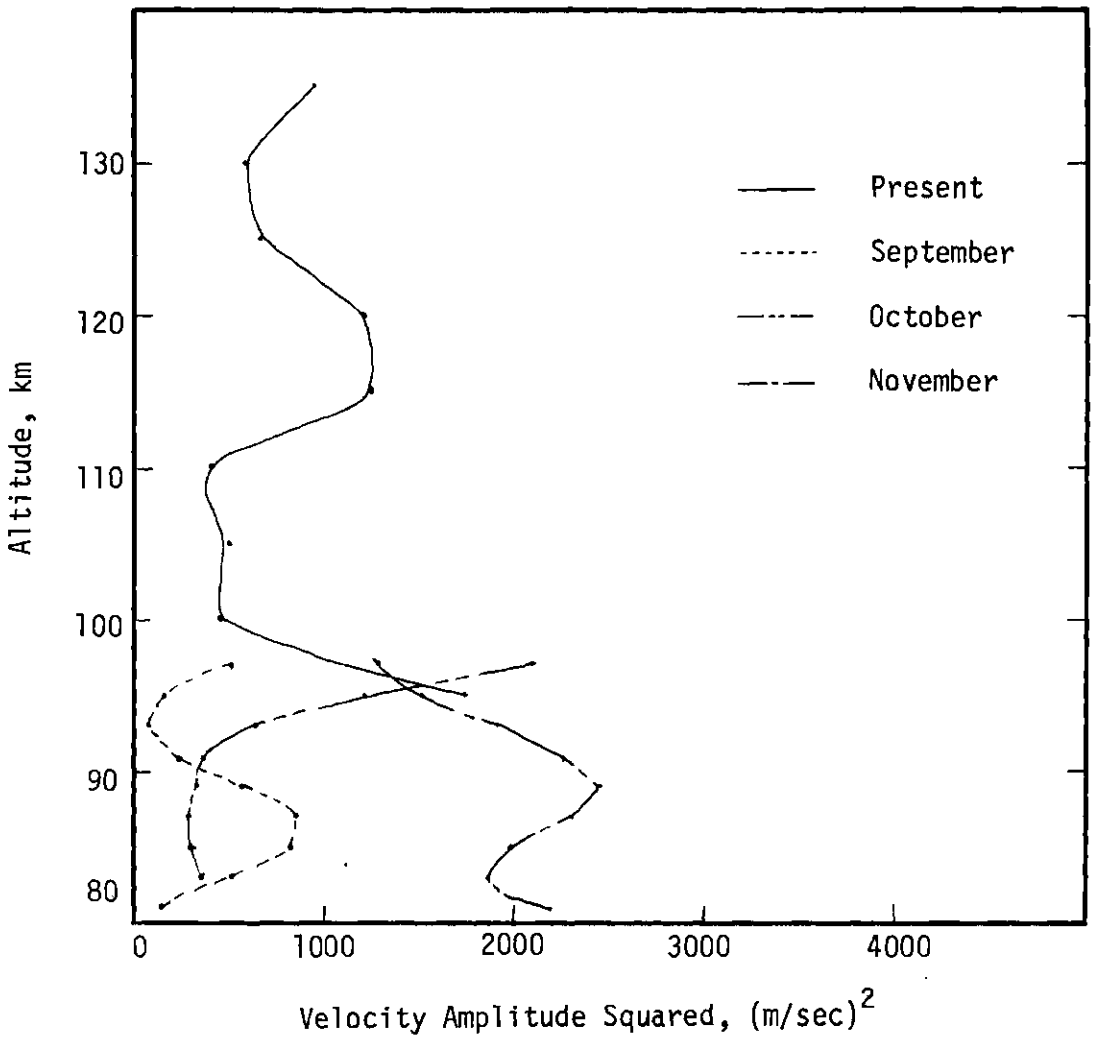

Figure 19. The Square of Velocity Amplitude Versus Height for the 12 Hour Period. Data for the Months of September, October and November of 1961 by Roper and Elford [1965] are Shown for Comparison.

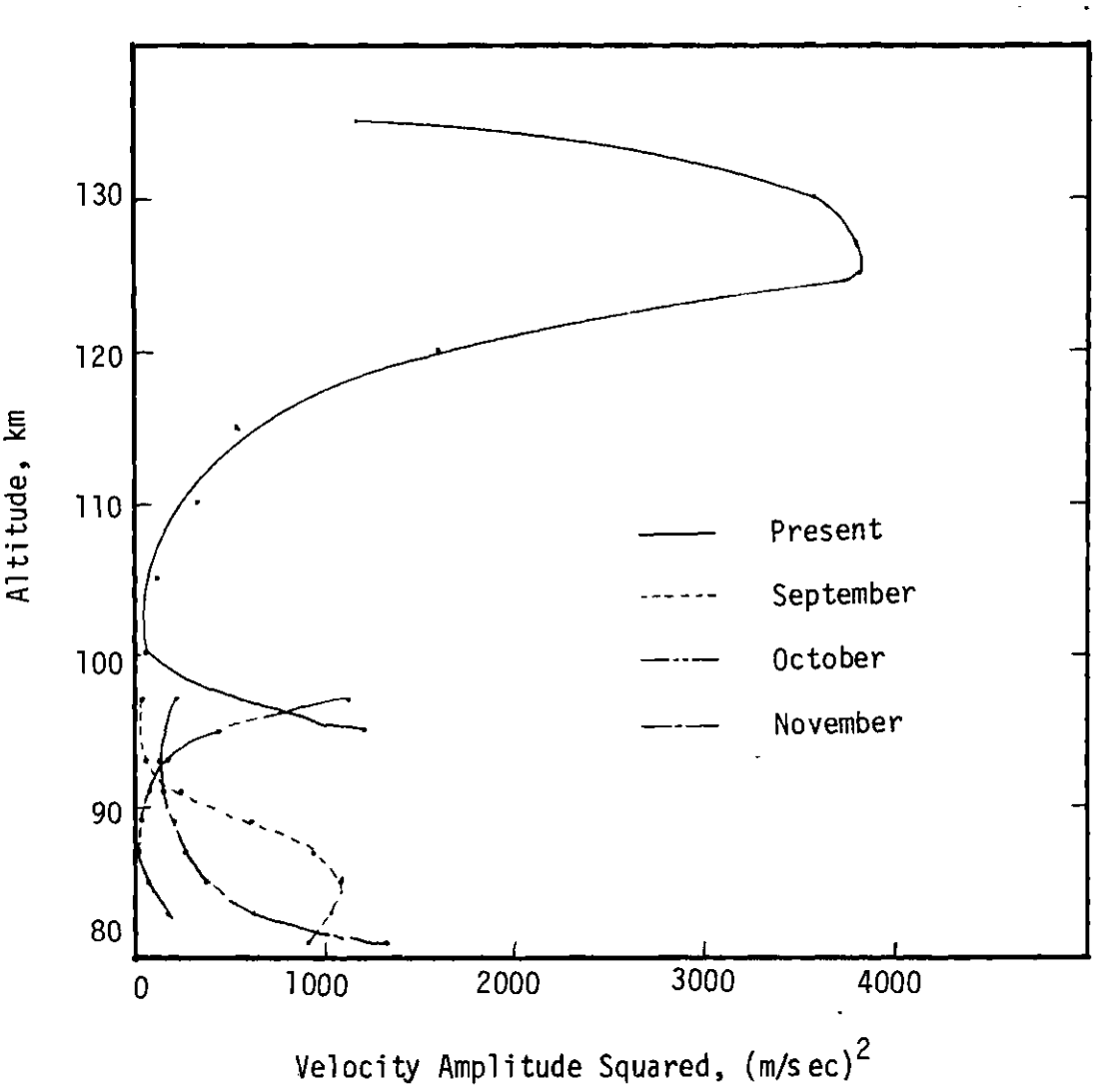

Figure 20. The Square of Velocity Amplitude Versus Height for the 8 Hour Period. Data for the Months of September, October and November of 1961 by Roper and Elford [1965] are Shown for Comparison.

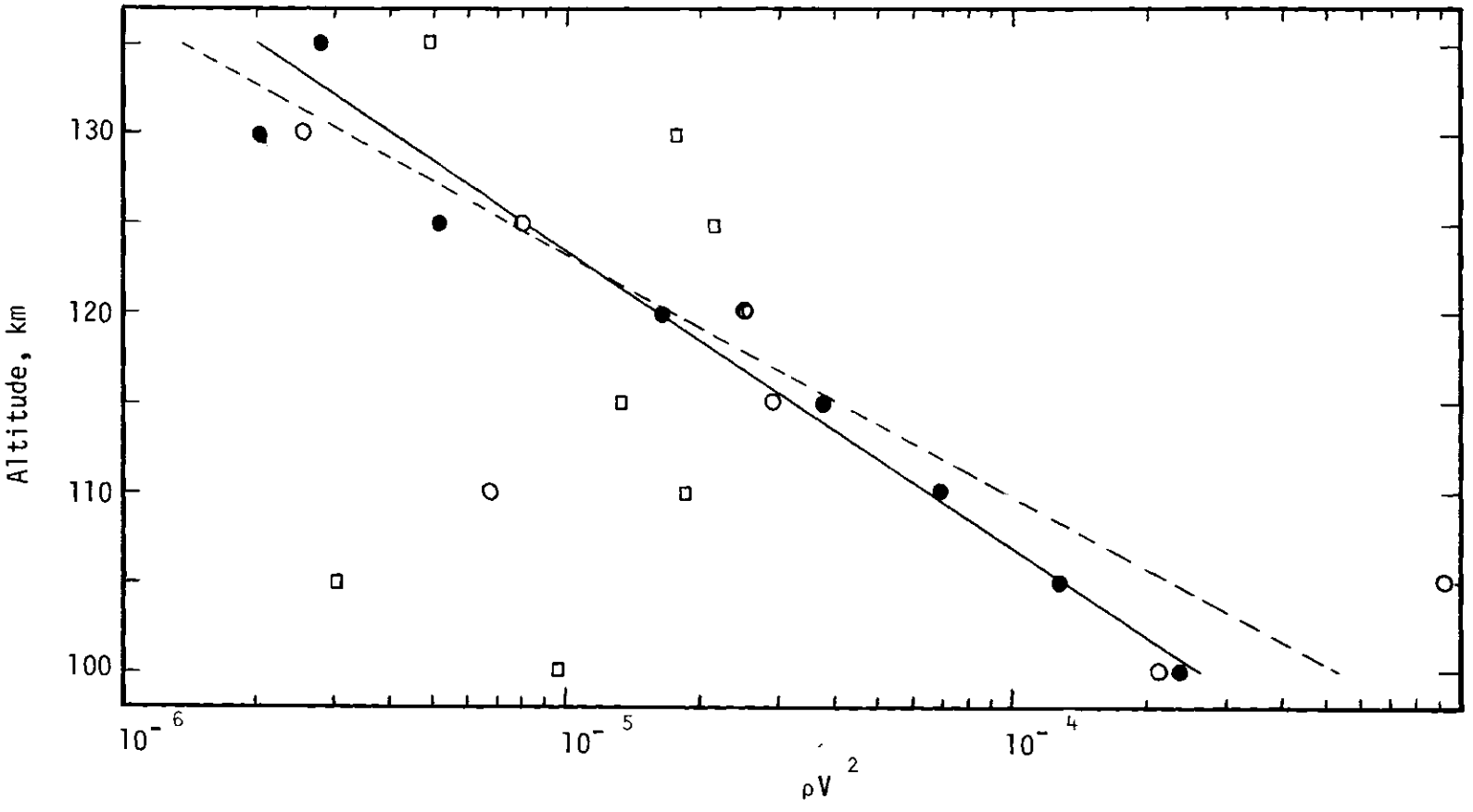

Figure 21. Semi-log Plot of Energy Versus Height for the 24 (Solid Dots), 12 (Open Circles) and 8 (Squares) Hour Periods. The Two Straight Lines are Subjective Fits of the 24 and 12 Hour Periods.

ρV^2 with height to be

$$\rho V^2 \sim \exp(-z/z_0) \qquad \text{(III-12)}$$

for wave motion which he attributed mostly to internal gravity waves where z_0 is a characteristic length of the dissipation. Internal gravity waves are small scale motions which were postulated by Hines [1960] to be important even in the height region around 100 km altitude. The gravity waves have vertical wavelengths of the order of 12 km near the 100 km region and have very small periods in comparison with the tidal harmonics. The main forcing function of the gravity waves is the force of gravity.

The values of z_0 calculated by the Groves' method for tidal wave motions are shown in Table 5. Notice that the calculated z_0 value for the 8 hour period is approximately infinite. Thus if one can accept the results of Figure 20, then the 8 hour period acts as if it has no dissipative forces acting on it in this height range.

For comparison, z_0 values which were calculated from data from Kochanski [1964], Roper [1966], and the geometrical method are shown in Table 5 also. Note that the z_0 values from the 4 sets of data agree very well with each other with the exception of the 12 hour period from Roper's data. However, Roper's data were for the month of June, 1961 only and this is during the season of the year for which the 12 hour period is thought to be strongest. Thus this calculation of z_0 for the semidiurnal component may not be good for any other time of the year.

Table 5. Calculated Values of the Characteristic Length z_0.

Analysis	z_0	Effective Height Range	Reference
Kochanski			
1) Gravity Wave Motion	7.6	70-140 km	Kochanski [1964]
Meteor Data Groves's Method			
1) 24 hour period	6.5	83-97 km	
2) 12 hour period	∞		Roper [1966] and Justus & Roper [1968]
Chemical Release Data Geometrical Method			
1) 24 hour period	5.1	90-120 km	Woodrum and Justus [1968]
2) 12 hour period	5.0		
Chemical Release Data Groves' Method			
1) 24 hour period	7.3	95-135 km	Present Analysis
2) 12 hour period	5.9		
3) 8 hour period	∞		

The actual zonal and meridional components of the prevailing, 24 hour, and 12 hour winds can also be obtained from the Groves' analysis. These components could be calculated for any hour of the day; but for convenience in comparing the results of the present analysis with other results, winds at 6 P.M. were taken. The component winds of the prevailing and tidal winds are shown in Figures 22 and 23. The prevailing wind in this case was calculated separately with each calculation of the tidal components. The three calculations agreed very well and hence, the average prevailing wind is shown in Figure 22.

Vertical wavelengths for the tidal and prevailing winds were calculated by three methods. Method one calculated the wavelength by considering the phase. The wavelength is the vertical distance required for the wind to rotate 360°. It should be noted that all the results showed that the tidal and prevailing winds rotate clockwise with increasing height.

Method two calculated the wavelength by subjective analysis of Figures 22 and 23. Method three calculated the wavelength by correlation analysis of the component curves in these figures. The averages of these results with the indicated standard deviations are shown in Table 6 under the heading of Groves Method. The standard deviations show a measure of the self consistency of each of the three methods but do not necessarily correspond to the actual possible error in each value.

Phase differences between the northward and eastward components of the tidal and prevailing winds were calculated by a subjective

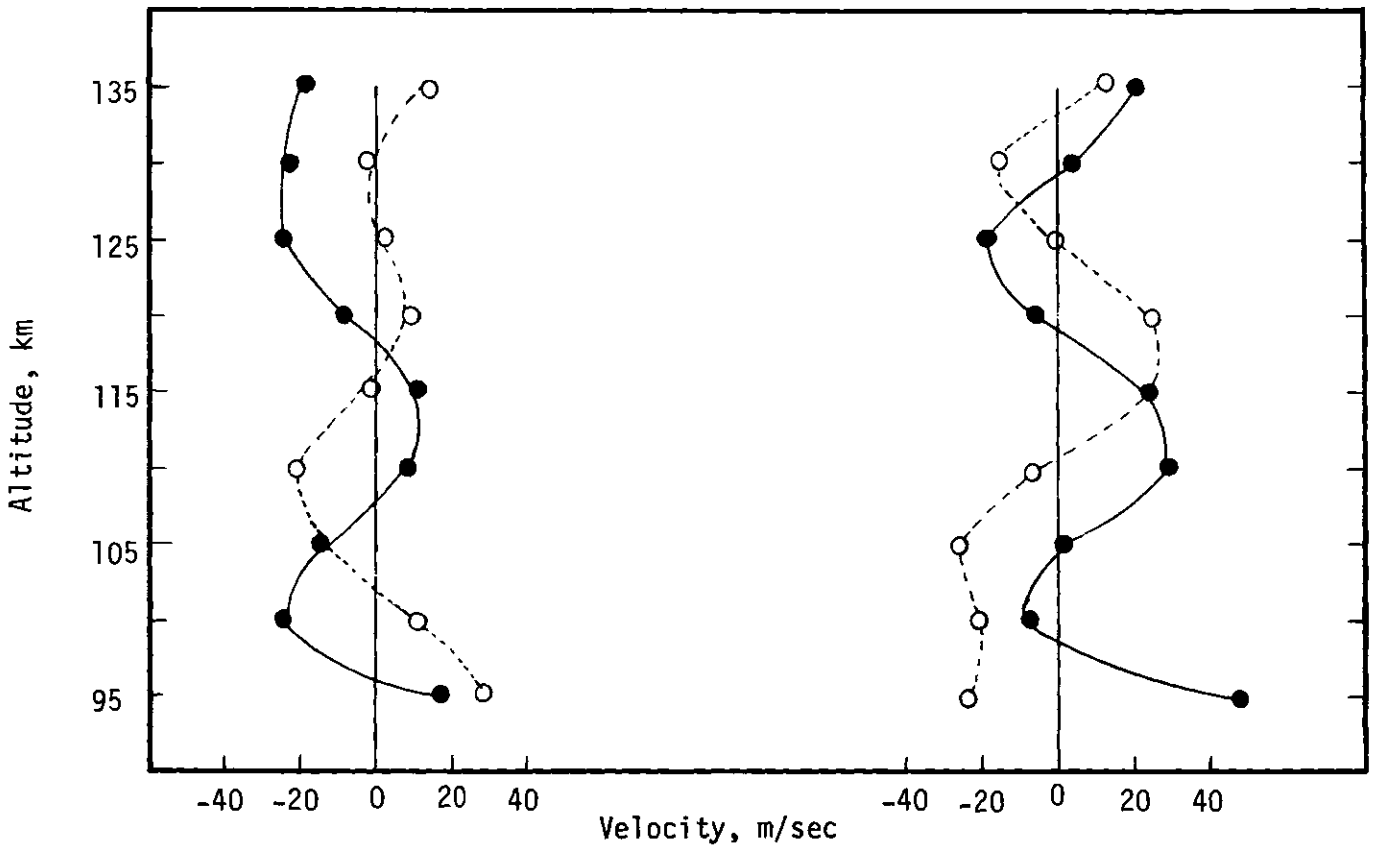

Figure 22. Calculated Northward (Solid Dots) and Eastward (Open Circles) Components of the Prevailing (Left Plot) and 24 Hour (Right Plot) Winds.

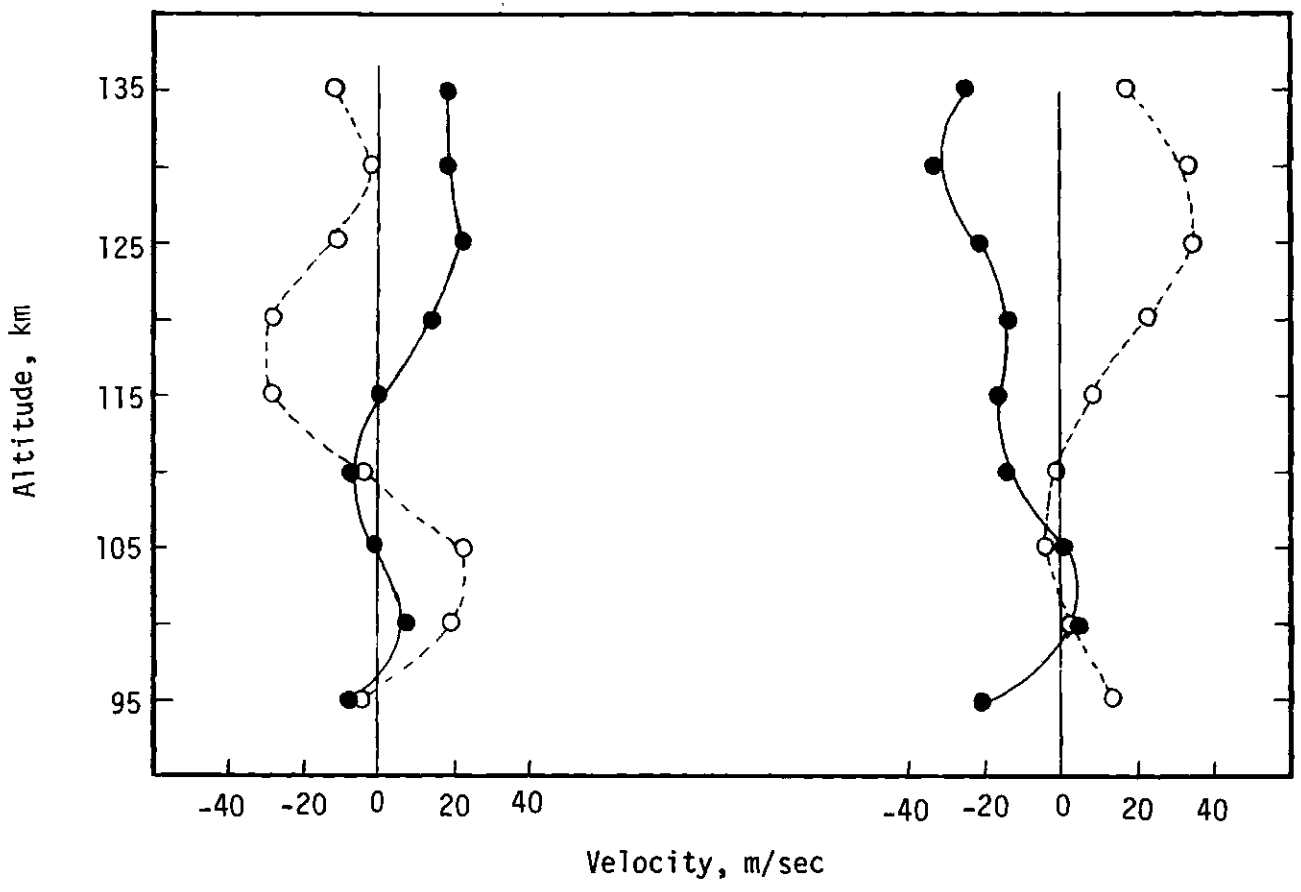

Figure 23. Calculated Northward (Solid Dots) and Eastward (Open Circles) Components of the 12 (Left Plot) and 8 (Right Plot) Hour Winds.

Table 6. Comparisons of the Calculated Wavelengths, Phase Difference, and Average Amplitudes.

Comparison	Geometrical Method	Groves Method
Wavelength		
(a) 24 hour	19 ± 1 km	25 ± 2 km
(b) 12 hour	≈ 60 km	36 ± 1 km
(c) Prevailing	27 ± 5 km	26 ± 4 km
Phase Difference		
(a) 24 hour	120° ± 7°	100° ± 11°
(b) 12 hour	- - - - - -	107° ± 3°
(c) Prevailing	123° ± 7°	102° ± 6°
Average Amplitudes		
(a) 24 hour	19 m/sec	23 m/sec
(b) 12 hour	≈ 15 m/sec	20 m/sec
(c) Prevailing	20 m/sec	20 m/sec

analysis and a cross correlation analysis of the component curves in the Figures 22 and 23. These values together with the values of the average amplitude of the tidal and prevailing winds are also shown in Table 6.

The 8 hour period is not considered in Table 6 because it is too small below an altitude of 120 km to extract any meaningful information about its wavelength and phase difference. The results of the Groves' analysis in Table 6 are compared with the results of vector analysis presented by the geometrical method. The two methods are seen to give very much the same results, especially for the phase differences and average amplitudes. The only significant difference between the two methods is in the calculated values of the 24 hour and 12 hour vertical wavelengths. However the 12 hour wavelength as calculated from the geometrical method is so approximate that it cannot be considered incompatible with the 36 km wavelength calculated by the Groves method.

There is a difference in the calculated wavelength for the 24 hour period, however. One possible cause for the difference could be the fact that the Groves analysis uses actual times for each wind datum whereas the vector method uses an averaged time for a group of wind data points. This would seem to indicate that the Groves method is better.

Theory predicts that for a nondissipative atmosphere the wavelength of the (1,3) mode of the diurnal tide is about 20 km, which agrees well with the results of the vector method. However, if dissipation occurs, as the results in both analyses show, then the

expected wavelength would be longer than 20 km. This seems to agree with the results of the Groves method. Further tidal analysis work will be needed to distinguish which of the two methods give the better results.

Variance

The experimental analysis thus far has been concerned with the very large scale motion of the atmosphere. It would also be interesting to see if some information could be obtained about the smaller scale oscillations. The "variance" curves of Figure 10 might give us this information.

As Hines [1966] has pointed out, the variance calculated from the averaging of wind profiles into different time groups could be produced by at least four processes: (1) irregular winds which are attributable to internal gravity waves, (2) day-to-day and seasonal variation of the systematic winds, (3) scatter introduced by the variation of rocket launch times within each group, and (4) additional systematic components such as eight-and six-hour tides, which are not accounted for in the geometrical method of tidal extraction.

By using the results of Kochanski [1964], Hines [1966] has divided his computed variance into a component produced by gravity waves and a component produced by other effects. Kochanski extracted "irregular" winds, which he identified as gravity waves, from a number of single wind profiles. He did this by inspection of the oscillations in the speed versus height curves. Hines has pointed out that Kochanski's method cannot identify and extract large scale gravity

waves which may be present and that the method is "subject to challenge" on the basis of subjective decisions which must be made in the analysis. The result expressed in equation III-5 also shows for a single mode that oscillations in the speed curves could be produced by unequal amplitudes of the northward and eastward tidal components and/or a phase difference between these components of something other than 90°. A superposition of different tidal modes could very well be a major contributor to the total winds. Hence, the total winds may also show oscillations in the speed curves due to the results of equation III-5. Thus, Kochanski's method would also be subject to challenge on the grounds of the results expressed by equations III-5 and III-7 with the possibility of $A \neq B$ or $\phi \neq 90^{c}$. So the results of Kochanski [1964] must be viewed with great suspicion. However, he calculated an amplitude of about 60 m/sec for oscillations due to gravity waves at about 105 km altitude. Hines [1966] calculated an average variance of about 65 m/sec.

The average variance for the P.M., midnight and A.M. curves of Figure 10 are 66, 64 and 52 m/sec respectively.

Velocity Difference

In an attempt to better establish the magnitude of the small scale oscillations, a further analysis was performed involving pairs of wind profiles. Two wind profiles, which have rocket launch times that are different by an amount of an integral multiple of a day plus or minus fifteen minutes, were subtracted from each other to give a velocity difference. Since the wind profiles have a time difference of an integral multiple of a day, then all contribution from the 24 hour tidal harmonic sequence should be excluded from the velocity difference.

So the velocity difference should be caused mostly by irregular winds which include gravity waves and the possible nonharmonic oscillations shown by the Groves analysis. Day-to-day variations of the systematic winds would also be included in the velocity difference but should play a minor role as compared with the irregular winds. Provided the velocity differences are taken over at most a few days interval then seasonal variations of the systematic winds should not be present to any significant extent in the computed velocity difference. Figure 17 shows the average speed squared of the 33 and 20 hour nonharmonic motion is about 900 m^2/sec^2. Figures 24 and 25 show that the average square of the velocity differences is about 8000 m^2/sec^2. Hence the nonharmonic motions should influence the velocity difference measurements in only a small way if any.

A total of 38 pairs of wind profiles were obtained for which the time difference within each pair extended from one day through fifteen days. Figures 24 and 25 show the plots of a 5 km average of the square of the calculated velocity differences versus the time difference in days. The indicated heights on these figures are the midpoint heights of the 5 km average. The straight lines are least square fits to the data points. The straight lines show that there is little or no significant increase in the amplitude of the velocity differences with an increase in the time difference. The reason for this can be seen by the following analysis.

Comparison With Correlation Analysis. The procedure of performing an average of the square of the velocity difference can be related to the calculation of the correlation function described in Appendix G

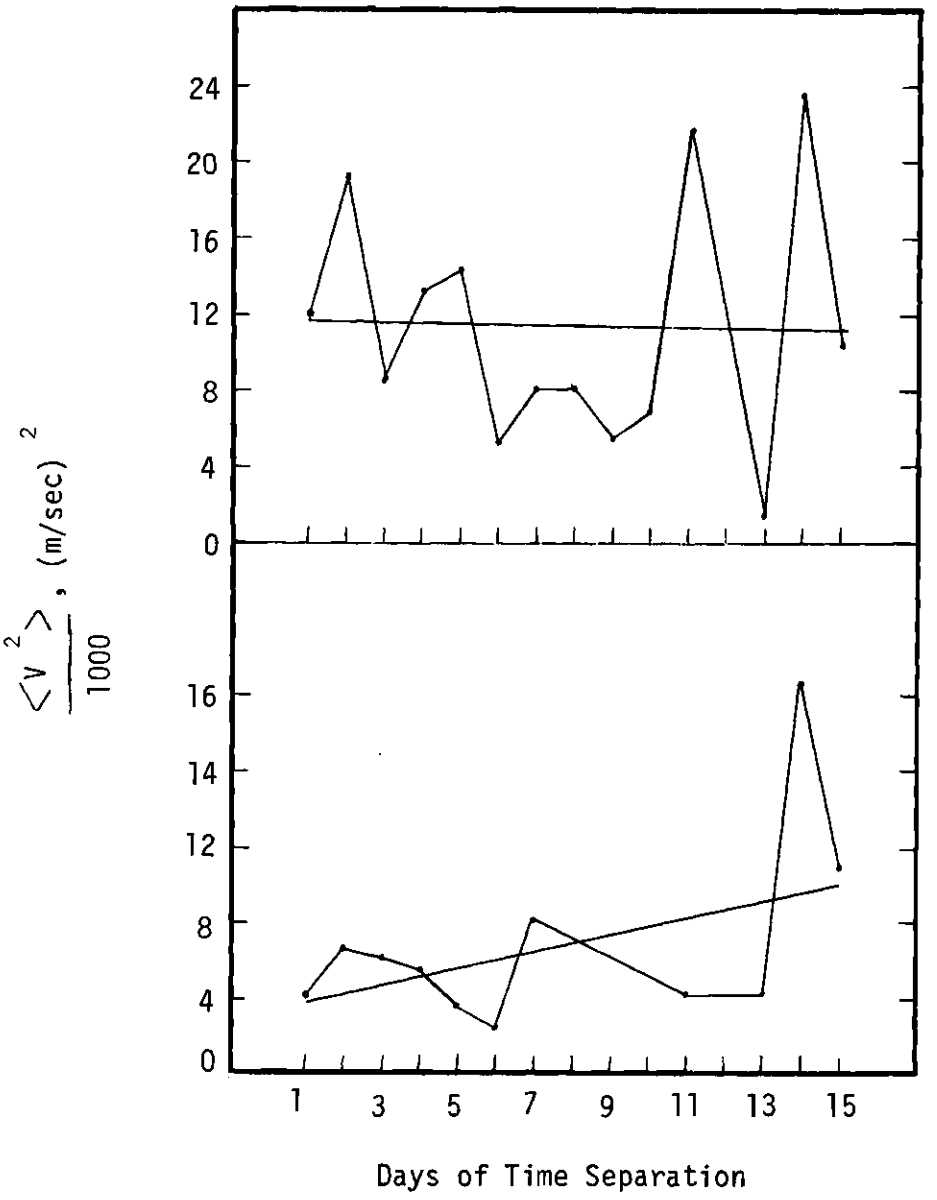

Figure 24. Square of the Velocity Difference Averaged Over a Five Kilometer Height Interval with the Midpoints of the Two Height Intervals at 97 km (Lower) and 102 km (Upper) Versus Days of Time Separation of the Wind Profiles. The Straight Lines are Least-squares Fits of the Data.

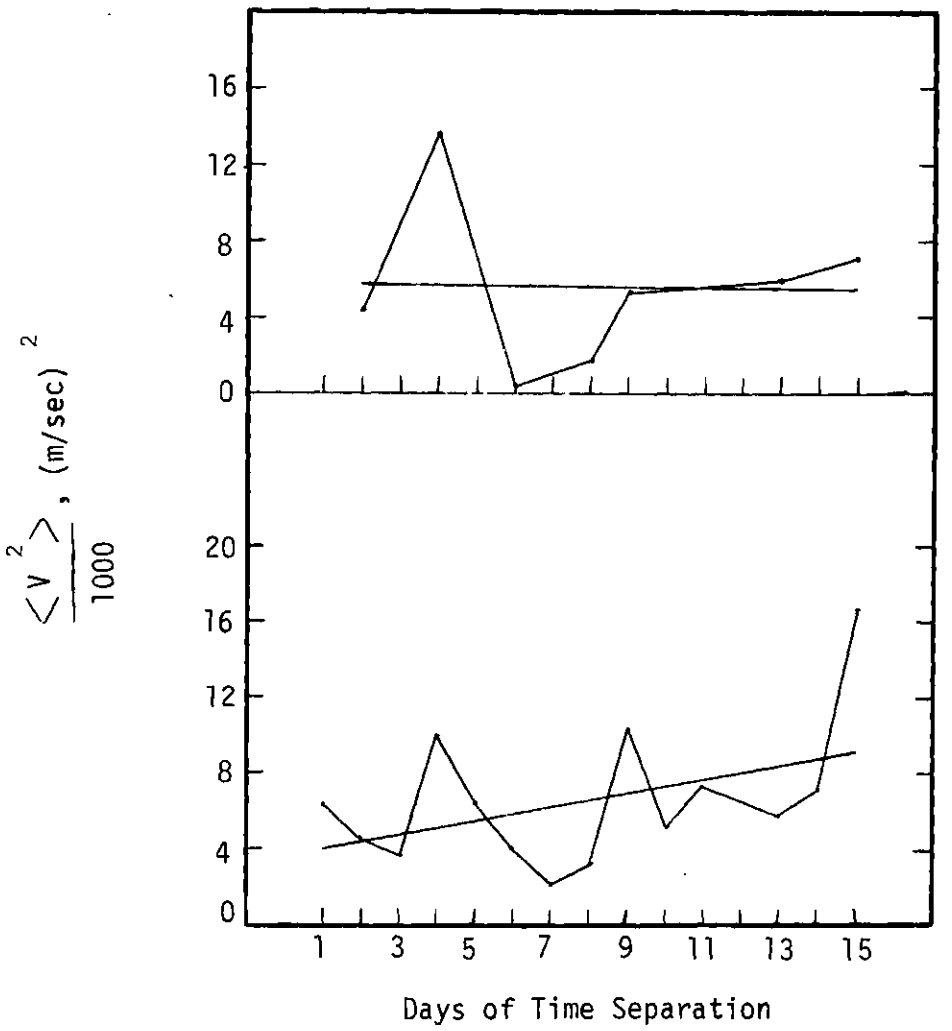

Figure 25. Square of the Velocity Difference Averaged Over a Five Kilometer Height Interval with the Midpoints of the Two Height Intervals at 107 km (Lower) and 112 km (Upper) Versus Days of Time Separation of the Wind Profiles. The Straight Lines are Least-squares Fits of the Data.

in the following manner.

$$V_d^2 = \langle [V(t) - V(t + \delta t]^2 \rangle \qquad \text{(III-13)}$$

where V_d is the velocity difference, t is time, δt is an integral multiple of a day and the angle brackets denote an average.

$$V_d^2 = 2 \langle V^2(t) \rangle - 2 \langle V(t)\, V(t + \delta t) \rangle \qquad \text{(III-14)}$$

where the average of the velocity squared is independent of time. By equation C-1, we get

$$V^2 = 2 \langle V^2(t) \rangle [1 - G(\delta t)] \qquad \text{(III-15)}$$

where $G(\delta t)$ is the correlation function.

Figure 26 shows a plot of $\dfrac{V_d^2}{2 \langle V^2(t) \rangle}$ versus period for the type of motions expected to be contained in the velocity differences. The solid curve gives the correlation function for a wind component with only one mode of oscillation. When the wind component is made up of oscillations with many different periods as are expected to be present in the velocity difference then the correlation function behaves like the dotted line. The other curve in Figure 26 represents the expected value of $\dfrac{V_d^2}{2 \langle V^2(t) \rangle}$ for the velocity difference data.

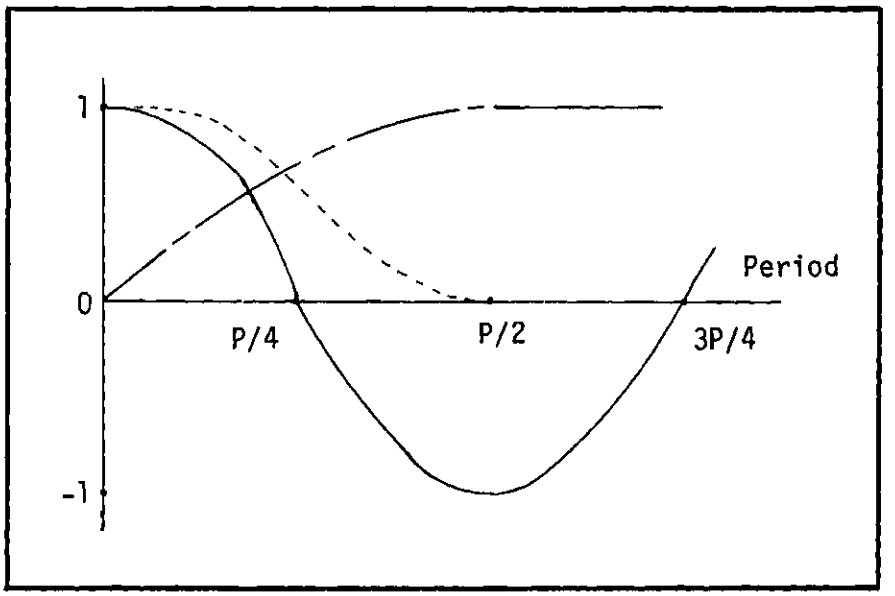

Figure 26. Correlation Function. Solid Line Gives Correlation Function for One Mode of Oscillation. Dotted Line gives Correlation Function for a Superposition of Several Modes of Oscillations. The Other Line Represents the Expected Value of $\frac{V_d^2}{2 < V^2(t) >}$ For the Velocity Difference Data.

Thus the calculated curves in Figures 24 and 25 must represent that part of the curve in Figure 26 for which the correlation curve has already descended to zero.

Since the velocity difference data does not show any significant change with time difference, then in order to get a rough estimate of the amplitude of the small scale motions versus altitude, all the velocity difference data were averaged together for each height. Figure 27 shows these results. The abscissa of Figure 27 is actually $\left(\frac{1}{2} V_d^2\right)^{1/2}$ instead of just V_d. The reason for this is seen in equation III-15. The square of the velocity difference approaches twice the square of the velocity amplitude of the atmospheric oscillation. If the velocity differences are attributed to gravity waves, then Figure 27 shows the variation of the gravity wave winds with height directly. The probable error of the mean for the curve in Figure 27 ranges from 10.2 m/sec at 92 km to 27.6 m/sec at 103 km altitude with an average probable error of about 20 m/sec.

The curve in Figure 27 indicates an increase in the gravity wave wind up to about 102-105 km altitude with a maximum of about 60 to 70 m/sec at about 105 km. Then the gravity wave wind decreases slightly or stays constant immediately above 105 km altitude. Kochanski [1964] observed a similar nature for the irregular winds which he attributed to gravity waves; however, his method of analysis is very questionable. If the curve in Figure 27 is attributed to gravity waves only, then the average gravity wave wind is about 53 m/sec for the observed height interval.

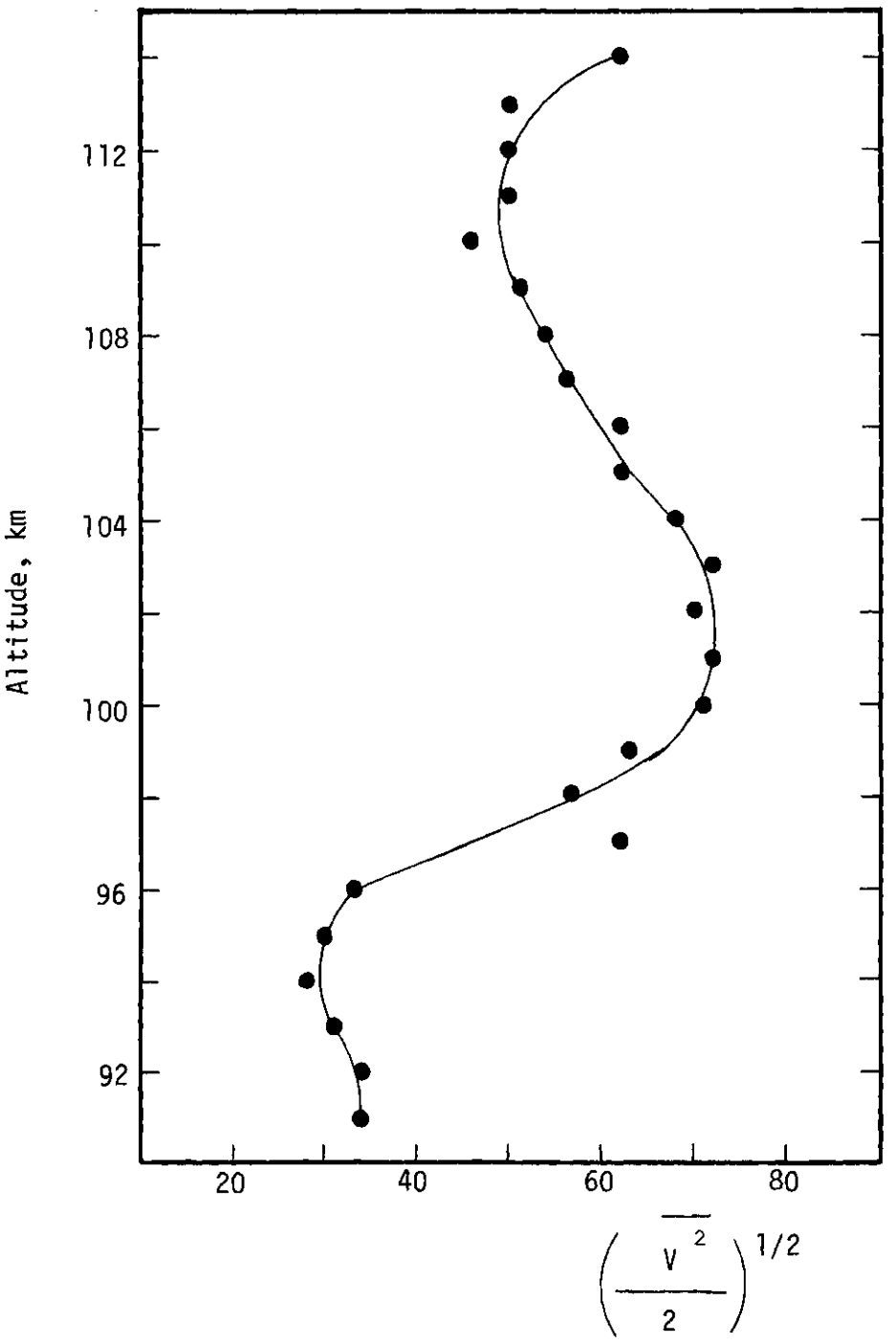

Figure 27. Velocity Difference Averaged Over All Time Separations Versus Height.

As was mentioned earlier in this chapter, Kochanski proposed that the variation of the energy contained in the gravity wave motion had an exponential form with height given by equation III-12. For the purpose of fitting this exponential function to the velocity difference data, a semi-log plot of the energy versus height was made and is shown in Figure 28. This figure shows the energy contained in the irregular motion is rather constant below an altitude of 100 km and then decays exponentially above this altitude with a z_0 value of 4.3 km. This value is seen to be of the same order of magnitude, although somewhat smaller than the value which Kochanski obtained (7.6 km given in Table 5).

A similar plot can also be made for the variance data computed from the geometrical method and is shown in Figure 29. The z_0 values for the PM, midnight and AM data are 6.6, 6.6 and 6.0 km respectively.

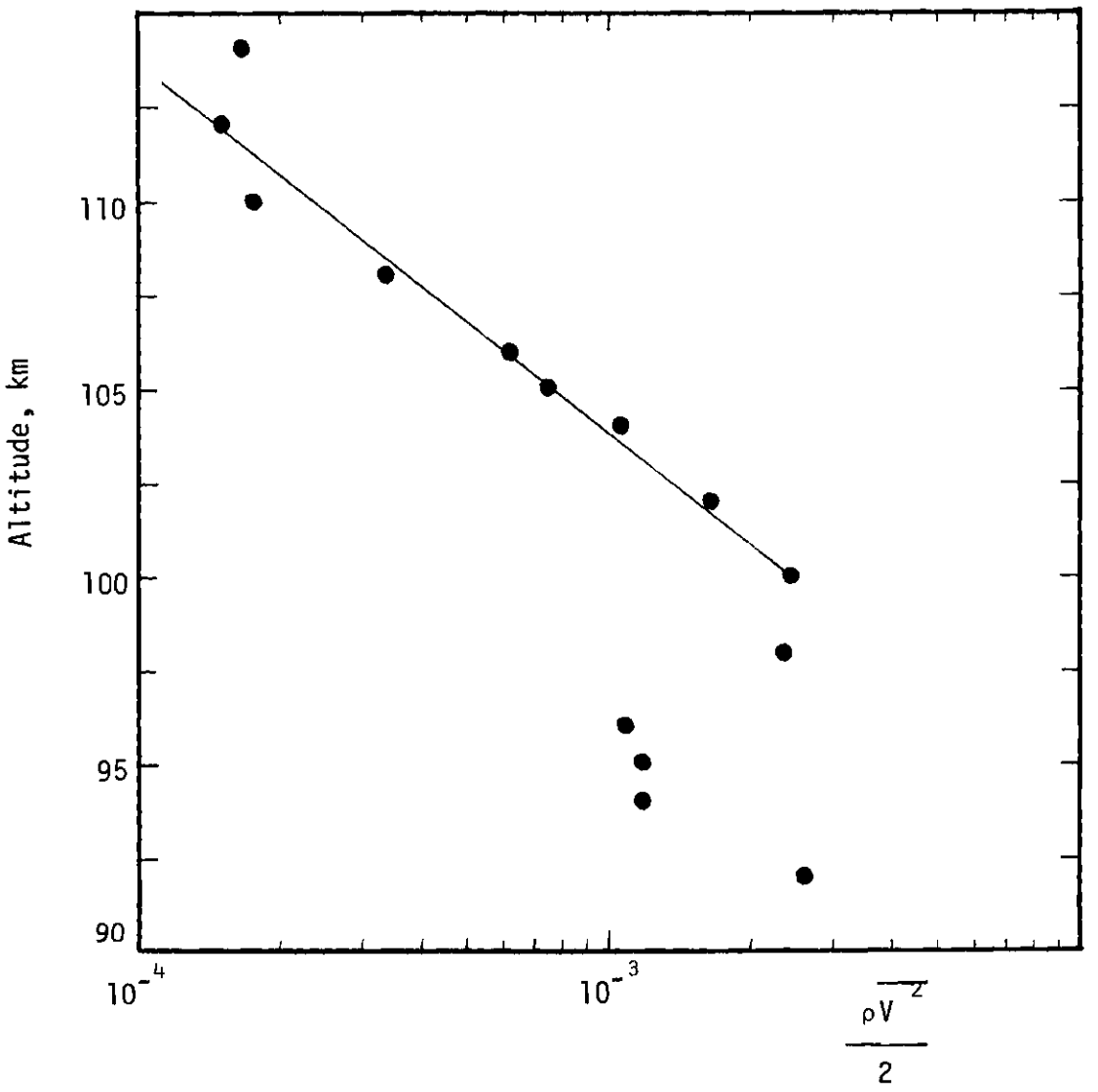

Figure 28. Semi-log Plot of Energy Contained in the Velocity Difference Versus Altitude. The Straight Line is a Subjective Fit of the Data Over Indicated Altitude.

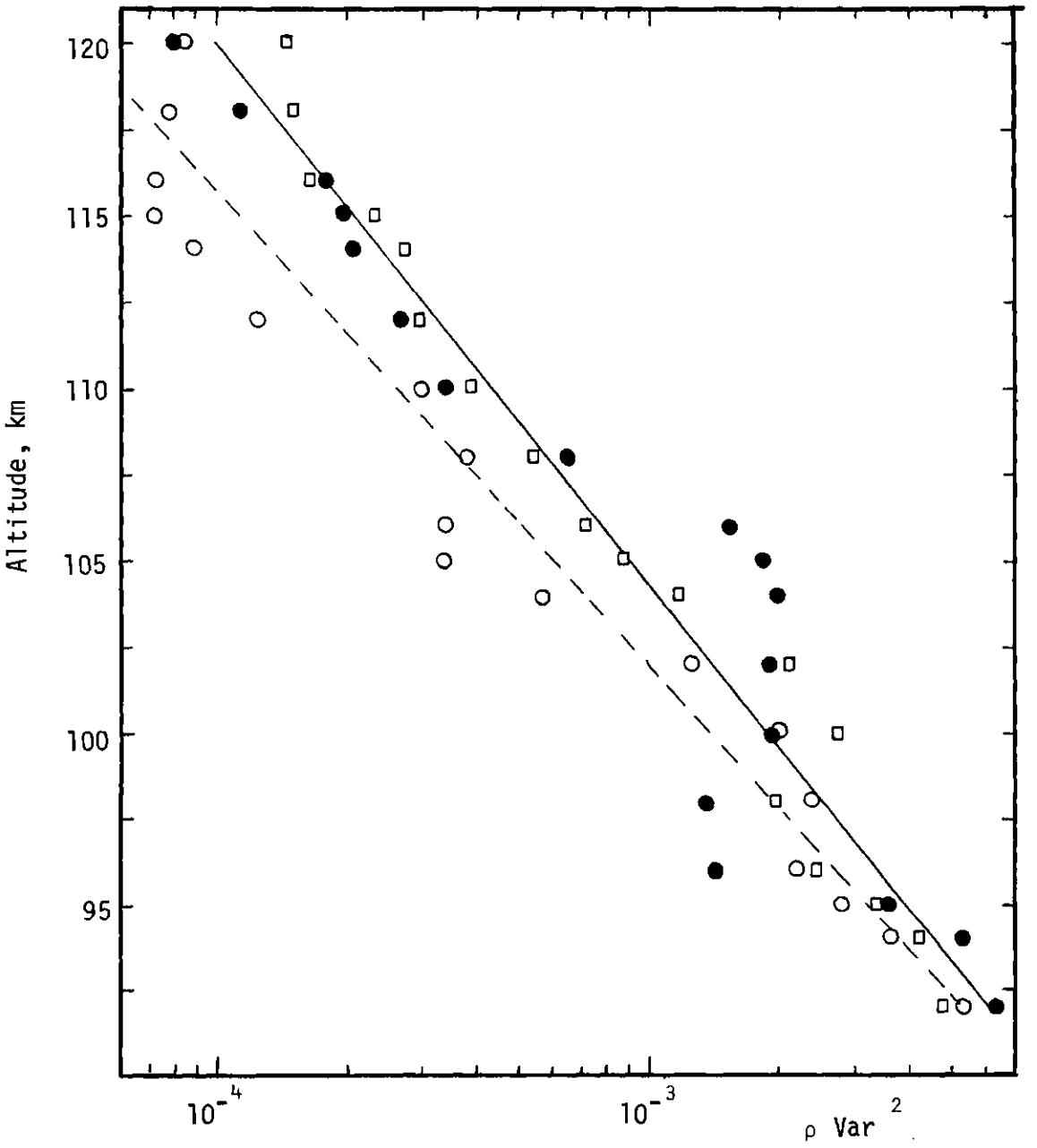

Figure 29. Semi-log Plot of Energy Contained in the Variance as Computed for the Time Groups of Dusk (Solid Dots), Midnight (Squares) and Dawn (Open Circles) Versus Altitude. The Straight Lines are Subjective Fits of the Data.

CHAPTER IV

CONCLUSIONS

Table 7 and 8 give a summary of the conclusions which can be drawn from the two methods of analyzing the experimental data presented here. Table 7 also shows the predicted values of the different parameters for the tidal waves from the tidal theory given in Chapter II.

Both analyses computed a prevailing wind whose height variation can most easily be explained by some wavelike motion. The computed velocity amplitudes, wavelengths and phase differences for the prevailing wind by the two methods agree very well.

The calculated vertical wavelengths of the propagating diurnal tide agree well with the wavelength of the (1,3) mode. The Groves method seems to show some influence of the viscous dissipation of the tidal energy in its calculated wavelength. Its calculated wavelength was 25 km which was a little longer than the predicted value of 20 km.

The calculated vertical wavelength of the semidiurnal tide seems to agree well with the wavelength of the (2,4) mode. It was thought earlier that the (2,2) mode was the main contributor to the semidiurnal oscillation in the height range around 100 km. The (2,2) mode is the main contributor to the semidiurnal oscillation in the lower atmosphere.

The phase difference between the northward and eastward velocity

Table 7: Tidal Parameters

	Theoretical (linearized theory with no dissipation)	Geometrical	Groves
Prevailing Wind			
a) Sense of rotation	----------	Clockwise	Clockwise
b) Velocity Amp.	----------	23 m/sec	20 m/sec
c) Vertical Wavelength	----------	27 km	26 km
d) Phase Difference	----------	123°	102°
Diurnal Tide			
a) Sense of rotation	Clockwise	Clockwise	Clockwise
b) Vel. Amp.	100 m/sec	19 m/sec	23 m/sec
c) Vertical Wavelengths	20 km	19 km	25 km
d) Phase Difference	≈ 90°	120°	100°
Semidiurnal Tide			
a) Sense of rotation	Clockwise	Undetermined	Clockwise
b) Vel. Amp.	≈ 100 m/sec	≈ 15 m/sec	20 m/sec
c) Vertical Wavelength	40 km or 100 km	≈ 60 km	36 km
d) Phase Difference	≈ 90°	Undetermined	107°

Table 8. Energy Dissipation

Analysis	Average Magnitude (m/sec)	z_o (km)	Height Range (km)	Reference
Kochanski				
1) Gravity Wave	45	7.6	70-140	Kochanski [1964]
Velocity Difference	53	4.3	91-114	Present Analysis
Hines				
1) Variance	65	--	90-130	Hines [1966]
Geometrical Method				
1) Variance	61	6.4	90-120	Woodrum and Justus [1968]
2) Diurnal	25	5.1		
3) Semidiurnal	15	5.0		
Meteor Data Groves Method				
1) Diurnal	55	6.5	83-97	Roper [1966] and Justus and Roper [1968]
2) Semidiurnal	48	∞		
Chemical Release Data Groves Method				
1) Diurnal	23	7.3	95-135	Present Analysis
2) Semidiurnal	20	5.9		
3) 8 hour period	24	∞		

components for both the diurnal and semidiurnal tides were calculated to be significantly larger than the value of 90° which was predicted by linearized tidal theory for a single mode of oscillation.

The calculated velocity amplitudes for both the diurnal and semidiurnal oscillations were very much smaller than the predicted amplitudes. One reason is due to the neglect of the nonlinear velocity terms in the tidal theory. These nonlinear terms become very important above the altitude of 100 km. The effect of the nonlinear terms would be to reduce the theoretically predicted velocity amplitudes and thus bring the predicted and actual amplitudes into closer agreement. Also, the viscous dissipation of energy becomes important above 100 km and hence this process would tend to reduce the predicted amplitude even more if these effects were taken into account in the theory.

Table 8 shows that both the tidal wave motion and the small scale wave motion suffer energy dissipation for the altitude range 90 - 120 km. Kochanski suggested an energy variation with height of the wave motion given by Equation III-12, where the parameter z_0 is a characteristic length of the dissipation. When the value of z_0 approaches infinity, this means that energy remains approximately constant with heights (i.e no significant dissipation takes place). Table 8 shows that the values of z_0 range from 4.3 to 7.6 for the wave motion given here with only two exceptions. The z_0 value calculated for the semi-diurnal tide from data presented by Roper [1966] is for one month only and is suspected to be peculiar to that one month. An infinite value of z_0 was also calculated for the 8 hour period from the Groves

analysis of the chemical release data. However the amplitude of the 8 hour period is very small below about 120 km and becomes large only in the height range 120-135 km for this set of data. This importance of the 8 hour period has not been observed generally in the lower atmosphere. However, no one has previously been able to separate the 8 hour periodic motion experimentally from the total winds in the altitude range just above 100 km. So the significance of the 8 hour motion in this height range depends on whether future experimental measurements also show an important 8 hour periodic motion.

Table 8 also shows the average magnitude of the tidal and small scale motions. The velocity difference analysis gives an average gravity wave of about 53 m/sec (if the velocity differences are attributed to gravity waves only). This analysis showed an increase of the irregular winds to a maximum of about 60 to 70 m/sec in the height range 102-105 km. Immediately above altitude 105 km, the irregular winds decrease slightly or stay constant.

The variance measurements made by Hines [1966] and the geometrical method presented here agree very well. As was suggested by Hines, the variance measurements are probably composed of a gravity wave component of about 40 to 45 m/sec and the rest is made up of variations in the systematic winds.

An energy spectrum analysis was also performed on the wind data for periodicites of 6 to 46 hours. As expected, this analysis showed that the 24 hour harmonics carry a large portion of the atmospheric energy. However, this analysis also indicated that a large amount of energy may also be carried by nonharmonic motions with periods of 16,

20, 33 and 36 hours. These motions may be caused by nonlinear interactions of the 24 hour harmonics.

In all cases the results showed a clockwise rotation of the wind vector with increasing height and a downward phase propagation. The downward phase propagation, as shown in Chapter II, corresponds to an upward energy propagation.

APPENDIX A

DEVELOPMENT OF THE THEORY

The theory of atmospheric tides has been developed, bit by bit, over the years by many different investigators. A very good collection of the theoretical works to the present time is given by Siebert [1961] and his presentation of the theory will be exhibited and expanded in this section.

The earth's atmosphere is a very complex system and many different parameters influence the atmospheric motions. It is impossible for the theory to consider all of the influences exerted by the atmosphere. Thus some of the less important influences are neglected.

Initial Equations

For this reason the earth is assumed to be a smoothed sphere rotating with a constant angular velocity $\underline{\omega}$. The acceleration due to gravity $\underline{g}$ is assumed to be independent of latitude and height. The direction of the vector $\underline{g}$ is taken to be radially down. The error introduced into the theory thus far is about 3%.

Let p_0, ρ_0, and T_0 represent the static pressure, static density and static temperature of the atmosphere. These quantities are assumed to be independent of latitude and longitude and dependent only on height z. The pressure, density, and temperature are related by the hydrostatic equation and the ideal gas equation.

$$\frac{dp_o}{dz} = \frac{\partial p_o}{\partial z} = -g\rho_o \qquad \text{(A-1)}$$

$$p_o = \frac{nRT_o}{V_v} = \frac{\rho_o}{M} RT_o = g\rho_o H \qquad \text{(A-2)}$$

where M is the mean molecular weight of air, V_v is the volume and H is the scale height as defined by equation I-1. The mean molecular weight of air is assumed to be constant and thus the humidity of the air is neglected. R is the universal gas constant which is equal to 8.3149 x 10^3 joules per kgm-mole-deg and n is the number of moles.

Eulerian Equations of Motion

The equations of motion that will be employed are the Eulerian equations of hydrodynamics referred to a rotating earth.

$$\frac{d\underline{V}}{dt} + 2\omega \times \underline{V} = -\frac{1}{\rho} \nabla p + \underline{g} - \nabla\Omega \qquad \text{(A-3)}$$

where $p = p_0 + \delta p$ and $\rho = \rho_o + \delta\rho$ are the actual pressure and density of the atmosphere with δp and $\delta\rho$ as variations in the pressure and density from the undisturbed condition, $\underline{V} = (u,v,w)$ is the velocity of the tidal wind with u, v, w as components in the southward, eastward, and vertical directions respectively, and Ω is the gravitational tidal potential. Note that equation A-3 neglects all effects due to friction and viscosity.

If we denote x, y, z as the southward, eastward and vertical coordinates respectively, then

$$\underline{V} = \underline{V}\,(x, y, z, t)$$

$$\frac{d\underline{V}}{dt} = \frac{\partial \underline{V}}{\partial x} u + \frac{\partial \underline{V}}{\partial y} v + \frac{\partial \underline{V}}{\partial z} w + \frac{\partial \underline{V}}{\partial t} \qquad \text{(A-4)}$$

The three nonlinear terms on the right side of equation A-4 have been the subject of much discussion. In order for the mathematical theory to be solvable, these terms must be neglected. Thus it is vital to know the magnitude of the three nonlinear terms compared with the magnitude of the term $\frac{\partial \underline{V}}{\partial t}$. Pekeris [1951] shows a plot of the approximate ratio of these terms and this plot is shown in Figure 30. Note that the neglect of these terms is a fairly good approximation below an altitude of about 100 km. However above this height and certainly above 110 km, the approximation is not a very good one. One of the consequences of the nonlinear terms is that modes of oscillations will no longer be independent and will begin to interact with each other. A possible result of this interaction is the alteration of the amplitudes of some of the harmonic modes and there is a slight chance that some non-harmonic oscillations may be created [Shiren (1965)].

Thus it is shown that the nonlinear terms become appreciable in the middle of the height range which is being studied. Therefore, the theoretical equations developed in this section should be considered as only a first approximation for the upper half of the altitude range which is considered and the interpretation of the results should take this situation into consideration.

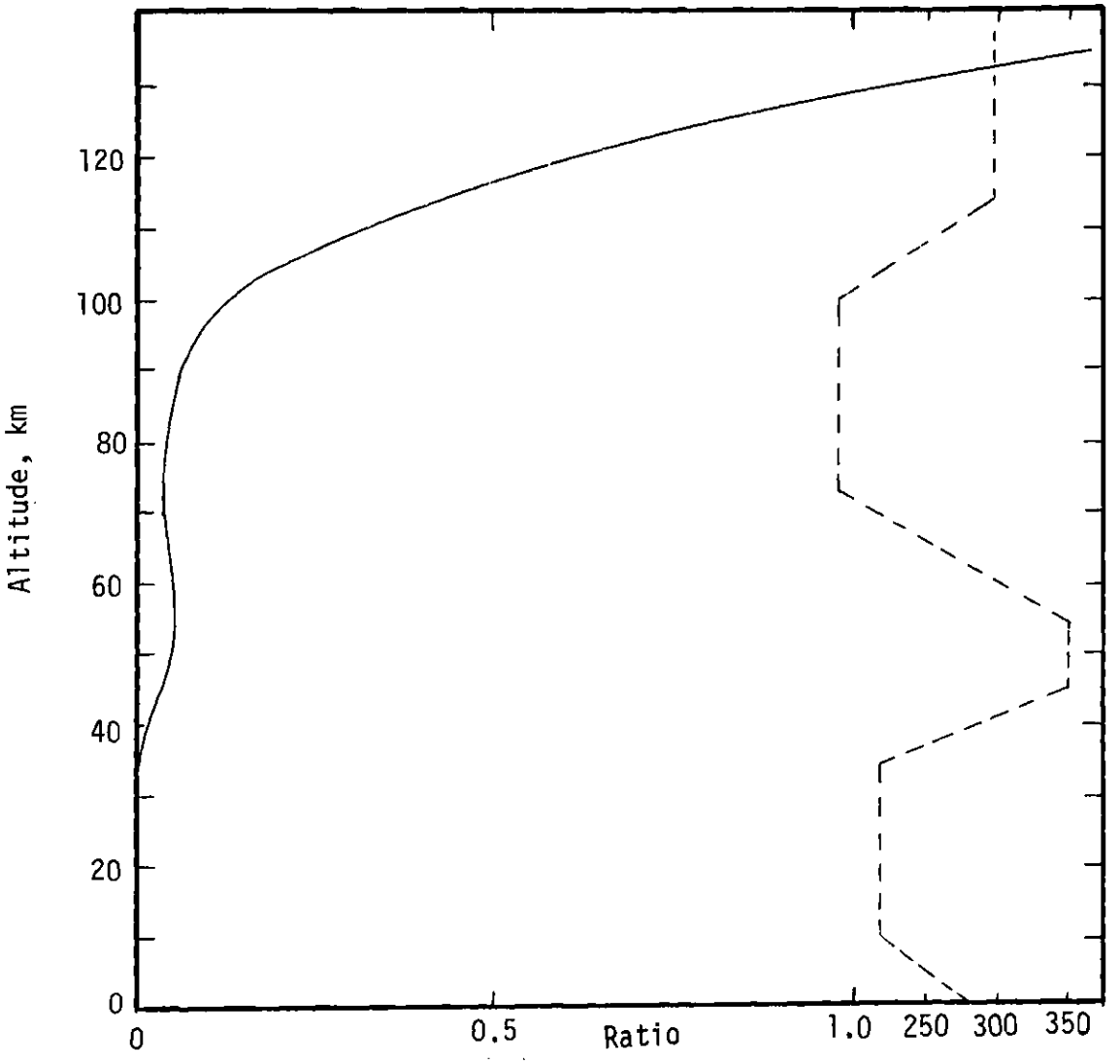

Figure 30. The Ratio of the Neglected Nonlinear Terms to the Term $\left| \frac{\partial \underline{V}}{\partial t} \right|$. The Dotted Curve Shows the Temperature Profile Used for the Calculation of the Ratio (After Pekeris [1951]).

Now consider the term

$$-\frac{1}{\rho}\nabla p = -\frac{1}{\rho_o + \delta\rho}\nabla(p_o + \delta p) \tag{A-5}$$

but

$$\nabla p_o = \hat{\imath}\frac{\partial p_o}{\partial x} + \hat{j}\frac{\partial p_o}{\partial y} + \hat{k}\frac{\partial p_o}{\partial z}$$

$$\nabla p_o = \hat{k}\frac{\partial p_o}{\partial z} \tag{A-6}$$

since the pressure depends only on the altitude z.

With the use of equations A-1 and A-6, we get from equation A-5

$$-\frac{1}{\rho}\nabla p = \frac{g\rho_o\hat{k}}{\rho_o + \delta\rho} - \frac{\nabla(\delta p)}{\rho_o + \delta\rho}$$

If the term $\frac{1}{\rho + \delta\rho}$ is expanded and only the first order terms are kept, then

$$-\frac{1}{\rho}\nabla p = g\,\hat{k}\left(1 - \frac{\delta\rho}{\rho_o}\right) - \frac{\nabla(\delta p)}{\rho_o}\left(1 - \frac{\delta\rho}{\rho_o}\right)$$

$$= -(-g\hat{k}) + (-g\hat{k})\frac{\delta\rho}{\rho_o} - \frac{\nabla(\delta p)}{\rho_o} + \nabla(\delta p)\frac{\delta\rho}{\rho_o^2}$$

$$-\frac{1}{\rho}\nabla p = -g + g\frac{\delta\rho}{\rho_o} - \frac{\nabla(\delta p)}{\rho_o} \tag{A-7}$$

If the nonlinear terms in equation A-4 are neglected, then with the use of equations A-4 and A-7, we get from equation A-3

$$\frac{\partial \underline{V}}{\partial t} + 2\,\omega \times \underline{V} = \frac{-1}{\rho_o}\,\nabla(\delta p) + \frac{\delta\rho}{\rho_o}\,\underline{g} - \nabla\Omega \qquad \text{(A-8)}$$

This equation is a vector equation and is actually

$$\frac{\partial u}{\partial t} + 2\,(w\omega_y - \omega_z v) = -\frac{\partial}{\partial x}\left(\frac{\delta p}{\rho_o} + \Omega\right) \qquad \text{(A-9)}$$

$$\frac{\partial v}{\partial t} + 2\,(\omega_z u - w\omega_x) = -\frac{\partial}{\partial y}\left(\frac{\delta p}{\rho_o} + \Omega\right) \qquad \text{(A-10)}$$

$$\frac{\partial w}{\partial t} + 2(\omega_x v - \omega_y u) = -\frac{1}{\rho_o}\frac{\partial}{\partial z}(\delta p) - \frac{\partial \Omega}{\partial z} - \frac{\delta\rho}{\rho_o}\,g \qquad \text{(A-11)}$$

The vertical velocity w is assumed to be very small in comparison with the horizontal velocities u and v. The vertical acceleration is also assumed negligible.

Now consider Figure 31. Note that ω_y is always zero, $\omega_z = \omega \cos\theta$ where θ is the colatitude, and $\omega_x = -\omega \sin\theta$. Now compare the two terms $2\omega_x v$ and $\frac{\delta\rho}{\rho_o}\,g$ in equation A-11. At about 100 km altitude, the values of the concerned quantities are about

$$g \simeq 10 \text{ m/sec}^2$$

$$\rho_o \simeq 10^{-6} \text{ kgm/m}^3$$

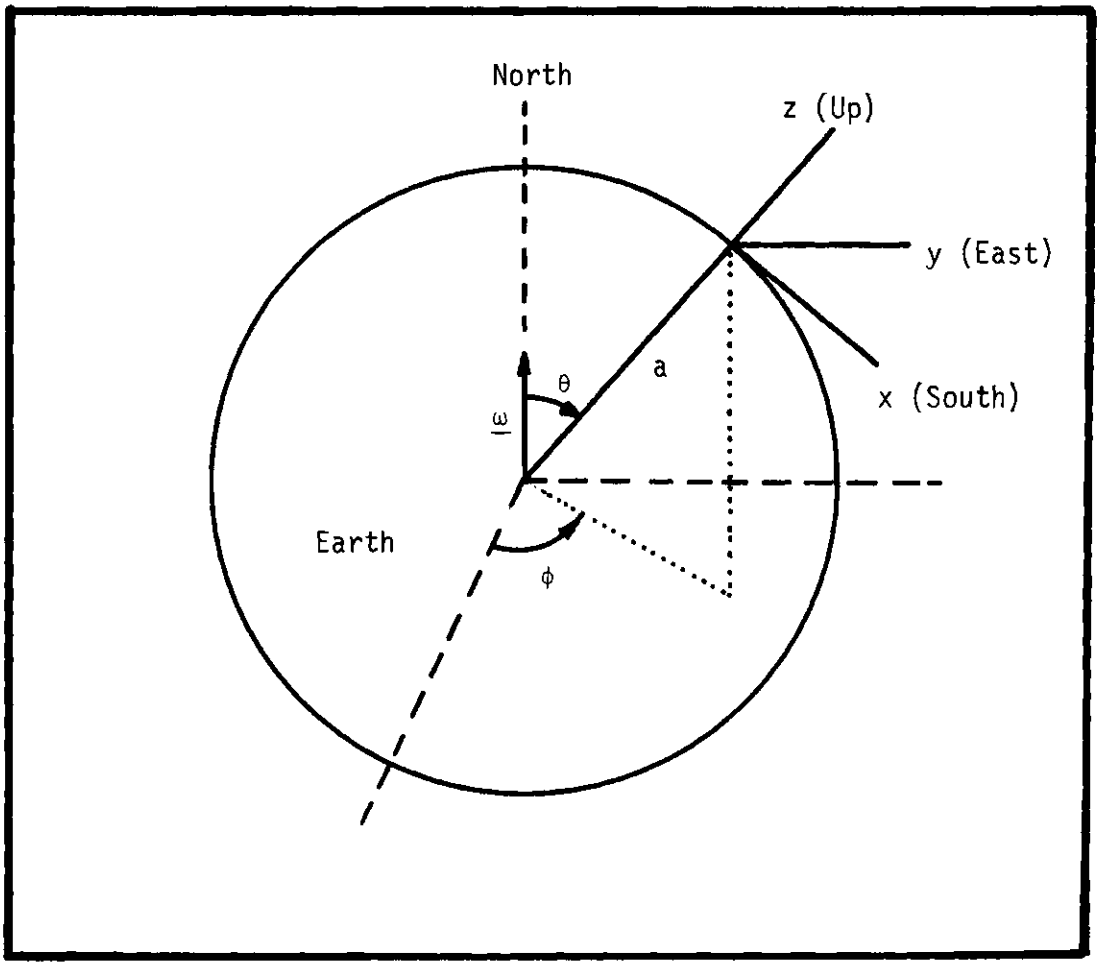

Figure 31. Coordinate Systems.

$$\delta\rho \simeq 10^{-8} \text{ kgm/m}^3$$

$$\omega \simeq \frac{2\pi}{24} = \frac{1}{14400} \text{ rad./sec.}$$

$$v \simeq 50 \text{ m/sec.}$$

$$\sin\theta \simeq 1$$

then

$$\frac{\delta\rho}{\rho_o} g \simeq 0.1 \text{ m/sec}^2$$

$$2\omega v \sin\theta \simeq 0.008 \text{ m/sec}^2$$

Thus $2\omega_x v$ is about one or two orders of magnitude less than $\frac{\delta\rho}{\rho_o} g$ and therefore can be neglected in a comparison.

To change the coordinate systems of equations A-9, A-10, A-11 from (x,y,z) to (r,θ,ϕ) where $r = a + z$ and ϕ is the longitude, we have

$$dx = r\, d\theta$$

$$dy = r \sin\theta\, d\phi$$

$$dz = dr$$

Since z is much less than the radius of the earth, then it is assumed that z can be neglected whenever it is compared with a, so

$$dx = a\, d\theta$$

$$dy = a \sin\theta\, d\phi$$

$$dz = dz$$

Thus equations A-9, A-10, A-11 become

$$\frac{\partial u}{\partial t} - 2\,\omega v \cos\theta = -\frac{1}{a}\frac{\partial}{\partial \theta}\left(\frac{\delta p}{\rho_o} + \Omega\right) \qquad \text{(A-12)}$$

$$\frac{\partial v}{\partial t} + 2\,\omega u \cos\theta = -\frac{1}{a \sin\theta}\frac{\partial}{\partial \phi}\left(\frac{\delta p}{\rho_o} + \Omega\right) \qquad \text{(A-13)}$$

$$\frac{\partial(\delta p)}{\partial z} = -g\,\delta\rho - \rho_o \frac{\partial \Omega}{\partial z} \qquad \text{(A-14)}$$

Pressure Variation as a Thermodynamic Process

The above equations describe the motion of the atmosphere caused by a pressure variation δp. The tidal pressure variations may also be treated as a thermodynamic process which can be described by the first law of thermodynamics for an ideal gas.

$$\delta Q = c_v\,dT + p\,d\left(\frac{1}{\rho}\right) \qquad \text{(A-15)}$$

where δQ is an infinitesimal amount of heat added per unit mass of air, c_v is the specific heat at constant volume, and T is the temperature. The quantity δQ may not be an exact differential.

If δQ is proportional to dT, then the changes of state are determined by

$$\delta Q = -\Gamma\,dT \qquad \text{(A-16)}$$

where $$T \sim \rho^{\gamma'-1}$$

$$\gamma' = \frac{c_p + \Gamma}{c_v + \Gamma} \qquad 0 \leq \Gamma < \infty \tag{A-17}$$

c_p is the specific heat at constant pressure.

Hence all the changes of state are connected with temperature changes with the exception of the isothermal changes of state, that is $\gamma' = 1$. The adiabatic changes of state occur when $\Gamma = 0$ which gives

$$\delta Q = 0$$

$$T \sim \rho^{\gamma - 1}$$

$$\gamma = \frac{c_p}{c_v} = 1.40$$

Chapman [1932] investigated the case where the tidal pressure is assumed to be excited exclusively by gravitation and he found that within the margin of the determined error the pressure changes take place adiabatically. Thus no change in δQ would occur. If the pressure variation is thermally excited, then

$$\delta Q = J\, dt \tag{A-18}$$

where J is the amount of heat absorbed or emitted by a unit mass of air per unit time.

Then equation A-15 becomes

$$J\, dt = c_v\, dT - \frac{p}{\rho^2}\, d\rho$$

$$J + \frac{P}{\rho^2} \frac{d\rho}{dt} = c_v \frac{dT}{dt}$$

But

$$R = M(c_p - c_v)$$

$$\frac{R}{c_v} = M(\gamma-1)$$

$$c_v = \frac{R}{M(\gamma-1)}$$

So

$$\frac{R}{M(\gamma-1)} \frac{dT}{dt} = \frac{p}{\rho^2} \frac{d\rho}{dt} + J \qquad \text{(A-19)}$$

Now we will assume that the ideal gas equation A-2 is valid for a disturbed atmosphere as well as the static variables.

$$p = \frac{R}{M} \rho T \qquad \text{(A-20)}$$

$$dp = \frac{R}{M} (T\, d\rho + \rho\, dT)$$

$$\frac{dp}{\frac{R}{M}\rho T} = \frac{d\rho}{\rho} + \frac{dT}{T}$$

$$\frac{dp}{p} = \frac{d\rho}{\rho} + \frac{dT}{T} \qquad \text{(A-21)}$$

$$\frac{1}{p} \frac{dp}{dt} = \frac{1}{\rho} \frac{d\rho}{dt} + \frac{1}{T} \frac{dT}{dt} \qquad \text{(A-22)}$$

Equation A-19 becomes by expansion

$$\frac{R}{M(\gamma-1)} \frac{dT}{dt} = \frac{p_o + \delta p}{(\rho_o + \delta\rho)^2} \frac{d\rho}{dt} + J$$

Now if the small variation terms, δp and $\delta\rho$, are neglected whenever compared to the static terms, p_o and ρ_o, and with the help of equation I-1, then

$$\frac{R}{M(\gamma-1)} \frac{dT}{dt} = \frac{gH}{\rho_o} \frac{d\rho}{dt} + J \qquad \text{(A-23)}$$

From equations A-20 and A-22, then

$$\frac{R}{M(\gamma-1)} \left[\frac{Mp}{R\rho} \left(\frac{1}{p} \frac{dp}{dt} - \frac{1}{\rho} \frac{d\rho}{dt}\right)\right] = \frac{p}{\rho^2} \frac{d\rho}{dt} + J$$

$$\frac{dp}{dt} = \frac{\gamma p}{\rho} \frac{d\rho}{dt} + (\gamma-1)\rho J$$

If the second order terms are neglected, then we have

$$\frac{dp}{dt} = \frac{p_o}{\rho_o} \gamma \frac{d\rho}{dt} + (\gamma-1)\rho_o J$$

$$\frac{dp}{dt} = \gamma gh \frac{d\rho}{dt} + (\gamma-1)\rho_o J \qquad \text{(A-24)}$$

where

$$\frac{dp}{dt} = \frac{dp_o}{dt} + \frac{d(\delta p)}{dt}$$

$$\frac{dp_o}{dt} = w \frac{\partial p_o}{\partial z} = - wg\rho_o \qquad \text{(A-25)}$$

since $p_o = p_o(z)$

$$\frac{d(\delta p)}{dt} = u \frac{\partial(\delta p)}{\partial x} + v \frac{\partial(\delta p)}{\partial y} + w \frac{\partial(\delta p)}{\partial z} + \frac{\partial(\delta p)}{\partial t}$$

The first two terms on the right involve the horizontal derivative of the pressure variation. It seems reasonable that the changes in the horizontal pressure variations are very small and hence these terms are neglected. The third term is multiplied by the vertical velocity which is assumed to be very small and since the term $\frac{\partial(\delta p)}{\partial z}$ is also small then the third term is neglected also

$$\frac{d(\delta p)}{dt} = \frac{\partial(\delta p)}{\partial t} \qquad \text{(A-26)}$$

Then

$$\frac{dp}{dt} = - wg\rho_o + \frac{\partial(\delta p)}{\partial t} \qquad \text{(A-27)}$$

Similarly

$$\frac{dp}{dt} = w \frac{\partial \rho_o}{\partial z} + \frac{\partial(\delta \rho)}{\partial t} \qquad \text{(A-28)}$$

$$\frac{dT}{dt} = w \frac{\partial T_o}{\partial z} + \frac{\partial(\delta T)}{\partial t} \qquad \text{(A-29)}$$

where $T = T_o + \delta T$.

Continuity Equation

To complete the set of initial equations, we will use the equation

of continuity.

$$\frac{d\rho}{dt} + \rho_o \chi = 0 \tag{A-30}$$

where

$$\chi = \nabla \cdot \underline{V} = \frac{1}{a \sin\theta} \frac{\partial}{\partial\theta} (u \sin\theta)$$

$$+ \frac{1}{a \sin\theta} \frac{\partial v}{\partial\phi} + \frac{\partial w}{\partial z} \tag{A-31}$$

Solution of the Initial Equations

Equations A-12, A-13, A-14, A-23 and A-29 give us five equations from which the five unknowns (u, v, w, δp, δT) will be solved.

First we assume that all the values (u, v, w, δp, $\delta\rho$, δT, χ, Ω, J) vary as $e^{i\sigma t}$ where σ is the angular frequency of the oscillation. Then equations A-12 and A-13 become

$$i\sigma u - 2\omega v \cos\theta = -\frac{1}{a} \frac{\partial k}{\partial\theta}$$

$$i\sigma v + 2\omega u \cos\theta = -\frac{1}{a \sin\theta} \frac{\partial k}{\partial\phi}$$

where

$$k = \frac{\delta p}{\rho_o} + \Omega$$

Solving these equations for u and v, we have

Solving these equations for u and v, we have

$$u = \frac{2\,\omega\, v \cos\theta}{i\sigma} - \frac{1}{i\,\sigma\, a}\,\frac{\partial k}{\partial \theta}$$

$$i\,\sigma\, v + \frac{4\,\omega^2\, v \cos^2\theta}{i\,\sigma} - \frac{2\,\omega}{i\,\sigma\, a}\cos\theta\,\frac{\partial k}{\partial \theta}$$

$$= \frac{1}{a \sin\theta}\,\frac{\partial k}{\partial \phi}$$

$$v = \frac{\dfrac{2\,\omega\cos\theta}{i\,\sigma\, a}\,\dfrac{\partial}{\partial\theta} - \dfrac{1}{a\sin\theta}\,\dfrac{\partial k}{\partial\phi}}{i\sigma + \dfrac{4\,\omega^2\cos^2\theta}{i\,\sigma}}$$

$$v = \frac{2\,\omega\cos\theta\,\dfrac{\partial k}{\partial\theta} - \dfrac{i\sigma}{\sin\theta}\,\dfrac{\partial k}{\partial\phi}}{4\,a\omega^2\left(\cos^2\theta - \dfrac{\sigma^2}{4\omega^2}\right)}$$

$$v = \frac{i\,\sigma}{4\,a\,\omega^2\left(f^2 - \cos^2\theta\right)}\left[\frac{i\cos\theta}{f}\,\frac{\partial}{\partial\theta} + \frac{1}{\sin\theta}\,\frac{\partial}{\partial\phi}\right] k \qquad \text{(A-32)}$$

where

$$f = \frac{\sigma}{2\,\omega} \qquad \text{(A-33)}$$

Then u becomes

$$u = \frac{2\,\omega\cos\theta}{4\,a\,\omega^2\,(f^2-\cos^2\theta)}\left[\frac{i\cos\theta}{f}\frac{\partial}{\partial\theta}+\frac{1}{\sin\theta}\frac{\partial}{\partial\phi}\right]k$$

$$-\frac{1}{i\,\sigma\,a}\frac{\partial k}{\partial\phi}$$

$$=\frac{1}{4\,a\,\omega^2\,(f^2-\cos^2\theta)}\left\{\left[\frac{2\,i\,\omega\cos^2\theta}{f}-\frac{4\,a\,\omega^2\,(f^2-\cos^2\theta)}{i\,\sigma\,a}\right]\frac{\partial k}{\partial\theta}\right.$$

$$\left.+\frac{\sigma\cot\theta}{f}\frac{\partial k}{\partial\phi}\right\}$$

$$u = \frac{1}{4\,a\,\omega^2\,(f^2-\cos^2\theta)}\left\{\left[\frac{4\,i\,\omega^2\cos^2\theta}{\sigma}-\frac{4\,a\,\omega^2\,\sigma^2}{i\,\sigma\,a\,4\omega^2}+\right.\right.$$

$$\left.\left.\frac{4\,a\,\omega^2\cos^2\theta}{i\,\sigma\,a}\right]\frac{\partial k}{\partial\theta}+\frac{\sigma\cot\theta}{f}\frac{\partial k}{\partial\phi}\right\}$$

$$u = \frac{\sigma}{4\,a\,\omega^2\,(f^2-\cos^2\theta)}\left[i\frac{\partial}{\partial\theta}+\frac{\cot\theta}{f}\frac{\partial}{\partial\phi}\right]k \quad \text{(A-34)}$$

By the substitution of A-31 and A-33 into A-30, we get

$$\chi = \frac{1}{a\sin\theta}\frac{\partial}{\partial\theta}\left\{\frac{\sigma\sin\theta}{4\,a\,\omega^2\,(f^2-\cos^2\theta)}\left[i\frac{\partial}{\partial\theta}+\frac{\cot\theta}{f}\frac{\partial}{\partial\phi}\right]k\right\}$$

$$+\frac{1}{a\sin\theta}\frac{\partial}{\partial\phi}\left\{\frac{i\,\sigma}{4\,a\,\omega^2\,(f^2-\cos^2\theta)}\left[\frac{i\cos\theta}{f}\frac{\partial}{\partial\theta}+\frac{1}{\sin\theta}\frac{\partial}{\partial\phi}\right]k\right\}$$

$$+\frac{\partial w}{\partial z}$$

$$\chi - \frac{\partial w}{\partial z} = \frac{i\sigma}{4a^2\omega^2}\left\{\frac{1}{\sin\theta}\frac{\partial}{\partial\theta}\left[\frac{\sin\theta}{f^2-\cos^2\theta}\frac{\partial k}{\partial\theta}\right.\right.$$

$$+ \frac{1}{i f \sin\theta}\frac{\cos\theta}{f^2-\cos^2\theta}\frac{\partial^2 k}{\partial\theta\partial\phi} + \frac{1}{i f \sin\theta}$$

$$\left(-\frac{\sin\theta}{f^2-\cos^2\theta}\frac{\partial k}{\partial\phi} -\right.$$

$$\left.\left.\frac{\cos\theta\,(2\cos\theta\sin\theta)}{(f^2-\cos^2\theta)^2}\frac{\partial k}{\partial\phi}\right) + \frac{i}{f\sin\theta}\frac{\cos\theta}{f^2-\cos^2\theta}\frac{\partial^2 k}{\partial\theta\partial\phi}\right.$$

$$\left. + \frac{1}{\sin^2\theta}\frac{1}{f^2-\cos^2\theta}\frac{\partial^2 k}{\partial\phi^2}\right\}$$

$$\chi - \frac{\partial w}{\partial z} = \frac{i\sigma}{4a^2\omega^2} F(k) \qquad \text{(A-34)}$$

where

$$F = \frac{1}{\sin\theta}\frac{\partial}{\partial\theta}\left(\frac{\sin\theta}{f^2-\cos^2\theta}\frac{\partial}{\partial\theta}\right)$$

$$+ \frac{1}{f^2-\cos^2\theta}\left(\frac{i}{f}\frac{f^2+\cos^2\theta}{f^2-\cos^2\theta}\frac{\partial}{\partial\phi} + \frac{1}{\sin^2\theta}\frac{\partial^2}{\partial\phi^2}\right) \qquad \text{(A-35)}$$

Now to evaluate the quantity $\frac{\partial w}{\partial z}$, let us substitute the continuity equation A-30 into equation A-23.

$$\frac{R}{M(\gamma-1)}\frac{dT}{dt} = -gH\chi + J$$

By equation A-29, this becomes

$$\frac{R}{M(\gamma-1)} \left[w \frac{\partial T_o}{\partial z} + \frac{\partial (\delta T)}{\partial t} \right] = - g H \chi + J$$

By equation I-1,

$$H = \frac{R T_o}{M g}$$

$$\frac{\partial T_o}{\partial z} = \frac{Mg}{R} \frac{\partial H}{\partial z} \qquad \text{(A-36)}$$

$$\frac{R}{M(\gamma-1)} \left[\frac{w M g}{R} \frac{\partial H}{\partial z} + i \sigma \delta T \right] = - g H \chi + J$$

$$\frac{w g}{\kappa \gamma} \frac{\partial H}{\partial z} \frac{R}{M \kappa \gamma} i \sigma \delta T = - g H \chi + J$$

where

$$\kappa = \frac{\gamma - 1}{\gamma} = \frac{c_p - c_v}{c_p}$$

For dry air, $\kappa = \frac{2}{7}$.

$$i \sigma \delta T = \frac{\kappa M}{R} \left(\gamma J - g \gamma H \chi - \frac{w g}{\kappa} \frac{\partial H}{\partial z} \right) \qquad \text{(A-37)}$$

By substituting equation A-30 into A-24, we get

$$\frac{dp}{dt} = \gamma g H (-\rho_o \chi) + (\gamma - 1) \rho_o J$$

From equation A-27, we get

$$-w g \rho_o + \frac{\partial(\delta p)}{\partial t} = -\gamma g \rho_o H \chi + (\gamma - 1) \rho_o J$$

$$i \sigma \delta p = w g \rho_o - \gamma g \rho_o H \chi + (\gamma-1) \rho_o J \qquad \text{(A-38)}$$

$$i \sigma \frac{\partial(\delta p)}{\partial z} = \frac{\partial w}{\partial z} g \rho_o + w g \frac{\partial \rho_o}{\partial z} - \gamma g \frac{\partial \rho_o}{\partial z} H \chi$$

$$- \gamma g \rho_o \frac{\partial H}{\partial z} \chi - \gamma g \rho_o H \frac{\partial \chi}{\partial z}$$

$$+ (\gamma-1) \frac{\partial \rho_o}{\partial z} J + (\gamma-1) \rho_o \frac{\partial J}{\partial z}$$

From equation A-2

$$P_o = g \rho_o H$$

$$\frac{\partial p_o}{\partial z} = g \frac{\partial \rho_o}{\partial z} H + g \rho_o \frac{\partial H}{\partial z} \qquad \text{(A-39)}$$

So

$$i \sigma \frac{\partial(\delta p)}{\partial z} = \frac{\partial w}{\partial z} g \rho_o + w g \frac{\partial \rho_o}{\partial z} - \gamma \chi \frac{\partial p_o}{\partial z} - \gamma g \rho_o H \frac{\partial \chi}{\partial z}$$

$$+ \quad (\gamma-1) \quad \frac{\partial \rho_o}{\partial z} \quad J \quad + \quad (\gamma-1) \; \rho_o \quad \frac{\partial J}{\partial z}$$

By the use of equations A-1 and A-14, we get

$$i \; \sigma \; g \; \delta\rho - i \; \sigma \; \rho_o \quad \frac{\partial \Omega}{\partial z} \quad = \quad \frac{\partial w}{\partial z} \quad g \; \rho_o \quad + w \; g \quad \frac{\partial \rho_o}{\partial z} \quad + g \; \rho_o \; \gamma \; \chi$$

$$- \gamma \; g \; \rho_o \; H \quad \frac{\partial \chi}{\partial z} \quad + \quad (\gamma-1) \quad \frac{\partial (\rho_o \; J)}{\partial z} \qquad \text{(A-40)}$$

By combining the continuity equation A-30 and equation A-28, we get

$$\frac{d\rho}{dt} \quad = \quad - \rho_o \; \chi \quad = \quad w \; \frac{\partial \rho_o}{\partial z} \quad + \quad i \; \sigma \; \delta\rho$$

$$\frac{\partial \rho_o}{\partial z} \quad = \quad - \quad \frac{\rho_o}{w} \quad \chi \quad - \quad \frac{i \; \sigma}{w} \quad \delta\rho \qquad \text{(A-41)}$$

After substitution of A-40, we get from equation A-39

$$- \; i \; \sigma \; g \; \delta\rho - i \; \sigma \; \rho_o \; \frac{\partial \Omega}{\partial z} \quad = \quad \frac{\partial w}{\partial z} \quad g \; \rho_o \quad - i \; \sigma \; g \; \delta\rho - g \; \rho_o \; \chi$$

$$+ g \; \rho_o \; \gamma \; \chi - \gamma \; g \; \rho_o \; H \quad \frac{\partial \chi}{\partial z} \quad + \quad (\gamma-1) \quad \frac{\partial (\rho_o J)}{\partial z}$$

$$\frac{\partial w}{\partial z} \quad = \quad \gamma \; H \quad \frac{\partial \chi}{\partial z} \quad - \quad (\gamma-1) \; \chi \quad - \frac{\gamma - 1}{g \; \rho_o} \quad \frac{\partial (\rho_o J)}{\partial z} \quad - \quad \frac{i \; \sigma}{g} \quad \frac{\partial \Omega}{\partial z} \qquad \text{(A-42)}$$

From equation A-39, we get

$$\frac{\partial \rho_o}{\partial z} = \frac{1}{g H} \frac{\partial p_o}{\partial z} - \frac{\rho_o}{H} \frac{\partial H}{\partial z}$$

$$\frac{1}{\rho_o} \frac{\partial \rho_o}{\partial z} = - \frac{1}{H} \left(1 + \frac{\partial H}{\partial z}\right) \qquad \text{(A-43)}$$

Now

$$k = \frac{\delta p}{\rho_o} + \Omega$$

$$\frac{\partial k}{\partial z} = \frac{\partial}{\partial z} \left(\frac{\delta p}{\rho_o}\right) + \frac{\partial \Omega}{\partial z}$$

But from equation A-38, we have

$$\frac{\delta p}{\rho_o} = \frac{1}{i \sigma} \left[w g - \gamma g H \chi + (\gamma - 1) J \right]$$

$$\frac{\partial}{\partial z} \frac{\delta p}{\rho_o} = \frac{1}{i \sigma} \frac{\partial w}{\partial z} g - \gamma g \frac{\partial H}{\partial z} \chi - \gamma g H \frac{\partial \chi}{\partial z} + (\gamma - 1) \frac{\partial J}{\partial z}$$

So

$$\frac{\partial k}{\partial z} = \frac{1}{i\sigma} g \frac{\partial w}{\partial z} - \gamma g \chi \frac{\partial H}{\partial z} - \gamma g H \frac{\partial \chi}{\partial z} + (\gamma - 1) \frac{\partial J}{\partial z}$$

$$+ \frac{\partial \Omega}{\partial z}$$

With the substitution of equation A-42, we get

$$\frac{\partial k}{\partial z} = \frac{1}{i\sigma}\left[g\gamma H \frac{\partial \chi}{\partial z} - g(\gamma-1)\chi - \frac{(\gamma-1)}{\rho_o}\frac{\partial(\rho_o J)}{\partial z} \right.$$

$$- i\sigma \frac{\partial \Omega}{\partial z} - \gamma g \chi \frac{\partial H}{\partial z} - \gamma g H \frac{\partial \chi}{\partial z}$$

$$\left. + (\gamma-1)\frac{\partial J}{\partial z} \right] + \frac{\partial \Omega}{\partial z}$$

$$\frac{i\sigma}{g\gamma}\frac{\partial k}{\partial z} = -\kappa\chi - \frac{\kappa}{g}\frac{\partial J}{\partial z} - \frac{\kappa J}{g\rho_o}\frac{\partial \rho_o}{\partial z} - \chi\frac{\partial H}{\partial z}$$

$$+ \frac{\kappa}{g}\frac{\partial J}{\partial z}$$

$$= -\left(\kappa + \frac{\partial H}{\partial}\right)\chi - \frac{\kappa J}{g\rho_o}\frac{\partial \rho_o}{\partial z}$$

By substitution of equation A-43, we get

$$\frac{i\sigma}{g\gamma}\frac{\partial k}{\partial z} = -\left(\kappa + \frac{\partial H}{\partial z}\right)\chi + \frac{\kappa J}{gH}\left(1 + \frac{\partial H}{\partial z}\right) \qquad \text{(A-44)}$$

By differentiating equation A-34, we get

$$\frac{\partial \chi}{\partial z} - \frac{\partial^2 w}{\partial z^2} = \frac{i\sigma}{4a^2\omega^2} F\left(\frac{\partial k}{\partial z}\right)$$

$$\frac{\partial^2 w}{\partial z^2} = \frac{\partial \chi}{\partial z} - \frac{i\sigma}{4\, a^2\, \omega^2} F\left(\frac{\partial k}{\partial z}\right) \qquad \text{(A-45)}$$

Also differentiating equation A-42, we get

$$\frac{\partial^2 w}{\partial z^2} = \gamma H \frac{\partial^2 \chi}{\partial z^2} + \gamma \frac{\partial H}{\partial z} \frac{\partial \chi}{\partial z} - (\gamma-1) \frac{\partial \chi}{\partial z}$$

$$- \frac{(\gamma-1)}{g\rho_o} \frac{\partial^2 (\rho_o J)}{\partial z^2} + \frac{(\gamma-1)}{g\rho_o^2} \frac{\partial \rho_o}{\partial z} \frac{\partial (\rho_o J)}{\partial z}$$

$$- \frac{i\,\sigma}{g} \frac{\partial^2 \Omega}{\partial z^2} \qquad \text{(A-46)}$$

Now, the term $\frac{i\,\sigma}{g} \frac{\partial^2 \Omega}{\partial z^2}$ is very small and can be neglected. Then if A-45 and A-46 are equated, we get

$$\frac{\partial \chi}{\partial z} - \frac{i\sigma}{4\, a^2\, \omega^2} F\left(\frac{\partial k}{\partial z}\right) = \gamma H \frac{\partial^2 \chi}{\partial z^2} + \gamma \frac{\partial H}{\partial z} \frac{\partial \chi}{\partial z} - \gamma \frac{\partial \chi}{\partial z}$$

$$+ \frac{\partial \chi}{\partial z} - \frac{(\gamma-1)}{g\rho_o} \frac{\partial^2 (\rho_o J)}{\partial z^2} + \frac{\gamma - 1}{g\, \rho_o^2} \frac{\partial \rho_o}{\partial z} \frac{\partial (\rho_o J)}{\partial z}$$

$$\gamma H \frac{\partial^2 \chi}{\partial z^2} + \gamma \left(\frac{\partial H}{\partial z} - 1\right) \frac{\partial \chi}{\partial z} - \frac{\gamma - 1}{g} \frac{\partial^2 J}{\partial z^2} - \frac{2(\gamma-1)}{g\, \rho_o} \frac{\partial \rho_o}{\partial z} \frac{\partial J}{\partial z}$$

$$- \frac{(\gamma-1)\ J}{g\rho_o} \frac{\partial^2 \rho_o}{\partial z^2} + \frac{(\gamma-1)}{g\ \rho_o} \frac{\partial \rho_o}{\partial z} \frac{\partial J}{\partial z}$$

$$+ \frac{(\gamma-1)\ J}{g\rho_o^{\ 2}} \frac{\partial \rho_o}{\partial z} \frac{\partial \rho_o}{\partial z} + \frac{g\gamma}{4\ a^2\ \omega^2} F\left(\frac{i\sigma}{g\gamma} \frac{\partial k}{\partial z}\right) = 0$$

Divide by γ and substitute $\kappa = \frac{\gamma - 1}{\gamma}$ into this equation and we have

$$H \frac{\partial^2 \chi}{\partial z^2} + \left(\frac{\partial H}{\partial z} - 1\right) \frac{\partial \chi}{\partial z} - \frac{\kappa}{g} \frac{\partial}{\partial z} \left(\frac{\partial J}{\partial z}\right) - \frac{\kappa}{g} \left[\frac{J}{\rho_o} \frac{\partial^2 \rho_o}{\partial z^2}\right.$$

$$\left. - \frac{J}{\rho_o^{\ 2}} \frac{\partial \rho_o}{\partial z} \frac{\partial \rho_o}{\partial z} + \frac{1}{\rho_o} \frac{\partial \rho_o}{\partial z} \frac{\partial J}{\partial z}\right]$$

$$+ \frac{g}{4\ a^2\ \omega^2} F\left(\frac{i\ \sigma}{g\ \gamma} \frac{\partial k}{\partial z}\right) = 0 \qquad \text{(A-47)}$$

Now note that

$$\frac{\partial}{\partial z}\left[\left(\frac{1}{\rho_o} \frac{\partial \rho_o}{\partial z}\right) J\right] = \frac{\partial}{\partial z}\left[-\frac{1}{H}\left(1 + \frac{\partial H}{\partial z}\right) J\right]$$

$$= \frac{J}{\rho_o} \frac{\partial^2 \rho_o}{\partial z^2} - \frac{J}{\rho o^2} \frac{\partial \rho_o}{\partial z} \frac{\partial \rho_o}{\partial z} + \frac{1}{\rho_o} \frac{\partial \rho_o}{\partial z} \frac{\partial J}{\partial z}$$

By substitution of this and equation A-44 into A-47, we get

$$H\frac{\partial^2\chi}{\partial z^2} + \left(\frac{\partial H}{\partial z} - 1\right)\frac{\partial\chi}{\partial z} - \frac{\kappa}{g}\frac{\partial}{\partial z}\left[\frac{\partial J}{\partial z} - \frac{1}{H}\left(1 + \frac{\partial H}{\partial z}\right)J\right]$$

$$- \frac{g}{4\,a^2\,\omega^2} F\left[\left(\kappa + \frac{\partial H}{\partial z}\right)\chi - \frac{\kappa J}{gH}\left(1 + \frac{\partial H}{\partial z}\right)\right] = 0 \qquad \text{(A-48)}$$

Series Expansion

Equation A-48 is a partial differential equation for χ and can be solved by the method of separation of variables. We can expand χ and J in terms of the eigenfunctions $\psi_n(\theta,\phi)$ of the operator F.

$$\chi = \sum_n \chi_n(z)\,\psi_n(\theta,\phi)\,e^{i\sigma t}$$

$$J = \sum_n J_n(z)\,\psi_n(\theta,\phi)\,e^{i\sigma t} \qquad \text{(A-49)}$$

Then equation A-48 becomes

$$\sum_n \psi_n(\theta,\phi)\,e^{i\sigma t}\left\{H\frac{\partial^2\chi_n}{\partial z^2} + \left(\frac{\partial H}{\partial z} - 1\right)\frac{\partial\chi_n}{\partial z}\right.$$

$$\left. - \frac{\kappa}{g}\frac{\partial}{\partial z}\left[\frac{\partial J_n}{\partial z} - \frac{1}{H}\left(1 + \frac{\partial H}{\partial z}\right)J_n\right]\right\}$$

$$- \sum_n \frac{g}{4\,a^2\,\omega^2} F\left[\left(\kappa + \frac{\partial H}{\partial z}\right)\right. \chi_n(z)\,\psi_n(\theta,\phi)e^{i\sigma t}$$

$$- \frac{\kappa}{g\ H} \left(1 + \frac{\partial H}{\partial z} \right) \ J_n(z) \ \ \psi_n(\theta,\phi)\ e^{i\sigma t} \Bigg] = 0$$

Now the functions $\psi_n(\theta,\phi)$ form a complete set of orthogonal functions, so this equation must also be true for every n. Divide by $\psi_n(\theta,\phi)e^{i\sigma t}$ and group terms.

$$H \frac{\partial^2 \chi_n}{\partial z^2} + \left(\frac{\partial H}{\partial z} - 1 \right) \frac{\partial \chi_n}{\partial z} - \left(\kappa + \frac{\partial H}{\partial z} \right) \chi_n \ \frac{F(\psi_n)}{\psi_n} \ \ \frac{g}{4\ a^2\ \omega^2}$$

$$= \frac{\kappa}{g} \left\{ \frac{\partial}{\partial z} \left[\frac{\partial J_n}{\partial z} - \frac{1}{H} \left(1 + \frac{\partial H}{\partial z} \right) \ J_n \right] \right.$$

$$\left. - \frac{g}{4\ a^2\ \omega^2} \ \frac{1}{H} \ \left(1 + \frac{\partial H}{\partial z} \right) J_n \ \frac{F(\psi_n)}{\psi_n} \right\}$$

Now we know that

$$F(\psi_n) = c\ \psi_n$$

where c is a constant. Define a constant $\frac{1}{h_n}$ such that

$$F(\psi_n) = - \frac{4\ a^2\ \omega^2}{g\ h_n} \ \psi_n \qquad \text{(A-50)}$$

Later it will be shown that h_n are equivalent depths. Then

$$H \frac{\partial^2 \chi_n}{\partial z^2} + \left(\frac{\partial H}{\partial z} - 1 \right) \frac{\partial \chi_n}{\partial z} + \left(\kappa + \frac{\partial H}{\partial z} \right) \frac{\chi_n}{h_n}$$

$$= \frac{\kappa}{g} \left\{ \left(1 + \frac{H}{z} \right) \frac{J_n}{H h_n} + \frac{\partial}{\partial z} \left[\frac{\partial J_n}{\partial z} \right.\right.$$

$$\left.\left. - \frac{1}{H} \left(1 + \frac{\partial H}{\partial z} \right) J_n \right] \right\} \qquad \text{(A-51)}$$

By combining equations A-42 and A-43, we get

$$\frac{\partial w}{\partial z} = \gamma H \frac{\partial \chi}{\partial z} - \gamma \chi + \chi - \frac{\gamma - 1}{g} \frac{\partial J}{\partial z} - \frac{(\gamma-1)J}{g \rho_o} \frac{\partial \rho_o}{\partial z}$$

$$- \frac{i\sigma}{g} \frac{\partial \Omega}{\partial z}$$

$$\frac{\partial w}{\partial z} = \gamma H \frac{\partial \chi}{\partial z} - \gamma \chi + \chi - \frac{\gamma - 1}{g} \frac{\partial J}{\partial z} + \frac{(\gamma-1)J}{g H} \left(1 + \frac{\partial H}{\partial z} \right)$$

$$- \frac{i\sigma}{g} \frac{\partial \Omega}{\partial z}$$

So equation A-34 becomes

$$\chi - \gamma H \frac{\partial \chi}{\partial z} + \gamma \chi - \chi + \frac{\gamma - 1}{g} \frac{\partial J}{\partial z} - \frac{(\gamma-1)J}{g H} \left(1 + \frac{\partial H}{\partial z} \right)$$

$$- \frac{i\sigma}{g} \frac{\partial \Omega}{\partial z} = \frac{i\sigma}{4\, a^2\, \omega^2} F\left(\frac{\delta p}{\rho_o} + \Omega\right) \tag{A-52}$$

Now assume that the following terms can be expanded in terms of the eigenfunctions of F as

$$u = \sum_n u_n(z)\, \psi_n(\theta,\phi) e^{i\sigma t} \tag{A-53}$$

$$v = \sum_n v_n(z)\, \psi_n(\theta,\phi) e^{i\sigma t} \tag{A-54}$$

$$w = \sum_n w_n(z)\, \psi_n(\theta,\phi) e^{i\sigma t} \tag{A-55}$$

$$\delta\rho = \sum_n \delta p_n(z)\, \psi_n(\theta,\phi) e^{i\sigma t} \tag{A-56}$$

$$\delta T = \sum_n \delta T_n(z)\, \psi_n(\theta,\phi) e^{i\sigma t} \tag{A-57}$$

$$\Omega = \sum_n \Omega_n(z)\, \psi_n(\theta,\phi) e^{i\sigma t} \tag{A-58}$$

Substitute equations A-53 thru A-58 into A-52 and remember that $\psi_n(\theta,\phi)$ is a set of orthogonal functions and thus the equation must be true for every value of n.

$$\left[- \gamma H \frac{\partial \chi_n}{\partial z} + \gamma \chi_n + \frac{\gamma - 1}{g} \frac{\partial J_n}{\partial z} - \frac{(\gamma-1) J_n}{g H} \left(1 + \frac{\partial H}{\partial z}\right)\right.$$

$$- \frac{i\sigma}{g} \frac{\partial \Omega_n}{\partial z} \Big] \psi_n e^{i\sigma t} = \frac{i\sigma}{4 a^2 \omega^2} F\Big[\Big(\frac{\delta p_n}{\rho_o} + \Omega_n\Big) \psi_n\Big] e^{i\sigma t} \qquad \text{(A-59)}$$

But

$$F\left[\left(\frac{\delta p_n}{\rho_o} + \Omega_n\right)\psi_n\right] = \left(\frac{\delta p_n}{\rho_o} + \Omega_n\right) F(\psi_n)$$

$$= \left(\frac{\delta p_n}{\rho_o} + \Omega_n\right)\left(- \frac{4 a^2 \omega^2}{g h_n} \psi_n\right)$$

So from equation A-59

$$\frac{\delta p_n}{\rho_o} + \Omega_n = \frac{\gamma g h_n}{i\sigma} \left(H \frac{\partial \chi_n}{\partial z} - \chi_n - \frac{\kappa}{g} \frac{\partial J_n}{\partial z} + \frac{\kappa}{g H} J_n \right.$$

$$\left. + \frac{\kappa J_n}{g H} \frac{\partial H}{\partial z} + \frac{i\sigma}{g\gamma} \frac{\partial \Omega_n}{\partial z} \right)$$

Since the term $\frac{\partial \Omega_n}{\partial z}$ is of the order $\frac{h_n \Omega_n}{a} << \Omega_n$, then it will be neglected in comparison with Ω_n. Also note that

$$\left(H \frac{\partial}{\partial z} - 1\right)\left(\chi_n - \frac{\kappa J_n}{g H}\right) = H \frac{\partial \chi_n}{\partial z} - \chi_n + \frac{\kappa J_n}{g H}$$

$$- \frac{\kappa}{g} \frac{\partial J_n}{\partial z} + \frac{\kappa J_n}{g H} \frac{\partial H}{\partial z}$$

So

$$\frac{\delta p_n}{\rho_o} + \Omega_n = \frac{\gamma g h_n}{i \sigma} \left(H \frac{\partial}{\partial z} - 1 \right) \left(\chi_n - \frac{\kappa J_n}{g H} \right) \qquad \text{(A-60)}$$

When equations A-53 thru A-58 are combined with equation A-38, we get

$$\delta p_n = \frac{g \gamma}{i \sigma} \left(\frac{\rho_o}{\gamma} w_n - \rho_o H \chi_n + \frac{\kappa \rho_o}{g} J_n \right)$$

Then equation A-60 becomes

$$\frac{g}{i \sigma} \left(w_n - \gamma H \chi_n + \frac{\kappa \gamma}{g} J_n \right) + \Omega_n = \frac{\gamma g h_n}{i \sigma} \left(H \frac{\partial}{\partial z} - 1 \right) \left(\chi_n - \frac{\kappa J_n}{g H} \right)$$

$$w_n = \gamma H \chi_n - \frac{\kappa \gamma}{g} J_n - \frac{i\sigma}{g} \Omega_n + \gamma h_n \left(H \frac{\partial}{\partial z} - 1 \right) \left(\chi_n - \frac{\kappa J_n}{g H} \right)$$

$$w_n = - \frac{i \sigma}{g} \Omega_n + \gamma \left[\left(\chi_n - \frac{\kappa J_n}{g H} \right) H + \left(H h_n \frac{\partial}{\partial z} - h_n \right) \left(\chi_n - \frac{\kappa J_n}{g H} \right) \right]$$

$$w_n = -\frac{i\sigma}{g}\Omega_n + \gamma\left(H h_n \frac{\partial}{\partial z} + H - h_n\right)\left(\chi_n - \frac{\kappa J_n}{g H}\right) \qquad \text{(A-61)}$$

By substitution of equations A-53 thru A-58 into equation A-32, we get

$$v_n\psi_n = \frac{i\sigma}{4 a \omega^2 (f^2 - \cos^2\theta)}\left(\frac{i\cos\theta}{f}\frac{\partial}{\partial\theta} + \frac{1}{\sin\theta}\frac{\partial}{\partial\phi}\right)$$

$$\left[\left(\frac{\delta p_n}{\rho_o} + \Omega_n\right)\psi_n\right]$$

or considering v_n as an operator, we have

$$v_n = \frac{i\sigma}{4 a \omega^2 (f^2 - \cos^2\theta)}\left(\frac{\delta p_n}{\rho_o} + \Omega_n\right)\left(\frac{i\cos\theta}{f}\frac{\partial}{\partial\theta} +\right.$$

$$\left.\frac{1}{\sin\theta}\frac{\partial}{\partial\phi}\right)$$

With the help of equation A-60, this becomes

$$v_n = \frac{i\sigma}{4 a \omega^2 (f^2 - \cos^2\theta)}\frac{\gamma g h_n}{i\sigma}\left[\left(H\frac{\partial}{\partial z} - 1\right)\left(\chi_n - \frac{\kappa J_n}{g H}\right)\right]$$

$$\left(\frac{i\cos\theta}{f}\frac{\partial}{\partial\theta} + \frac{1}{\sin\theta}\frac{\partial}{\partial\phi}\right)$$

$$v_n = \frac{\gamma g h_n}{4 a \omega^2 (f^2 - \cos^2\theta)} \left[\left(H \frac{\partial}{\partial z} - 1\right)\left(\chi_n - \frac{\kappa J_n}{g H}\right)\right]$$

$$\left(\frac{i \cos\theta}{f} \frac{\partial}{\partial\theta} + \frac{1}{\sin\theta} \frac{\partial}{\partial\phi}\right) \qquad \text{(A-62)}$$

By substitution of equations A-53 thru A-58 into equation A-34, we get

$$u_n \psi_n = \frac{\sigma}{4 a \omega^2 (f^2 - \cos^2\theta)} \left(i \frac{\partial}{\partial\theta} + \frac{\cot\theta}{f} \frac{\partial}{\partial\phi}\right)$$

$$\left[\left(\frac{\delta p_n}{\rho_o} + \Omega_n\right) \psi_n\right]$$

$$u_n = \frac{\sigma}{4 a \omega^2 (f^2 - \cos^2\theta)} \left(\frac{\delta p_n}{\rho_o} + \Omega_n\right)\left(i \frac{\partial}{\partial\theta} + \frac{\cot\theta}{f} \frac{\partial}{\partial\phi}\right) \qquad \text{(A-63)}$$

By substitution of equations A-53 thru A-58 into equation A-37, we get

$$\delta T_n \psi_n = \frac{\kappa M}{i\sigma R} \left(\gamma J_n \psi_n - g \gamma H \chi_n \psi_n - \frac{g}{\kappa} \frac{\partial H}{\partial z} w_n \psi_n\right)$$

$$\delta T_n = \frac{\kappa M}{i \sigma R} \left(\gamma J_n - g \gamma H \chi_n - \frac{g}{\kappa} \frac{\partial H}{\partial z} w_n\right) \qquad \text{(A-64)}$$

Transformation to Scale Height Corrected Altitude

Thus equations A-60, A-61, A-62, A-63 and A-64 give the solutions of u_n, v_n, w_n, δp_n, and δT_n in terms of χ_n, Ω_n, J_n and their derivatives. These equations can be simplified by a transformation to scale height corrected altitudes. Define the scale height corrected altitude x as

$$x = \int_o^z \frac{d\xi}{H(\xi)} \tag{A-65}$$

Define $y_n(x)$ as

$$y_n(x)\ e^{x/2} = \chi_n(z) - \frac{\kappa J_n(z)}{g\ H(z)} \tag{A-66}$$

From equations A-1 and A-2

$$\frac{\partial p_o}{\partial z} = - g\ \rho_o$$

$$p_o = g\ \rho_o\ H$$

$$\frac{\partial p_o}{\partial_z} = \frac{p_o}{H}$$

$$\frac{dp_o}{p_o} = - \frac{dz}{H}$$

$$\ell n\ p_o(x) = - x + \text{constant}$$

where $\text{constant} = \ell n\ p_o(o)$

$$\ell n\ \frac{p_o(x)}{p_o(o)} = -x$$

$$p_o(x) = p_o(0)\ e^{-x} \qquad \text{(A-67)}$$

Solving equation A-66 for $\chi_n(z)$ and then differentiating with respect to z, we get

$$\frac{\partial \chi_n}{\partial z} = \frac{\partial y_n}{\partial x} e^{x/2} \frac{\partial x}{\partial z} + \frac{1}{2} y_n e^{x/2} \frac{\partial x}{\partial z} + \frac{\kappa}{g\ H} \frac{\partial J_n}{\partial z}$$

$$- \frac{\kappa\ J_n}{g\ H^2} \frac{\partial H}{\partial z}$$

From equation A-65, we get

$$\frac{\partial x}{\partial z} = \frac{1}{H}$$

So

$$\frac{\partial \chi_n}{\partial z} = \frac{1}{H} \frac{\partial y_n}{\partial x} e^{x/2} + \frac{1}{2\ H} y_n e^{x/2} + \frac{\kappa}{g\ H} \frac{\partial J_n}{\partial z}$$

$$- \frac{\kappa J_n}{g\ H^2} \frac{\partial H}{\partial z}$$

$$\frac{\partial^2 \chi_n}{\partial z^2} = \frac{1}{2H^2}\frac{\partial y_n}{\partial x}e^{x/2} + \frac{1}{H^2}\frac{\partial^2 y_n}{\partial x^2}e^{x/2} - \frac{1}{H^2}\frac{\partial y_n}{\partial x}e^{x/2}\frac{\partial H}{\partial z}$$

$$+ \frac{1}{4H^2}y_n e^{x/2} + \frac{1}{2H^2}\frac{\partial y_n}{\partial x}e^{x/2} - \frac{1}{2H^2}y_n e^{x/2}\frac{\partial H}{\partial z}$$

$$+ \frac{\kappa}{gH}\frac{\partial^2 J_n}{\partial z^2} - \frac{\kappa}{gH^2}\frac{\partial J_n}{\partial z}\frac{\partial H}{\partial z} - \frac{\kappa J_n}{gH^2}\frac{\partial^2 H}{\partial z^2}$$

$$- \frac{\kappa}{gH^2}\frac{\partial H}{\partial z}\frac{\partial J_n}{\partial z} + \frac{2\kappa J_n}{gH^3}\frac{\partial H}{\partial z}\frac{\partial H}{\partial z}$$

When the last two equations are substituted into the differential equation A-51, we get

$$\frac{1}{2H}\frac{y_n}{x}e^{x/2} + \frac{1}{H}\frac{\partial^2 y_n}{\partial x^2}e^{x/2} - \frac{1}{H}\frac{\partial y_n}{\partial x}e^{x/2}\frac{\partial H}{\partial z}$$

$$+ \frac{1}{4H}y_n e^{x/2} + \frac{1}{2H}\frac{\partial y_n}{\partial x}e^{x/2} - \frac{1}{2H}y_n e^{x/2}\frac{\partial H}{\partial z}$$

$$+ \frac{\kappa}{g}\frac{\partial^2 J_n}{\partial z^2} - \frac{\kappa}{gH}\frac{\partial J_n}{\partial z}\frac{\partial H}{\partial z} - \frac{\kappa J_n}{gH}\frac{\partial^2 H}{\partial z^2}$$

$$- \frac{\kappa}{gH}\frac{\partial H}{\partial z}\frac{\partial J_n}{\partial z} + \frac{2\kappa J_n}{gH^2}\frac{\partial H}{\partial z}\frac{\partial H}{\partial z} + \frac{1}{H}\frac{\partial y_n}{\partial x}e^{x/2}\frac{\partial H}{\partial z}$$

$$+ \frac{1}{2H} y_n e^{x/2} \frac{\partial H}{\partial z} + \frac{\kappa}{gH} \frac{\partial J_n}{\partial z} \frac{\partial H}{\partial z} - \frac{\kappa J_n}{gH^2} \frac{\partial H}{\partial z} \frac{\partial H}{\partial z}$$

$$- \frac{1}{H} \frac{\partial y_n}{\partial x} e^{x/2} - \frac{1}{2H} y_n e^{x/2} - \frac{\kappa}{gH} \frac{\partial J_n}{\partial z} + \frac{\kappa J_n}{gH^2} \frac{\partial H}{\partial z}$$

$$+ \frac{\kappa}{h_n} y_n e^{x/2} + \frac{\kappa^2 J_n}{g h_n H} + \frac{1}{h_n} y_n e^{x/2} \frac{\partial H}{\partial z} + \frac{\kappa J_n}{gH h_n} \frac{\partial H}{\partial z}$$

$$= \frac{\kappa J_n}{gH h_n} + \frac{\kappa J_n}{gH h_n} \frac{\partial H}{\partial z} + \frac{\kappa}{g} \frac{\partial^2 J_n}{\partial z^2} - \frac{\kappa}{gH} \frac{\partial J_n}{\partial z}$$

$$+ \frac{\kappa J_n}{gH^2} \frac{\partial H}{\partial z} - \frac{\kappa}{gH} \frac{\partial H}{\partial z} \frac{\partial J_n}{\partial z} - \frac{\kappa J_n}{gH} \frac{\partial^2 H}{\partial z^2}$$

$$+ \frac{\kappa J_n}{gH^2} \frac{\partial H}{\partial z} \frac{\partial H}{\partial z}$$

The combining of like terms gives us

$$\frac{\partial^2 y_n}{\partial x^2} \left(\frac{e^{x/2}}{H} \right) - \frac{1}{4} y_n \left(\frac{e^{x/2}}{H} \right) + \frac{\kappa H}{h_n} y_n \left(\frac{e^{x/2}}{H} \right)$$

$$+ \frac{H}{h_n} \frac{\partial H}{\partial z} y_n \left(\frac{e^{x/2}}{H} \right) = \frac{J_n}{g H h_n} \kappa \quad (1 - \kappa) \bar{e}^{x/2}$$

$$\frac{\partial^2 y_n}{\partial x^2} - \frac{1}{4} \left[1 - \frac{4}{h_n} \left(\kappa H + H \frac{\partial H}{\partial z} \right) \right] \quad y_n(x) = \frac{\kappa}{g \gamma h_n} J_n(x) \, e^{-x/2}$$

But

$$\frac{\partial H}{\partial z} = \frac{\partial H}{\partial x} \frac{\partial x}{\partial z} = \frac{1}{H} \frac{\partial H}{\partial x}$$

$$\frac{\partial^2 y_n}{\partial x^2} - \frac{1}{4} \left[1 - \frac{4}{h_n} \left(\kappa H + \frac{\partial H}{\partial x} \right) \right] y_n = \frac{\kappa}{\gamma g h_n} J_n \, e^{x/2} \qquad \text{(A-68)}$$

This is the differential equation for χ_n in terms of the new variables.

To transform equations A-60, A-61, A-62, A-63 and A-64, note that

$$\frac{\partial}{\partial z} = \frac{\partial x}{\partial z} \frac{\partial}{\partial x} = \frac{1}{H} \frac{\partial}{\partial x}$$

So equation A-63 becomes

$$u_n = \frac{\gamma g h_n}{4 a \omega^2 (f^2 - \cos^2 \theta)} \left(\frac{\partial y_n}{\partial x} e^{x/2} + \frac{1}{2} y_n e^{x/2} + \frac{\kappa}{g} \frac{\partial J_n}{\partial z} \right.$$

$$- \frac{\kappa J_n}{g H} \frac{\partial H}{\partial z} - \frac{\kappa}{g} \frac{\partial J_n}{\partial z} + \frac{\kappa J_n}{g H} \frac{\partial H}{\partial z} - y_n e^{x/2}$$

$$- \frac{\kappa}{g} \frac{J_n}{H} + \frac{\kappa J_n}{g H} \left(\frac{\partial}{\partial \theta} - \frac{i \cot \theta}{f} \frac{\partial}{\partial \phi} \right)$$

$$u_n = \frac{\gamma g h_n e^{x/2}}{4 a \omega^2 (f^2 - \cos^2 \theta)} \left(\frac{\partial y_n}{\partial x} - \frac{1}{2} y_n \right) \left(\frac{\partial}{\partial \theta} - \frac{i \cot \theta}{f} \frac{\partial}{\partial \phi} \right) \quad \text{(A-69)}$$

From equation A-62

$$v_n = \frac{i \gamma g h_n}{4 a \omega^2 (f^2 - \cos^2 \theta)} \left(\frac{\partial y_n}{\partial x} e^{x/2} + \frac{1}{2} y_n e^{x/2} + \frac{\kappa}{g} \frac{\partial J_n}{\partial z} \right.$$

$$- \frac{\kappa J_n}{g H} \frac{\partial H}{\partial z} - \frac{\kappa}{g} \frac{\partial J_n}{\partial z} + \frac{\kappa J_n}{g H} \frac{\partial H}{\partial z} - y_n e^{x/2}$$

$$\left. - \frac{\kappa J_n}{g H} + \frac{\kappa J_n}{g H} \right) \left(\frac{\cos \theta}{f} \frac{\partial}{\partial \theta} - \frac{i}{\sin \theta} \frac{\partial}{\partial \phi} \right)$$

$$v_n = \frac{i \gamma g h_n e^{x/2}}{4 a \omega^2 (f^2 - \cos^2 \theta)} \left(\frac{\partial y_n}{\partial x} - \frac{1}{2} y_n \right) \left(\frac{\cos \theta}{f} \frac{\partial}{\partial \theta} - \frac{i}{\sin \theta} \frac{\partial}{\partial \phi} \right)$$

(A-70)

From equation A-61

$$w_n = - \frac{i\sigma}{g} \Omega_n + \gamma \left(h_n \frac{\partial y_n}{\partial x} e^{x/2} + \frac{h_n}{2} y_n e^{x/2} + \frac{h_n \kappa}{g} \frac{\partial J_n}{\partial z} \right.$$

$$- \frac{h_n \kappa J_n}{g H} \frac{\partial H}{\partial z} - \frac{h_n \kappa}{g} \frac{\partial J_n}{\partial z} + \frac{\kappa J_n}{g H} \frac{\partial H}{\partial z}$$

$$+ H y_n e^{x/2} + \frac{\kappa J_n}{g} - \frac{\kappa J_n}{g} - h_n y_n e^{x/2}$$

$$\left. - \frac{h_n \kappa J_n}{g H} + \frac{h_n \kappa J_n}{g H} \right)$$

$$w_n = - \frac{i \sigma}{g} \Omega_n + \gamma h_n e^{x/2} \left[\frac{\partial y_n}{\partial x} + \left(\frac{H}{h_n} - \frac{1}{2} \right) y_n \right] \qquad \text{(A-71)}$$

From equation A-60, we have

$$\delta p_n = \frac{\gamma h_n p_o}{i \sigma H} \left(H \frac{\partial}{\partial z} - 1 \right) \left(\chi_n - \frac{\kappa J_n}{g H} \right) - \frac{p_o \Omega_n}{g H}$$

From the derivation of equations A-60 and with the use of equation A-66, we get

$$\delta p_n = \frac{\gamma h_n p_o}{i \sigma H} \left(\frac{\partial y_n}{\partial x} e^{x/2} - \frac{1}{2} y_n e^{x/2} \right) - \frac{p_o \Omega_n}{g H}$$

With the use of equation A-67, we have

$$\delta p_n = \frac{p_o(0)}{H} \left[- \frac{\Omega_n}{g} e^{-x} + \frac{\gamma h_n}{i\sigma} e^{-x/2} \left(\frac{\partial y_n}{\partial x} - \frac{1}{2} y_n \right) \right] \qquad \text{(A-72)}$$

From equation A-64, we get

$$\delta T_n = \frac{\kappa M}{i \sigma R} \left(\gamma J_n - g\gamma H \chi_n \right) - \frac{g M}{i \sigma R} \frac{\partial H}{\partial z} w_n$$

$$= \frac{\kappa M}{i \sigma R} \left(\gamma J_n - g\gamma H y_n e^{x/2} - \gamma \kappa J_n \right)$$

$$- \frac{g M}{i \sigma R H} \frac{\partial H}{\partial x} w_n$$

$$= \frac{\kappa M}{i\sigma R} J_n - \frac{\kappa M g \gamma H}{i \sigma R} y_n e^{x/2} - \frac{g M}{i \sigma R H} \frac{\partial H}{\partial x}$$

$$\left\{ - \frac{i\sigma}{g} \Omega_n + \gamma h_n e^{x/2} \left[\frac{\partial y_n}{\partial x} + \left(\frac{H}{h_n} - \frac{1}{2} \right) y_n \right] \right\}$$

$$\delta T_n = \frac{M}{R} \left\{ \frac{\Omega_n}{H} \frac{\partial H}{\partial x} - \frac{\gamma g h_n}{i \sigma} e^{x/2} \left[\frac{\kappa H}{h_n} + \frac{1}{H} \frac{\partial H}{\partial x} \left(\frac{\partial}{\partial x} \right. \right. \right.$$

$$+ \frac{H}{h_n} - \frac{1}{2}\Big)\Big] y_n + \frac{\kappa J_n}{i\sigma}\Big\} \qquad \text{(A-73)}$$

Note that if $f \ll 1$, i.e. for oscillations with longer than a 12 hour period, equations A-69 and A-70 have zeros in the denominator for certain values of θ. However it was shown by Brillouin in 1932 that the numerators disappear for these values of θ and that no singularities are present.

Thus the formal development of the theory is finished with equations A-69, A-70, A-71, A-72 and A-73. In order to examine the tidal oscillations further, we must know the form of the functions H, Ω and J. In addition, the differential equations A-50 and A-68 must be solved under certain boundary conditions. In general, this cannot be done. However, with the help of some very simplying assumptions, some of the more general motion of the atmosphere can be obtained.

The boundary conditions which are imposed on the solutions of equation A-68 are discussed in detail in Chapter II and will not be reiterated here.

Eigenvalue Calculation for Isothermal Atmosphere

For an example, let us calculate the eigenvalues of a free isothermal atmosphere and a free atmosphere in adiabatic equilibrium. To consider the conditions for free oscillations of the atmosphere, we must first set the exciting forces J_n and Ω_n equal to zero. Then the boundary condition at ground level becomes from equation II-9.

$$\left[\frac{\partial y_n}{\partial x} + \left(\frac{H}{h_n} - \frac{1}{2} \right) y_n \right]_{x = 0} = 0 \qquad \text{(A-74)}$$

Now the only unknown function in equation A-68 is H(x). For an isothermal atmosphere H(x) is constant or

$$H(x) = H(0) \qquad \text{(A-75)}$$

When this is substituted into equation A-68, we get

$$\frac{\partial^2 y_n}{\partial x^2} - \frac{1}{4} \left(1 - \frac{4 \kappa H(0)}{\hat{h}_n} \right) y_n = 0 \qquad \text{(A-76)}$$

For $\hat{h}_n > 4 \kappa H(0)$, solutions of this will be

$$y_n(x) = A_n \exp \left[-\frac{x}{2} \left(1 - \frac{4 \kappa H(0)}{\hat{h}_n} \right)^{1/2} \right]$$

$$+ B_n \exp \left[\frac{x}{2} \left(1 - \frac{4 \kappa H(0)}{\hat{h}_n} \right)^{1/2} \right]$$

By the boundary condition for large x which is discussed in Chapter II, this becomes

$$y_n(x) = A_n \exp \left[-\frac{x}{2} \left(1 - \frac{4 \kappa H(0)}{\hat{h}_n} \right)^{1/2} \right]$$

By substitution of this into the lower boundary condition A-74,

we get

$$\left[-\frac{1}{2}\left(1 - \frac{4\kappa H(0)}{\hat{h}_n}\right)^{1/2} y_n(x) + \frac{H(0)}{\hat{h}_n}\, y_n(x) - \frac{1}{2}\, y_n(x) \right]_{x=0} = 0$$

$$-\frac{1}{2}\left(1 - \frac{4\kappa H(0)}{\hat{h}_n}\right)^{1/2} - \frac{1}{2} + \frac{H(0)}{\hat{h}_n} = 0$$

$$\frac{1}{4} - \frac{\kappa H(0)}{\hat{h}_n} = \frac{H^2(0)}{\hat{h}_n^2} - \frac{H(0)}{\hat{h}_n} + \frac{1}{4}$$

$$\hat{h}_n \left(H(0) - \kappa H(0)\right) = H^2(0)$$

$$\hat{h}_n = \frac{\gamma\ H^2(0)}{\gamma\ H(0) - \gamma\ H(0) + H(0)}$$

$$\hat{h}_n = \gamma\ H(0) \qquad \text{(A-77)}$$

This is the eigenvalue that Laplace obtained for the case where γ was set equal to one.

Eigenvalue Calculation for Atmosphere in Adiabatic Equilibrium

For the case of adiabatic equilibrium, the density and pressure are connected by a power law which is valid for both the disturbed and undisturbed atmosphere.

$$\frac{p}{p_o} = \left(\frac{\rho}{\rho_o}\right)^{\gamma} \tag{A-78}$$

where $\gamma = \frac{c_p}{c_v}$ and $\frac{p_o}{\rho_o^{\gamma}}$ is a constant.

If equation A-78 is expanded and only first order terms are kept, then we get

$$\frac{p}{p_o} = \frac{p_o + \delta p}{p_o} = 1 + \frac{\delta p}{p_o}$$

$$\left(\frac{\rho}{\rho_o}\right)^{\gamma} = \left(\frac{\rho_o + \delta\rho}{\rho_o}\right)^{\gamma} = 1 + \gamma \frac{\delta\rho}{\rho_o}$$

or

$$\delta p = \gamma \frac{p_o}{\rho_o} \delta\rho$$

But from equation A-2, we get

$$\delta p = \gamma \; g \; H \; \delta\rho \tag{A-79}$$

Now we know

$$\frac{p_o}{\rho_o^{\gamma}} = \text{constant} \tag{A-80}$$

$$\frac{g \; H}{\rho_o^{\gamma - 1}} = \text{constant}$$

or

$$\frac{g}{\rho_o^{\gamma-1}} \frac{\partial H}{\partial x} - \frac{g \; H \; (\gamma-1)}{\rho_o^{\gamma-2}} \frac{\partial \rho_o}{\partial x} = 0$$

$$\frac{\partial H}{\partial x} = (\gamma-1) \; H \; \rho_o \frac{\partial \rho_o}{\partial x}$$

However from equation A-80

$$\frac{1}{\rho_o^{\gamma}} \frac{\partial p_o}{\partial x} - \frac{\gamma \; p_o}{\rho_o^{\gamma-1}} \frac{\partial \rho_o}{\partial x} = 0$$

$$\rho_o \frac{\partial \rho_o}{\partial x} = \frac{1}{\gamma \; p_o} \frac{\partial p_o}{\partial x}$$

With the help of equation A-67, this becomes

$$\rho_o \frac{\partial \rho_o}{\partial x} = - \frac{1}{\gamma}$$

So

$$\frac{\partial H}{\partial x} = - \frac{\gamma - 1}{\gamma} H = - \kappa H$$

$$\ell n\, H = - \kappa x + \text{constant}$$

But at $x = 0$, $\ell n\, H(0) = \text{constant}$

so

$$H(x) = H(0)\, e^{- \kappa x} \tag{A-81}$$

When this equation is substituted into equation A-68, we get

$$\frac{\partial^2 y_n}{\partial x^2} - \frac{1}{4} \left[1 - \frac{4 \kappa H(x)}{\hat{h}_n} + \frac{4\kappa}{\hat{h}_n} H(x) \right] y_n = 0$$

or

$$\frac{\partial^2 y_n}{\partial x^2} - \frac{1}{4} y_n = 0 \tag{A-82}$$

Solutions of this equation are

$$y_n(x) = A_n e^{- \frac{1}{2} x} + B_n e^{\frac{1}{2} x}$$

Again, the upper boundary condition forces $B_n = 0$. So when $y_n(x)$ is substituted into equation A-74 to take account of the lower boundary

condition, we get

$$\left[-\frac{1}{2} y_n(x) + \left(\frac{H(x)}{\hat{h}_n} - \frac{1}{2} \right) y_n(x) \right]_{x = 0} = 0$$

or

$$-\frac{1}{2} + \frac{H(o)}{\hat{h}_n} - \frac{1}{2} = 0$$

$$h_n = H(o) \tag{A-83}$$

This is the condition which Lamb (1924) derived.

Derivation of Laplace's Tidal Equation

Oceanic Tides

The equation A-50 first appeared in Laplace's theory of oceanic tides. It is rather easy to derive it for tides in a homogeneous ocean. For this purpose, we must assume an incompressible fluid and that the density is constant, i. e. $\rho = \rho_o$ = constant. Let $z = 0$ be the surface of the earth and $z = h$ be the surface of the undisturbed ocean. Let variations of the surface elevations be denoted by $\zeta(\theta,\phi,t)$. Then $z = h + \zeta$ is the surface of the disturbed ocean. Then the variation in the density can be represented by

$$\delta\rho = \begin{cases} 0 & \text{if } z > h + \zeta \\ \rho_o & \text{if } z < h + \zeta \end{cases} \tag{A-84}$$

and

$$\zeta = \frac{1}{\rho_o} \int_h^z \delta\rho \, dz' , \quad z \geq h + \zeta \tag{A-85}$$

Now assuming that the variation of Ω with respect to z is very small, we get from equation A-14

$$\frac{\partial}{\partial z} (\delta p) = - g \, \delta\rho$$

or

$$\int_o^\zeta d(\delta p) = - \int_o^\zeta g \, \delta\rho \, dz$$

$$\delta p(\zeta) - \delta p(0) = - g \, \rho_o \, \zeta$$

Assume that $\delta p(\zeta) = 0$, i.e. free surface.

$$\frac{\delta p}{\rho_o} = g \, \zeta \tag{A-86}$$

By consideration of equation A-86 and the fact that Ω depends only on ζ now, then equations A-12 and A-13 tell us that u and v do not

depend on z. Also from the continuity equation A-30, we have

$$\frac{d\rho}{dt} = -\rho_o \chi$$

But because of incompressibility of the fluid

$$\frac{d\rho}{dt} = 0$$

So

$$\chi = 0 \qquad \text{(A-87)}$$

Assume that the time dependence of ζ is exp $(i\sigma t)$ where σ is the frequency of the oscillation. Then by using equation A-87 and the fact that $w(o) = 0$ and $w(\zeta) = \frac{\partial \zeta}{\partial t} = i\sigma\zeta$, we can integrate equation A-31 to get

$$\int_o^{h+\zeta} \frac{\partial w}{\partial z}\, dz = -\left[\frac{1}{a \sin\theta}\frac{\partial}{\partial\theta}(u \sin\theta) + \frac{1}{a \sin\theta}\frac{\partial v}{\partial\phi}\right]\int_o^{h+\zeta} dz$$

$$w(h+\zeta) + \left[\frac{1}{a \sin\theta}\frac{\partial}{\partial\theta}(u \sin\theta) + \frac{1}{a \sin\theta}\frac{\partial v}{\partial\phi}\right](h+\zeta) = 0$$

But

$$w(h+\zeta) = \frac{\partial}{\partial t}(h+\zeta) = \frac{\partial \zeta}{\partial t} = i\sigma t$$

So

$$\frac{h}{a \sin \theta} \frac{\partial}{\partial \theta} (u \sin \theta) + \frac{h}{a \sin \theta} \frac{\partial v}{\partial \phi} + i\sigma t = 0 \qquad \text{(A-88)}$$

Now define the surface elevation of the equilibrium tide as

$$\bar{\zeta} = -\frac{\Omega}{g} \qquad \text{(A-89)}$$

By substituting equations A-32, A-34, A-86 and A-89 into equation A-88, we get

$$F(\zeta - \bar{\zeta}) + \frac{4 a^2 \omega^2}{g h} \zeta = 0 \qquad \text{(A-90)}$$

where F is defined by equation A-35.

This equation is the fundamental equation of free and forced tidal oscillations of a homogeneous ocean covering the whole earth at a uniform depth of h. The effect of mutual attraction of the disturbed masses, which is appreciable for an ocean of water, is not considered here.

Atmospheric Tides

If we assume a free oceanic oscillation ($\bar{\zeta} = 0$) and expand ζ in terms of the eigenfunctions $\psi_n(\theta,\phi)$ then equation A-90 becomes identical to equation A-50 if $h = h_n$. Hence this is the reason the separation constant h_n is called the "equivalent depth."

Now let us determine the eigenfunctions $\psi_n(\theta,\phi)$ in the case of a nonrotating earth. From equation A-50

$$\frac{F(\psi_n)}{\omega^2} + \frac{4\,a^2}{g\,h_n}\,\psi_n = 0$$

With the help of equations A-30 and A-31, this becomes

$$\frac{1}{\sin\theta}\frac{\partial}{\partial\theta}\left(\frac{\sin\theta}{\frac{\sigma^2}{4} - \omega^2\cos^2\theta}\frac{\partial}{\partial\theta}\right)\psi_n$$

$$+ \frac{1}{\frac{\sigma^2}{4} - \omega^2\cos^2\theta}\left[\frac{i\left(\frac{1}{2}\sigma\,\omega + \frac{1}{\sigma}\,2\,\omega^3\cos^2\theta\right)}{\frac{\sigma^2}{4} - \omega^2\cos^2\theta}\frac{\partial}{\partial\phi} + \frac{1}{\sin^2\theta}\frac{\partial^2}{\partial\phi^2}\right]\psi_n$$

$$+ \frac{4\,a^2}{g\,h_n}\,\psi_n = 0$$

Now setting $\omega = 0$, we have

$$\frac{4}{\sigma^2}\frac{1}{\sin\theta}\frac{\partial}{\partial\theta}\left(\sin\theta\frac{\partial}{\partial\theta}\right)\psi_n + \frac{4}{\sigma^2}\left(\frac{1}{\sin^2\theta}\frac{\partial^2}{\partial\phi^2}\right)\psi_n$$

$$+ \frac{4\,a^2}{g\,h_n}\,\psi_n = 0$$

or

$$\frac{1}{\sin\theta}\frac{\partial}{\partial\theta}\left(\sin\theta\frac{\partial\psi_n}{\partial\theta}\right) + \frac{1}{\sin^2\theta}\frac{\partial^2\psi_n}{\partial\phi^2} + \frac{a^2\sigma^2}{g\,h_n}\,\psi_n = 0 \qquad \text{(A-91)}$$

This is the well known spherical harmonics equation and we know solutions for it exist only if

$$\frac{a^2 \sigma^2}{g h_n} = n(n+1) \qquad n = 1, 2, 3 \ldots$$

so

$$h_n = \frac{a^2 \sigma^2}{n (n+1) g} \qquad n = 1, 2, 3 \ldots \qquad \text{(A-92)}$$

Equation A-92 tells us that a forced oscillation of frequency σ will have many equivalent depths h_n.

Eigenfunctions for Non-rotating Earth

The solution of equation A-91 then becomes

$$\psi_n(\theta,\phi) = P_n^s (\theta)\, e^{i s \phi} \qquad \text{(A-93)}$$

where s is an integer and $-n \leq s \leq n$. The $P_n^s(\theta)$ are the Associated Legendre Polynomials.

Hence, for each h_n there are $2n + 1$ different functions. This is due to the fact that for the non-rotating earth, h_n is independent of the parameter s. The nodal lines of equation A-93 on a sphere consist of 2s meridians and n - s parallels of the colalitude. If $s > 0$ then the wave is traveling westward. If $s < 0$ then the wave is traveling eastward. A standing zonal oscillation is given by $s = 0$.

Eigenfunctions for Rotating Earth

Now let us consider the solutions of equation A-91 for the case

of a rotating earth. Equation A-93 will no longer be sufficient. Hough [1898] was the first to solve this problem. He developed a new set of orthogonal spherical functions which are denoted as $\Theta^{s}_{\lambda,n}(\theta)$ and are called the Hough Functions. It is generally assumed that these functions are complete but Hough showed that for $\lambda = 1$ and $s = 1$, the Legendre Polynomial $P^{1}_{2}(\theta)$ is orthogonal to each member of $\Theta^{1}_{1,n}(\theta)$. The consequences of this were considered by Lindzen [1965] and will be shown later in this appendix. For the moment let us assume that the Hough Functions are complete. Then the solution of equation A-91 which was found by Hough is

$$\psi_n(\theta,\phi) = \Theta^{s}_{\lambda,n}(\theta)\, e^{is\phi} \qquad \text{(A-94)}$$

Both σ and λ denote the frequency of the forced oscillation. The quantity σ is measured in units of sec^{-1} and λ is in commensurable parts of the day.

Now if equation A-94 is substituted into equation A-50, we have

$$\frac{1}{\sin\theta}\frac{\partial}{\partial\theta}\left(\frac{\sin\theta}{f^2-\cos^2\theta}\frac{\partial\Theta^{s}_{\lambda,n}}{\partial\theta}\right)$$

$$+\frac{1}{f^2-\cos^2\theta}\left[\frac{-s}{f}\frac{f^2+\cos^2\theta}{f^2-\cos^2\theta}\Theta^{s}_{\lambda,n}+\frac{-s^2}{\sin^2\theta}\Theta^{s}_{\lambda,n}\right]$$

$$+\frac{4a^2\omega^2}{g h_n}\Theta^{s}_{\lambda,n} = 0$$

By making the substitution $\mu = \cos\theta$, we have

$$\frac{\partial}{\partial\mu}\left(\frac{1-\mu^2}{f^2-\mu^2}\frac{\partial\Theta^s_{\lambda,n}}{\partial\mu}\right) - \frac{1}{f^2-\mu^2}\left(\frac{s}{f}\frac{f^2+\mu^2}{f^2-\mu^2} + \frac{s^2}{1-\mu^2}\right)\Theta^s_{\lambda,n}$$

$$+ \frac{4a^2\omega^2}{g\,h_n}\Theta^s_{\lambda,n} = 0 \qquad \text{(A-95)}$$

This equation is Laplace's Tidal Equation for longitudinal wave number s and radial frequency σ. In order to solve this equation, specific values of f and s must be assumed. Then each function $\Theta^s_{\lambda,n}$ will have one equivalent depth h_n, i.e. h_n will depend on the three variables f (or λ or σ), s and n. Since the observed phenomenon is defined on a sphere, then the most advantageous way of representing the Hough Functions would probably be by a series expansion in terms of the Associated Legendre Polynomials. In general the equation A-95 is solved by assuming

$$\Theta^s_{\lambda,n}(\mu) = \sum_\nu C^{s,\nu}_{\lambda,n} P^s_\nu(\mu) \qquad \text{(A-96)}$$

Thus we have shown that for ocean tides, the Hough Functions (equation A-96) determine the latitude dependence of the surface elevation. For atmospheric tides, equation A-96 determine the latitude dependence of the quantity (according to equation A-60)

$$\chi_n - \frac{\kappa J_n}{g H} \qquad \text{(A-97)}$$

Correction for Incompleteness of Hough Functions

It was mentioned earlier that for $\lambda = 1$ ($\sigma = \omega$) and $s = 1$, the Hough Functions $\Theta^1_{1,n}(\mu)$ were not complete. So let us consider this situation. Since the Hough Functions are not complete then equation A-49 is incorrect if $\psi_n(\theta,\phi)$ is taken as $\Theta^1_{1,n}(\mu)\ e^{i\,s\,\phi}$ only. We should have

$$J = \left[\frac{}{J(z)}\ P_2^1(\mu) + \sum_n J_n(z)\ \Theta^1_{1,n}(\mu) \right] e^{i(\omega t + \phi)} \qquad \text{(A-98)}$$

This is particularly important because it is found that most of asymmetry in J is accounted for by the P_2^1 term. Now let us concern ourselves only with the following term

$$J' = \overline{J(z)}\ P_2^1(\mu)\ e^{i(\omega t + \phi)} \qquad \text{(A-99)}$$

From equations A-12, A-13, A-14, A-30 and A-24, we have

$$i\,\omega\,u - 2\,\omega\,v\cos\theta = -\frac{1}{a}\frac{\partial}{\partial\theta}\left(\frac{\delta p}{\rho_o}\right) \qquad \text{(A-100)}$$

$$i\,\omega\,v + 2\,\omega\,u\cos\theta = -\frac{1}{a\sin\theta}\frac{\partial}{\partial\phi}\left(\frac{\delta p}{\rho_o}\right) \qquad \text{(A-101)}$$

$$\frac{\partial(\delta p)}{\partial z} = -g\,\delta\,\rho \qquad \text{(A-102)}$$

$$i\,\omega\,\delta\rho + w\,\frac{\partial \rho_o}{\partial z} + \rho_o \chi = 0 \qquad \text{(A-103)}$$

$$i\,\omega\,\delta p + w\,\frac{\partial p_o}{\partial z} = \gamma\, g\, H \left(i\,\omega\,\delta\rho + w\,\frac{\partial \rho_o}{\partial z} \right)$$

$$+ (\gamma - 1)\,\rho_o\, J \qquad \text{(A-104)}$$

From equations A-1 and A-2

$$\frac{1}{p_o}\,\frac{\partial p_o}{\partial z} = -\,\frac{1}{H} \qquad \text{(A-105)}$$

Now it is advantageous to make the transformations

$$u' = \sqrt{\rho_o}\; u,\; v' = \sqrt{\rho_o}\; v,\; w' = \sqrt{\rho_o}\; w,$$

$$\delta p' = \frac{1}{\sqrt{\rho_o}}\;\delta p, \qquad \delta\rho' = \frac{1}{\sqrt{\rho_o}}\;\delta\rho$$

Then from equations A-99 and A-100, we have

$$u' = \frac{2\,v'}{i}\cos\theta - \frac{1}{i\,a\,\omega}\,\frac{\partial(\delta p')}{\partial\theta}$$

$$v' = -\,\frac{2\,u'}{i}\cos\theta - \frac{1}{i\,a\,\omega\sin\theta}\,\frac{\partial(\delta p')}{\partial\phi}$$

$$v' = 4\, v' \cos^2\theta - \frac{2\cos\theta}{a\,\omega}\,\frac{\partial(\delta p')}{\partial\theta}$$

$$- \frac{1}{i\,a\,\omega\sin\theta}\,\frac{\partial(\delta p')}{\partial\phi}$$

$$v' = \frac{-1}{a\,\omega\,(1 - 4\cos^2\theta)}\left(2\cos\theta\,\frac{\partial}{\partial\theta} + \frac{1}{\sin\theta}\right)\delta p' \qquad \text{(A-106)}$$

$$u' = \frac{2\,i\cos\theta}{a\,\omega\,(1 - 4\cos^2\theta)}\left(2\cos\theta\,\frac{\partial}{\partial\theta} + \frac{1}{\sin\theta}\right)\delta p'$$

$$+ \frac{i}{a\,\omega}\,\frac{\partial}{\partial\theta}\,(\delta p')$$

$$u' = \frac{1}{a\,\omega\,(1 - 4\cos^2\theta)}\left(\frac{\partial}{\partial\theta} + 2\cot\theta\right)\delta p' \qquad \text{(A-107)}$$

Following Lindzen [1965], we let

$$\delta p' = \overline{\delta p(z)}\; P_2^1(\theta)$$

or

$$\delta p' = \overline{\delta p(z)}\; \sin\theta\cos\theta \qquad \text{(A-108)}$$

where normalization is neglected.

Then from equations A-107 and A-108, we have

$$u' = \frac{i\,\overline{\delta p(z)}}{a\,\omega}\left(\frac{\cos^2\theta - \sin^2\theta + 2\cot\theta\sin\theta\cos\theta}{1 - 4\cos^2\theta}\right)$$

$$u' = \frac{-i}{a\,\omega}\,\overline{\delta p(z)} \tag{A-109}$$

From equations A-108 and A-106, we have

$$v' = \frac{-\overline{\delta p(z)}}{a\,\omega}\left[\frac{2\cos\theta\,(\cos^2\theta - \sin^2\theta) + \cos\theta}{1 - 4\cos^2\theta}\right]$$

$$v' = \frac{\cos\theta}{a\,\omega}\,\overline{\delta p(z)} \tag{A-110}$$

From equations A-31, A-109 and A-110, we get

$$\chi = \frac{-i\,\overline{\delta p(z)}}{a^2\,\omega}\cot\theta + \frac{i\,\overline{\delta p(z)}}{a^2\omega}\cot\theta + \frac{\partial w}{\partial z}$$

or

$$\chi = \frac{\partial w}{\partial z} \tag{A-111}$$

By the use of equations A-111, A-102 and A-43, we have

$$i\,\omega\sqrt{\rho_o}\;\delta\rho' + \frac{1}{\sqrt{\rho_o}}\,w'\,\frac{\partial\rho_o}{\partial z} + \rho_o\left(\frac{1}{\sqrt{\rho_o}}\,\frac{\partial w'}{\partial z} - \frac{1}{2}\,\frac{w'}{\rho_o 3/2}\,\frac{\partial\rho_o}{\partial z}\right) = 0$$

$$\frac{w'}{2}\,\frac{1}{\rho_o}\,\frac{\partial \rho_o}{\partial z} + \frac{\partial w'}{\partial z} = -\,i\,\omega\,\delta\rho'$$

$$\left[\frac{\partial}{\partial z} - \frac{1}{2\,H}\left(1 + \frac{\partial H}{\partial z}\right)\right] w' = -\,i\,\omega\,\delta\rho' \qquad \text{(A-112)}$$

From equations A-101 and A-43, we have

$$\sqrt{\rho_o}\,\frac{\partial(\delta p')}{\partial z} + \frac{\delta p'}{2\sqrt{\rho_o}}\,\frac{\partial \rho_o}{\partial z} = -\,g\,\sqrt{\rho_o}\;\;\delta\rho'$$

$$\left[\frac{\partial}{\partial z} - \frac{1}{2\,H}\left(1 + \frac{\partial H}{\partial z}\right)\right] \delta p' = -\,g\,\delta\rho'$$

Now we set

$$\delta\rho' = \overline{\delta\rho(z)}\;\;\sin\theta\,\cos\theta \qquad \text{(A-113)}$$

then

$$\left[\frac{\partial}{\partial z} - \frac{1}{2\,H}\left(1 + \frac{\partial H}{\partial z}\right)\right]\overline{\delta p(z)} = -\,g\,\overline{\delta\rho(z)} \qquad \text{(A-114)}$$

Equation A-112 requires that

$$w' = \overline{w(z)}\;\;\sin\theta\,\cos\theta \qquad \text{(A-115)}$$

Then equations A-112, A-115, and A-114 can be combined to give

$$\left[\frac{\partial}{\partial z} - \frac{1}{2H}\left(1 + \frac{\partial H}{\partial z}\right)\right]\left(g\ \overline{w(z)} - i\,\omega\,\overline{\delta p(z)}\right) = 0 \qquad \text{(A-116)}$$

Solving this equation, we get

$$g\ \overline{w(z)} - i\,\omega\ \overline{\delta p(z)} = A \exp\left[\int_0^z \frac{1}{2H}\left(1 + \frac{dH}{dz}\right) dz\right]$$

Now

$$\frac{1}{2H}\left(1 + \frac{dH}{dz}\right) > 0$$

Therefore since the quantity $g\ \overline{w(z)} - i\,\omega\,\overline{\delta\ p(z)}$ must be bounded for large z, then A = 0 and

$$i\,\omega\ \overline{\delta p(z)} = g\ \overline{w(z)} \qquad \text{(A-117)}$$

But at z = 0 then w = w(z) = 0 and hence $\overline{\delta p(z)} = 0$. Thus the pressure oscillation due to the diurnal term P_2^1 at ground level is zero. However this does not mean that the pressure oscillation due to this term is zero for all z though. The quantity which results from this term and which is zero throughout the atmosphere is equation A-97 as is shown by Lindzen [1965]. Then by using equations A-97 and A-111, we get

$$\frac{\partial}{\partial z}\left(\frac{\overline{w(z)}}{\sqrt{\rho_0}}\right) = \kappa\,\frac{\overline{J(z)}}{g\,H} \qquad \text{(A-118)}$$

From equation A-64 and by considering the term with the vertical

velocity as small, we have

$$\delta T' = \frac{\kappa M}{i \omega R} \left(\gamma J' - g \gamma H \chi \right)$$

or

$$\overline{\delta T(z)} = \frac{K M}{i \omega R} \left(\gamma \overline{J(z)} - g \gamma H \frac{\kappa \overline{J(z)}}{g H} \right)$$

$$\overline{\delta T(z)} = \frac{K M}{i \omega R} \overline{J(z)} \qquad \text{(A-119)}$$

where

$$\delta T' = \overline{\delta T(z)} \; P_2^1(\mu) \qquad \text{(A-120)}$$

Thus when the diurnal oscillation is considered, the above equations for u', v', w', $\delta p'$ and $\delta T'$ must be added to the equations A-69 thru A-73.

Summary

In concluding Appendix A, let us group the final results together. First, equations A-69 thru A-73 are not in the most desirable notation. For example, equation A-69 uses u_n as an operator. A more desirable situation is to let u_n now represent $u_n \, \Theta^s_{\lambda,n} \, e^{i(\sigma t + s\phi)}$. Making similar changes for the other variables, we have

$$u_n = \frac{\gamma g h_n e^{x/2}}{4 a \omega^2 (f^2 - \cos^2 \theta)} \left(\frac{\partial y_n}{\partial x} - \frac{1}{2} y_n \right) \left(\frac{\partial}{\partial \theta} \right.$$

$$- \frac{i \cot \theta}{f} \frac{\partial}{\partial \phi} \Bigg) \Theta^s_{\lambda,n} e^{i(\sigma t + s\phi)} \tag{A-121}$$

$$v_n = \frac{i \gamma g h_n e^{x/2}}{4 a \omega^2 (f^2 - \cos^2 \theta)} \left(\frac{\partial y_n}{\partial x} - \frac{1}{2} y_n \right) \left(\frac{\cos \theta}{f} \frac{\partial}{\partial \theta} \right.$$

$$\left. - \frac{i}{\sin \theta} \frac{\partial}{\partial \phi} \right) \Theta^s_{\lambda,n} e^{i(\sigma t + s\phi)} \tag{A-122}$$

$$w_n = - \frac{i \sigma}{g} \Omega_n + \gamma h_n e^{x/2} \left[\frac{\partial y_n}{\partial x} + \left(\frac{H}{h_n} - \frac{1}{2} \right) y_n \right] \Theta^s_{\lambda,n} e^{i(\sigma t + s\phi)} \tag{A-123}$$

$$\delta p_n = \frac{p_o(0)}{H} \left[- \frac{\Omega_n}{g} e^{-x} + \frac{\gamma h_n}{i\sigma} e^{-x/2} \left(\frac{\partial y_n}{\partial x} \right. \right.$$

$$\left. \left. - \frac{1}{2} y_n \right) \right] \Theta^s_{\lambda,n} e^{i(\sigma t + s\phi)} \tag{A-124}$$

$$\delta T_n = \frac{M}{R} \left\{ \frac{\Omega_n}{H} \frac{\partial H}{\partial x} - \frac{\gamma g h_n}{i\sigma} e^{x/2} \left[\frac{\kappa H}{h_n} + \frac{1}{H} \frac{\partial H}{\partial x} \left(\frac{\partial}{\partial x} \right. \right. \right.$$

$$\left. \left. \left. + \frac{H}{h_n} - \frac{1}{2} \right) \right] y_n + \frac{\kappa J_n}{i \sigma} \right\} \Theta^s_{\lambda,n} e^{i(\sigma t + s\phi)} \tag{A-125}$$

The latitude dependence is given by the solutions of Laplace's Equation A-95, which are the Hough Functions. The altitude dependence is given by equation A-68. Due to the incompleteness of the Hough Functions for the diurnal oscillation, the following terms must be

added to the above equations whenever the diurnal oscillation is considered.

$$u = \frac{-i}{a\,\omega\,\rho_o}\,\overline{\delta p(z)}\;e^{i(\omega t + \phi)} \qquad \text{(A-126)}$$

$$v = \frac{\cos\theta}{a\,\omega\,\rho_o}\,\overline{\delta p(z)}\;e^{i(\omega t + \phi)} \qquad \text{(A-127)}$$

$$w = \overline{w(z)}\;P_2^1(\mu)\;e^{i(\omega t + \phi)} \qquad)$$

where

$$\frac{\partial}{\partial z}\left(\overline{w(z)}\right) = \frac{\kappa\,\overline{J(z)}}{g\,H}$$

$$\delta p = \frac{g\,\rho_o\,\overline{w(z)}}{i\;\omega}\;P_2^1(\mu)\;e^{i(\omega t + \phi)} \qquad \text{(A-129)}$$

$$\delta T = \frac{\kappa\,M}{i\omega R}\,\overline{J(z)}\;P_2^1(\mu)\;e^{i(\omega t + \phi)} \qquad \text{(A-130)}$$

Expansion of Hough Functions for Semidiurnal Oscillations

Siebert [1961] shows the expansion of the Hough Functions in terms of the Associated Legendre Polynomials for the semidiurnal oscillation. If $s = 2$, $f = 1$ and $\sigma = \frac{2\pi}{12}$ (hours)$^{-1}$, then

$$\Theta^2_{2,2}(\theta) = P^2_2 - 0.339\ P^2_4 + 0.041\ P^2_6 - 0.002\ P^2_8 + \ldots \quad \text{(A-131)}$$

$$h_2 = 7.85 \text{ km} \quad \text{(A-132)}$$

$$\Theta^2_{2,4}(\theta) = 0.202\ P^2_2 + P^2_4 - 0.819\ P^2_6 + 0.24\ P^2_8 - 0.04\ P^2_{10} + \ldots \quad \text{(A-133)}$$

$$h_4 = 2.11 \text{ km} \quad \text{(A-134)}$$

$$\Theta^2_{2,6}(\theta) = 0.13\ P^2_2 + 0.755\ P^2_4 + P^2_6 - 1.72\ P^6_8 + 0.88\ P^2_{10}$$

$$- 0.2\ P^2_{12} + \ldots \quad \text{(A-135)}$$

$$h_6 = 0.957 \text{ km} \quad \text{(A-136)}$$

Expansion of Hough Functions for Diurnal Oscillations

Lindzen [1966] shows the expansion of the Hough Functions for the diurnal oscillations. If $s = 1$, $f = \frac{1}{2}$ and $\sigma = \frac{2\pi}{24}$ (hours)$^{-1}$, then

$$\Theta^1_{1,-1}(\theta) = 0.8968\ \bar{P}^1_1 + 0.4401\ \bar{P}^1_3 + 0.04534\ \bar{P}^1_5$$

$$+ 0.0020\ \bar{P}^1_7 + \ldots \quad \text{(A-137)}$$

$$h_{-1} = -12.25 \text{ km} \quad \text{(A-138)}$$

$$\Theta^1_{1,-3}(\theta) = -0.2703\ P_1^{\bar{1}} + 0.4613\ P_3^{\bar{1}} + 0.7731\ P_5^{\bar{1}}$$

$$+ 0.3302\ P_7^{\bar{1}} + 0.0698\ P_9^{\bar{1}} + 0.0087\ P_{11}^{\bar{1}} \qquad \text{(A-139)}$$

$$h_{-3} = -1.751 \text{ km} \qquad \text{(A-140)}$$

$$\Theta^1_{1,3}(\theta) = 0.2842\ P_1^{\bar{1}} - 0.6402\ P_3^{\bar{1}} + 0.6195\ P_5^{\bar{1}} - 0.3337\ P_7^{\bar{1}}$$

$$+ 0.1152\ P_9^{\bar{1}} - 0.0276\ P_{11}^{\bar{1}} + 0.0049\ P_{13}^{\bar{1}} - 0.0007\ P_{15}^{\bar{1}} \qquad \text{(A-141)}$$

$$h_3 = 0.700 \text{ km} \qquad \text{(A-142)}$$

$$\Theta^1_{1,5}(\theta) = -0.0738\ P_1^{\bar{1}} + 0.1573\ P_3^{\bar{1}} - 0.0594\ P_5^{\bar{1}} - 0.2401\ P_7^{\bar{1}}$$

$$+ 0.5150\ P_9^{\bar{1}} - 0.5807\ P_{11}^{\bar{1}} + 0.4574\ P_{13}^{\bar{1}} - 0.2757\ P_{15}^{\bar{1}}$$

$$+ 0.1332\ P_{17}^{\bar{1}} - 0.0530\ P_{19}^{\bar{1}} + 0.0177\ P_{21}^{\bar{1}} - 0.0051\ P_{23}^{\bar{1}}$$

$$+ 0.0012\ P_{25}^{\bar{1}} + \ldots \qquad \text{(A-143)}$$

$$h_5 = 0.122 \text{ km} \qquad \text{(A-144)}$$

$$\Theta^1_{1,7}(\theta) = 0.0378\ P_1^{\bar{1}} - 0.0800\ P_3^{\bar{1}} + 0.0239\ P_5^{\bar{1}} + 0.1331\ P_7^{\bar{1}}$$

$$- 0.2388\ \bar{P}^{1}_{9} + 0.1500\ \bar{P}^{1}_{11} + 0.1089\ \bar{P}^{1}_{13} - 0.3795\ \bar{P}^{1}_{15}$$

$$+ 0.5197\ \bar{P}^{1}_{17} - 0.4977\ \bar{P}^{1}_{19} + 0.3785\ \bar{P}^{1}_{21} - 0.2386\ \bar{P}^{1}_{23}$$

$$+ 0.1283\ \bar{P}^{1}_{25} - 0.0591\ \bar{P}^{1}_{27} + 0.0216\ \bar{P}^{1}_{29} + \ldots \qquad \text{(A-145)}$$

$$h_7 = 0.049 \text{ km} \qquad \text{(A-146)}$$

where

$$\int_{-1}^{1} [P^{s}_{n}(\mu)]^2\, d\mu = 1$$

and

$$\bar{\bar{P}}^{s}_{n}(\mu) = \left(\frac{2n+1}{2} \frac{(n-s)!}{(n+s)!} \right)^{1/2} P^{s}_{n}(\mu)$$

and the sum of the coefficients is one. Thus for the diurnal oscillation the Hough Functions are normalized.

APPENDIX B

GROVES ANALYSIS

Many people have carried out Fourier analyses of meteor wind data by various methods. One of the major difficulties faced in such an analysis is that, in practice, wind data can be obtained only at distinct altitudes and times with relatively large intervals of height and time between these data points. One method of analysis was developed by G. V. Groves [1959] which seems to alleviate somewhat the problem of sparsely spaced data. According to Groves, his method removes the assumption that variations in the wind within the time and height intervals between data points are negligible by generalizing the least-squares solution so that parameters defining the time-and-height-variations of the wind may be determined.

Because of its ability to analyze sparsely spaced data, the Groves method of analysis seems as though it would be ideal for the analysis of wind data from chemilumious clouds. Hence, this appendix will give a general description of the Groves method as it was used to analyze wind data which was accumulated from 1962 through 1965. The following is not meant to be a rigorous derivation but only to give a general understanding of what the Groves method does.

General Least Squares Solution

Let V be the vector velocity of the atmospheric wind and let V = (u,v,w) where u, v, w are the southward, eastward and vertical

velocities. The velocities u, v, and w are determined experimentally and are assumed to be expressed as certain specified functions of height z and time t.

$$u = u(z,t, a_{1n})$$

$$v = v(z,t, a_{2n}) \qquad \text{(B-1)}$$

$$w = w(z,t\ a_{3n})$$

where a_{kn} (n = 1, ..., N; k = 1, 2, 3) are the parameters which are being sought.

The winds will have small random fluctuations due to errors in the experimental measurements and the wind structure. To minimize the errors caused by these fluctuations, we need to minimize the quantity

$$\varepsilon_i = u_i \ell + v_i m + w_i n - V_i \qquad \text{(B-2)}$$

where ℓ, m, n are unit vectors in the southward, eastward, and vertical directions and

$$u_i = u(z_i, t_i, a_{1n})$$

The velocities v_i and w_i are defined in a similar manner. The subscript i denotes the $i^{\underline{th}}$ evaluation of the wind.

Since the fluctuations are random, the ε_i are assumed to be independent of each other and to have a normal distribution with a zero mean and a standard deviation of σ_i. The probability that the values of ε_i for i = 1, . . ., M should be in the ranges $(\varepsilon_1, \varepsilon_1 + d\varepsilon_1)$ . . .

$(\varepsilon_M, \varepsilon_M + d\varepsilon_M)$ is

$$P(\varepsilon_1, \ldots \varepsilon_M)\, d\varepsilon_1 \ldots d\varepsilon_M = \prod_{i=i}^{M} \frac{e^{-\varepsilon_i^2/2\sigma_i^2}}{\sqrt{2\pi}\,\sigma_i}\, d\varepsilon_i \qquad \text{(B-3)}$$

The parameters a_{kn} are chosen so that the observed set of values $\varepsilon_1, \ldots, \varepsilon_M$ have a maximum probability, or $\sum_{i=1}^{M} \frac{\varepsilon_i^2}{\sigma_i^2}$ is a minimum with respect to the a_{kn}.

By differentiation, we get

$$\sum_{i=1}^{M} \omega_i^2\, \varepsilon_i \frac{\partial \varepsilon_i}{\partial a_{kn}} = 0 \qquad \text{(B-4)}$$

where the weighting factors ω_i are

$$\omega_i^2 = \frac{1}{\sigma_i^2} \qquad \text{(B-5)}$$

Solution for Parameters a_{kn}

Assume that equations B-1 are linear in a_{kn} so that equation B-2 becomes

$$\varepsilon_i = \varepsilon_{io} + \underline{A} \left[\frac{\partial \varepsilon_i}{\partial a_{11}} \frac{\partial \varepsilon_i}{\partial a_{12}} \ldots \frac{\partial \varepsilon_i}{\partial a_{3N}} \right]$$

$$\varepsilon_i = \varepsilon_{io} + \left[\frac{\partial \varepsilon_i}{\partial a_{11}} \quad . \quad . \quad . \quad . \quad . \quad \frac{\partial \varepsilon_i}{\partial a_{3N}} \right] \underline{A}' \tag{B-6}$$

where

$$\varepsilon_{io} = u(z_i, t_i, 0)\, \ell + v(z_i, t_i, 0)\, m$$

$$+ w(z_i, t_i, o)\, n - V_i$$

and for convenience we can let

$$\varepsilon_{io} = - V_i \tag{B-7}$$

The prime in equation B-6 indicates a transposed matrix. An underlined quantity indicates that it is a matrix. This practice will be followed throughout this appendix. The matrix $\underline{A}$ is defined as

$$\underline{A} = \left[a_{11} \quad a_{12} \, . \, . \, . \, . \, a_{3N} \right] \tag{B-8}$$

By substituting equation B-6 into equation B-5, Groves [1959] shows that equation B-5 becomes

$$\underline{S}\, \underline{\varepsilon_{o\omega}}' + \underline{S}\, \underline{S}'\, \underline{A}' = 0 \tag{B-9}$$

where

$$\underline{S} = \begin{bmatrix} \omega_1 \frac{\partial \varepsilon_1}{\partial a_{11}} & \omega_2 \frac{\partial \varepsilon_2}{\partial a_{11}} & \cdots & \omega_M \frac{\partial \varepsilon_M}{\partial a_{11}} \\ \omega_1 \frac{\partial \varepsilon_1}{\partial a_{12}} & & & \\ \vdots & & & \\ \omega_1 \frac{\partial \varepsilon_1}{\partial a_{3N}} & & \cdots & \omega_M \frac{\partial \varepsilon_M}{\partial a_{3N}} \end{bmatrix} \qquad \text{(B-10)}$$

and by using equation B-2, we get

$$\underline{S} = \begin{bmatrix} \omega_1 \ell \frac{\partial u_1}{\partial a_{11}} & \omega_2 \ell \frac{\partial u_2}{\partial a_{11}} & \cdots & \omega_M \ell \frac{\partial u_M}{\partial a_{11}} \\ \omega_1 \ell \frac{\partial u_1}{\partial a_{12}} & & & \\ \vdots & & & \\ \omega_1 n \frac{\partial w_1}{\partial a_{3N}} & & \cdots & \omega_M n \frac{\partial w_M}{\partial a_{3N}} \end{bmatrix}$$

and

$$\underline{\varepsilon_{o\omega}} = \begin{bmatrix} \omega_1 \varepsilon_{10} & \cdots & \omega_M \varepsilon_{Mo} \end{bmatrix}$$

$$\underline{\varepsilon_{o\omega}} = \begin{bmatrix} \omega_1 V_1 & \cdots & \omega_M V_M \end{bmatrix} \qquad \text{(B-12)}$$

Thus the solution of equation B-9 can easily be seen to be

$$\underline{A} = \left[\omega_1 V_1 \cdot \cdot \cdot \cdot \omega_M V_M \right] \quad \underline{T} \tag{B-13}$$

where

$$\underline{T} = \underline{S}' (\underline{S}\ \underline{S}')^{-1} \tag{B-14}$$

The Weighting Factors, ω_i

According to equation B-5, the weighting factors are equal to the inverse standard deviation of the quantities ε_i, or

$$\omega_i = \left(< \varepsilon_i^2 > \right)^{-\frac{1}{2}} \tag{B-15}$$

However, the distribution of ε_i is not known, so the weighting factors will have to be approximated. Groves [1959] took the following as his weighting factors:

$$\omega_i = \left\{ \sum_{n=1}^{N} \left[\left(\frac{\partial u_i}{\partial a_{1n}} \right)^2 + \left(\frac{\partial v_i}{\partial a_{2n}} \right)^2 + \left(\frac{\partial w_i}{\partial a_{3n}} \right)^2 \right] \right\}^{-1/2} \tag{B-16}$$

From equations B-6, B-7, and B-2, it can be shown that the above value of ω_i is proportional to the inverse standard deviation but is certainly not equal to it.

Height and Time Variations Taken into Account

If the initial data are spread intermittently over large height and time intervals, then equations B-1 are first assumed to be periodic

in time with a period of $2\pi/\lambda$. The variations in height are taken into account by expanding equations B-1 in a finite number of terms of a Fourier expansion as follows:

$$
\begin{aligned}
u &= u_o(z) + u_1(z) \sin \lambda t + \ldots + u_p(z) \sin p\lambda t \\
&\quad + u_1^*(z) \cos \lambda t + \ldots + u_p^*(z) \cos p\lambda t \\
v &= v_o(z) + v_1(z) \sin \lambda t + \ldots + v_q(z) \sin q\lambda t \\
&\quad + v_1^*(z) \cos \lambda t + \ldots + v_q^*(z) \cos q\lambda t \\
w &= w_o(z) + w_1(z) \sin \lambda t + \ldots + w_r(z) \sin r\lambda t \\
&\quad + w_1^*(z) \cos \lambda t + \ldots + w_r^*(z) \cos r\lambda t
\end{aligned}
\tag{B-17}
$$

where

$$
\begin{aligned}
u_j(z) &= u_{jo} + u_{j1} K + u_{j2} K^2 + \ldots + u_{jB_j} K^{B_j} \quad (j=0, \ldots,p) \\
u_j^*(z) &= u_{jo}^* + u_{j1}^* K + \ldots + u_{jB_j}^* K^{B_j} \quad (j=1, \ldots,p) \\
v_j(z) &= v_{jo} + v_{j1} K + \ldots + v_{jc_j} K^{c_j} \quad (j=0, \ldots,q) \\
v_j^*(z) &= v_{jo}^* + v_{j1}^* K + \ldots + v_{jc_j}^* K^{c_j} \quad (j=1, \ldots,q)
\end{aligned}
\tag{B-18}
$$

$$w_j(z) = w_{jo} + w_{j1} K + \ldots + w_{jd_j} K^{d_j} \qquad (j=0,\ldots,r)$$

$$w_j^*(z) = w_{jo}^* + w_{j1}^* K + \ldots + w_{jd_j}^* K^{d_j} \qquad (j=1,\ldots,r)$$

$$K = \frac{2z - (z_1 + z_2)}{z_1 - z_2} \qquad (B\text{-}19)$$

where z_1 and z_2 are the greatest and lowest heights under consideration respectively.

By comparing equations B-18 and B-16, we see that the coefficients a_{1n} are given as

$$a_{1n} = u_{jn} + u_{jn}^* \qquad (B\text{-}20)$$

Similarly, the coefficients a_{2n} and a_{3n} are also defined in terms of $v_{jn} + v_{jn}^*$ and $w_{jn} + w_{jn}^*$. So by equation B-16, we have the weighting factors as

$$\omega_i = \left[\sum_{j=0}^{p} \left(1 + K_i^2 + \ldots + K_i^{2B_j} \right) + \sum_{j=0}^{q} \left(1 + K_i^2 \ldots + K_i^{2c_j} \right) + \sum_{j=0}^{r} \left(1 + K_i^2 + \ldots + K_i^{2d_j} \right) \right]^{-\frac{1}{2}} \qquad (B\text{-}21)$$

From equation B-11, we have

$$\underline{S} = \begin{bmatrix} \{L_{jk}\} \\ \{M_{jk}\} \\ \{N_{jk}\} \end{bmatrix} \tag{B-22}$$

where

$$\{L_{jk}\} = \left[\underline{L_{oo}} \cdots \underline{L_{oB_o}} \cdots \underline{L_{po}} \cdots \underline{L_{pB_p}} \right]'$$

$$\{M_{jk}\} = \left[\underline{M_{oo}} \cdots \underline{M_{oc_o}} \cdots \underline{M_{qo}} \cdots \underline{M_{qc_q}} \right]' \tag{B-23}$$

$$\{N_{jk}\} = \left[\underline{N_{oo}} \cdots \underline{N_{od_o}} \cdots \underline{N_{qo}} \cdots \underline{N_{qd_q}} \right]'$$

$$\underline{L_{ok}} = \left[\omega_1 \ell K_1^k \cdots \omega_M \ell K_M^k \right] \qquad (k = 0, \ldots, B_o)$$

$$\underline{L_{jk}} = \begin{bmatrix} \omega_1 \ell K_1^k \sin j\lambda t_1 \cdots \omega_M \ell K_M^k \sin j\lambda t_M \\ \omega_1 \ell K_1^k \cos j\lambda t_1 \cdots \omega_M \ell K_M^k \cos j\lambda t_M \end{bmatrix}$$

$$(j = 1, \ldots p)$$

$$(k = 0, \ldots B_j)$$

$$\underline{M_{ok}} = \left[\omega_1 m K_1^k \cdots \omega_M m K_M^k \right] (k = 0, \ldots C_o)$$

$$\underline{M_{jk}} = \begin{bmatrix} \omega_1 m K_1^k \sin j\lambda t_1 \; . \; . \; . \; \omega_M m K_M^k \sin j \lambda t_M \\ \\ \omega_1 m K_1^k \cos j\lambda t_1 \; . \; . \; . \; \omega_M m K_M^k \cos j \lambda t_M \end{bmatrix} \quad \text{(B-24)}$$

$$(j = 1, \; . \; . \; . \; , q)$$

$$(k = 0, \; . \; . \; . \; , c_j)$$

$$\underline{N_{ok}} = \begin{bmatrix} \omega_1 n K_1^k \; . \; . \; . \; \omega_M n K_M^k \end{bmatrix} (k = 0, \; . \; . \; . \; , d_o)$$

$$\underline{N_{jk}} = \begin{bmatrix} \omega_1 n K_1^k \sin j \lambda t_1 \; . \; . \; . \omega_M n K_M^k \sin j \lambda t_M \\ \\ \omega_1 n K_1^k \cos j \lambda t_1 \; . \; . \; . \omega_M n K_M^k \cos j \lambda t_M \end{bmatrix}$$

$$(j = 1, \; . \; . \; ., \; r)$$

$$(k = 0, \; . \; . \; ., \; d_j)$$

By using equations B-22, B-23 and B-24, we can solve equation B-13 for the matrix $\underline{A}$ which gives the values of $u_j(z)$, $u_j^*(z)$, $v_j(z)$, $v_j^*(z)$, $w_j(z)$ and $w_j^*(z)$. Then the amplitudes of the $j^{\underline{th}}$ harmonics are given by

$$U_j(z) = \left(u_j{}^2(z) + u_j{}^{*2}(z) \right)^{1/2}$$

$$V_j(z) = \left(v_j{}^2(z) + v_j{}^{*2}(z) \right)^{1/2} \quad \text{(B-25)}$$

$$W_j(z) = \left(w_j{}^2(z) + w_j{}^{*2}(z) \right)^{1/2}$$

and their phase angles are

$$\phi_j(z) = -\tan^{-1}\left[\frac{u_j(z)}{u_j^*(z)}\right]$$

$$\mu_j(z) = -\tan^{-1}\left[\frac{v_j(z)}{v_j^*(z)}\right] \qquad \text{(B-26)}$$

$$\zeta_j(z) = -\tan^{-1}\left[\frac{w_j(z)}{w_j^*(z)}\right]$$

Values Used for the Present Experiment

To analyze the wind data for purposes of the present paper, the following parameter values were used. In equations B-17, we have

$$p = q = 1$$

$$r = o \qquad \text{(B-27)}$$

So $u = u_o(z) + u_1(z) \sin \lambda t + u_1^*(z) \cos \lambda t$

$v = v_o(z) + v_1(z) \sin \lambda t + v_1^*(z) \cos \lambda t \qquad \text{(B-28)}$

$w = 0$

Thus, equations B-28 show that we are fitting a prevailing wind component (u_o or v_o) plus a single periodic component with a period of $2\pi/\lambda$ to the wind data. The vertical velocity is assumed to be zero.

From equation B-19, we have

$$z_1 = 140 \text{ km}$$

$$z_2 = 90 \text{ km}$$

$$K = \frac{z - 115}{25} \tag{B-29}$$

From equations B-18, we have

$$B_o = B_1 = c_o = c_1 = 7$$

$$d_j = 0 \tag{B-30}$$

Thus for both the prevailing and the periodic winds, the altitude dependence of the winds is expanded in terms of a seventh order polynomial of the height variable z.

In order to calculate the weighting factors by equation B-21, it must first be understood that in the case here, the Groves analysis will analyze only one component of the total wind at one time. That is, either the north-south or east-west wind components will be analyzed at one time but not simultaneously. Hence for the purpose of computing the weighting factors, whenever we say p = 1 then we must then say that q = r = 0. Thus the weighting factors become

$$\omega_i = \left[\sum_{j=o}^{p=q} \left(1 + K_1^2 + K_2^4 + K_3^6 + K_4^8 + K_5^{10} + K_6^{12} + K_7^{14} \right) \right]^{-1/2}$$

$$\omega_i = \left[2 \left(1 + K_1^2 + \ldots + K_7^{14} \right) \right]^{-1/2} \qquad \text{(B-31)}$$

By using equation B-29, we see that the weighting factors weight the wind data falling in the middle of the height range under consideration most heavily, i.e.

$$\text{at } z = 90 \text{ km} \quad , \quad \omega_i = 1/4$$

$$\text{at } z = 115 \text{ km} \quad , \quad \omega_i = \frac{1}{\sqrt{2}}$$

$$\text{at } z = 140 \text{ km} \quad , \quad \omega_i = 1/4$$

Thus, this is a reasonable weighting function because the best wind data are most likely to fall in the middle of the height range whereas the worst data are most likely to fall around the extremities of the height range.

Since we are specifying 7th order polynomial fits in height, the shortest vertical wavelength that can be determined by the present analysis is

$$2 \left(\frac{\text{Height range}}{\text{Order of polynomial minus one}} \right)$$

or

$$2 \left(\frac{140 - 90}{6} \right) = \frac{50}{3} = 16.7 \text{ km}$$

This is sufficient for the present work because the main interest is in the tidal harmonics, for which the shortest vertical wavelength

is about 20 km for the 24 hour periodic oscillations.

Using these parameter values, a computer program was constructed which would do a Groves analysis on the available wind data. The amplitudes and phases for different periodic oscillations were calculated. All the phases were calculated with reference to the time of day after midnight when a maximum amplitude of oscillation occurred. Different periodic components were obtained by varying the frequency λ.

APPENDIX C

CORRELATION ANALYSIS

The vertical autocorrelation function for a single wind component u(z) is defined as

$$G(\delta z) = \frac{< u(z)\ u(z + \delta z) >}{\left\{< [u(z)]^2 > \ < [u(z + \delta z)]^2 >\right\}^{1/2}} \qquad \text{(C-1)}$$

where the averages are taken over a range of altitudes z. This equation is appropriate whenever the average value of the wind component is zero. If the average value of the wind component $\bar{u}$ is not zero, then the wind component u(z) must be replaced by $u(z) - \bar{u}$.

The cross correlation function of u(z) and v(z) is defined as

$$F(\delta z) = \frac{< u(z)\ v(z + \delta z) >}{\left\{ < [\ u(z)\ ]^2 > \ < [\ v(z + \delta z)\ ]^2 > \right\}^{1/2}} \qquad \text{(C-2)}$$

To see how these functions relate to the wavelength and phase differences of the wind components, consider the following hypothetical wind profile:

$$u(z) = A \sin (\zeta + \phi) \qquad \text{(C-3)}$$

$$v(z) = B \sin \zeta \qquad \text{(C-4)}$$

where ζ is an appropriately non-dimensionalized height variable and ϕ

is the phase difference between the u and v components. Then

$$G(\delta\zeta) = \frac{A^2 \int_0^{2\pi} \sin(\zeta + \phi) \sin(\zeta + \phi + \delta\zeta)\, d\zeta}{A^2 \int_0^{2\pi} \sin^2(\zeta + \phi)\, d\zeta}$$

or

$$G(\delta\zeta) = \cos(\delta\zeta) \tag{C-5}$$

where A and B are constants.

Thus

$$G = 1 \quad \text{at} \quad \delta\zeta = 0$$

$$G = 0 \quad \text{at} \quad \delta\zeta = \pi/2$$

Then the height interval between the values of G = 1 and G = 0 is equal to one quarter of the vertical wavelength. Although the actual wind profile is composed of components with many different wavelengths, a general cosine-like dependence for $G(\delta z)$ is still observed for the tidal motions and the analysis then gives the dominant wavelength.

If equations C-3 and C-4 are substituted into the cross correlation C-2, then we get

$$F(\delta\zeta) = \frac{AB \int_0^{2\pi} \sin(\zeta + \phi) \sin(\zeta + \delta\zeta)\, d\zeta}{AB \left\{ \int_0^{2\pi} [\sin(\zeta + \phi)]^2\, d\zeta \int_0^{2\pi} [\sin(\zeta + \delta\zeta)]^2\, d\zeta \right\}^{1/2}}$$

$$F(\delta\zeta) = \frac{\cos\phi\cos(\delta\zeta)\int_0^{2\pi}\sin^2\zeta\,d\zeta + \sin\phi\sin(\delta\zeta)\int_0^{2\pi}\cos^2\zeta\,d\zeta}{\int_0^{2\pi}\sin^2\zeta\,d\zeta}$$

$$F(\delta\zeta) = \cos\phi\cos(\delta\zeta) + \sin\phi\sin(\delta\zeta)$$

$$F(\delta\zeta) = \cos(\delta\zeta - \phi) \qquad \text{(C-6)}$$

Thus equation C-6 gives the same variation with $\delta\zeta$ as equation C-5 except displaced by an amount equal to the phase difference ϕ between the northward and eastward wind components.

APPENDIX D

DERIVATION OF EQUATION III-5

$$V_n = A \sin (k z + \phi_1) \tag{D-1}$$

$$V_e = B \sin (k z + \phi_2) \tag{D-2}$$

Let

$$\zeta = k z + \phi_1 \tag{D-3}$$

$$\phi = \phi_2 - \phi_1 \tag{D-4}$$

Then

$$V^2 = V_n^2 + V_e^2$$

$$= A^2 \sin^2 \zeta + B^2 \sin^2 (\zeta + \phi)$$

$$= A^2 + B^2 - A^2 \cos^2 \zeta - B^2 (\cos^2 \zeta \cos^2 \phi$$

$$+ \sin^2 \zeta \sin^2 \phi - \frac{1}{2} \sin 2\zeta \sin \phi)$$

$$= A^2 + B^2 - \left(\frac{1 + \cos 2\zeta}{2}\right) \left(A^2 + B^2 \cos^2 \phi \right)$$

$$- B^2 \sin^2 \phi \left(\frac{1 - \cos 2\zeta}{2}\right) + \frac{1}{2} B^2 \sin 2\zeta \sin 2\phi$$

$$V^2 = A^2 + B^2 - \frac{A^2}{2} - \frac{B^2}{2} - \frac{1}{2} [A^2 \cos 2\zeta + (B^2 \cos^2 \phi$$

$$- B^2 \sin^2 \phi) \cos 2\zeta - B^2 \sin 2\phi \sin 2\zeta] \qquad \text{(D-5)}$$

$$V^2 = \frac{1}{2}(A^2 + B^2) - \frac{1}{2} A^2 \cos 2\zeta - \frac{1}{2} B^2 \cos 2(\zeta + \phi) \qquad \text{(D-6)}$$

Now force equation D-6 to have the form

$$V^2 = \frac{1}{2} (A^2 + B^2) - C \cos (2\zeta + \alpha) \qquad \text{(D-7)}$$

$$V^2 = \frac{1}{2} (A^2 + B^2) = - C \cos 2\zeta \cos \alpha$$

$$+ C \sin 2\zeta \sin \alpha \qquad \text{(D-8)}$$

By comparison of equations D-5 and D-8, we get

$$C \cos \alpha = \frac{1}{2}(A^2 + B^2 \cos 2\phi) \qquad \text{(D-9)}$$

$$C \sin \alpha = \frac{1}{2} B^2 \sin 2\phi \qquad \text{(D-10)}$$

By solving equations D-9 and D-10 for C and α, one gets for the quantity C

$$C = A B \left[\cos^2 \phi + \frac{1}{4} \left(\frac{A}{B} - \frac{B}{A} \right)^2 \right]^{1/2} \qquad \text{(D-11)}$$

If we let

$$\alpha = \phi + \beta \qquad \text{(D-12)}$$

then equations D-9 and D-10 become

$$\cos \phi \cos \beta - \sin \phi \sin \beta = \frac{1}{2C} (A^2 + B^2 \cos 2 \phi) \qquad \text{(D-13)}$$

$$\sin \phi \cos \beta + \cos \phi \sin \beta = \frac{1}{2C} (B^2 \sin 2 \phi) \qquad \text{(D-14)}$$

The solution of equations D-13 and D-14 for cos β and sin β give

$$\sin \beta = \frac{\sin \phi}{2 C} (B^2 - A^2)$$

$$\cos \beta = \frac{\cos \phi}{2 C} (A^2 + B^2)$$

or

$$\tan \beta = \frac{B^2 - A^2}{B^2 + A^2} \tan \phi \qquad \text{(D-15)}$$

Thus, equation D-7 is actually equation III-5 where the quantities C and α are defined by equations D-11, D-12, and D-15.

APPENDIX E

DERIVATION OF EOUATION III-8

$$V_n = A \sin (k z + \phi_1) \tag{E-1}$$

$$V_e = B \sin (k z + \phi_2) \tag{E-2}$$

Let

$$\zeta = k z + \phi_1$$

$$\phi = \phi_2 - \phi_1$$

$$\theta = \text{wind heading}$$

Then

$$\tan \theta = \frac{V_e}{V_n}$$

$$= \frac{B \sin (\zeta + \phi)}{A \sin \zeta}$$

$$= \frac{B}{A} (\cos \phi + \sin \phi \cot \zeta)$$

$$\tan \theta = \frac{B}{A} \left[\cos \phi + \sin \phi \tan \left(\frac{\pi}{2} - \zeta \right) \right] \tag{E-3}$$

or

$$\frac{\cos \zeta}{\sin \zeta} = \frac{A \tan \theta - B \cos \phi}{B \sin \phi} \tag{E-4}$$

$$V^2 = V_n^2 + V_e^2$$

$$V^2 = A^2 \sin^2 \zeta + B^2 \sin^2 (\zeta + \phi)$$

$$V^2 = A^2 \sin^2 \zeta + B^2 \sin^2 \zeta \cos^2 \phi + B^2 \sin^2 \phi \cos^2 \zeta$$

$$+ 2 B^2 \sin \phi \cos \phi \sin \zeta \cos \zeta$$

By using equation E-4, we have

$$V^2 = \left[\left(A^2 + B^2 \cos^2 \phi\right) B^2 \sin^2 \phi + B^2 \sin^2 \phi \, (A \tan \theta - B \cos \phi)^2 \right.$$

$$\left. + 2 B^3 \sin^2 \phi \cos \phi \left(A \tan \theta - B \cos \phi\right)\right] \left[B^2 + A^2 \tan^2 \theta \right.$$

$$\left. - 2 A B \tan \theta \cos \phi\right]^{-1}$$

$$V^2 = \frac{A^2 B^2 \sin^2 \phi}{B^2 \cos^2 \theta + A^2 \sin^2 \theta - 2 A B \cos \phi \sin \theta \cos \theta} \tag{E-5}$$

Consider

$$a^2 \cos^2 (\theta - \alpha) + b^2 \sin^2 (\theta - \alpha) = B^2 \cos^2 \theta + A^2 \sin^2 \theta$$

$$- 2 A B \cos \phi \sin \theta \cos \theta \tag{E-6}$$

$$= a^2 (\cos\theta \cos\alpha + \sin\theta \sin\alpha)^2 + b^2 (\sin\theta \cos\alpha - \cos\theta \sin\alpha)^2$$

$$= (a^2 \cos^2\alpha + b^2 \sin^2\alpha) \cos^2\theta + (a^2 \sin^2\alpha + b^2 \cos^2\alpha) (\sin^2\theta) + 2 \sin\alpha \cos\alpha (a^2 - b^2) \sin\theta \cos\theta$$

or $$2 \sin\alpha \cos\alpha (a^2 - b^2) = -2 A B \cos\phi \quad \text{(E-7)}$$

$$a^2 \cos^2\alpha + b^2 \sin^2\alpha = B^2 \quad \text{(E-8)}$$

$$a^2 \sin^2\alpha + b^2 \cos^2\alpha = A^2 \quad \text{(E-9)}$$

Solving equations E-6, E-7 and E-8, we have

$$\sin 2\alpha = -\frac{2 A B \cos\phi}{a^2 - b^2} \quad \text{(E-10)}$$

$$a^2 \cos 2\alpha - b^2 \cos 2\alpha = B^2 - A^2$$

$$\cos 2\alpha = \frac{B^2 - A^2}{a^2 - b^2} \quad \text{(E-11)}$$

$$a^2 + b^2 = A^2 + B^2 \quad \text{(E-12)}$$

From equations E-9 and E-10, we have

$$\tan 2\alpha = \frac{2 A B \cos\phi}{A^2 - B^2} \quad \text{(E-13)}$$

From equations E-10 and E-11, we have

$$a = \frac{1}{2}\left(A^2 + B^2 \frac{B^2 - A^2}{\cos 2\alpha}\right)$$

$$= \frac{1}{2}\left[A^2\left(\frac{\cos 2\alpha - 1}{\cos 2\alpha}\right) + B^2\left(\frac{\cos 2\alpha + 1}{\cos 2\alpha}\right)\right]$$

$$= \frac{1}{2}\tan 2\alpha\left[A^2\left(\frac{\cos 2\alpha - 1}{\sin 2\alpha}\right) + B^2\left(\frac{\cos 2\alpha + 1}{\sin 2\alpha}\right)\right]$$

$$a^2 = \frac{1}{2}\tan 2\alpha\left(-A^2 \tan\alpha + \frac{B^2}{\tan\alpha}\right) \qquad \text{(E-14)}$$

Again, we have from equations E-10 and E-11

$$b^2 = \frac{1}{2}\left(A^2 + B^2 + \frac{A^2 - B^2}{\cos 2\alpha}\right)$$

$$= \frac{1}{2}\left[A^2\left(\frac{\cos 2\alpha + 1}{\cos 2\alpha}\right) + B^2\left(\frac{\cos 2\alpha - 1}{\cos 2\alpha}\right)\right]$$

$$b^2 = \frac{1}{2}\tan 2\alpha\left(\frac{A^2}{\tan\alpha} - B^2 \tan\alpha\right) \qquad \text{(E-15)}$$

From equations E-13 and E-14, we have

$$a^2b^2 = \frac{1}{4}\tan^2 2\alpha\left(-A^2 \tan\alpha + \frac{B^2}{\tan\alpha}\right)\left(\frac{A^2}{\tan\alpha} - B^2 \tan\alpha\right)$$

$$= \frac{1}{4} \tan^2 2\alpha \left(- A^4 + \frac{A^2 B^2}{\tan^2 \alpha} + A^2 B^2 \tan^2 \alpha - B^4 \right)$$

$$a^2 b^2 = \tan^2 2\alpha \left(- \frac{A^4 + B^4}{4} + A^2 B^2 \frac{1 + \tan^4 \alpha}{4 \tan^2 \alpha} \right)$$

Now note that

$$\frac{1}{\tan^2 2\alpha} = \frac{1 + \tan^4 \alpha - 2 \tan^2 \alpha}{4 \tan^2 \alpha}$$

$$= \frac{1 + \tan^4 \alpha}{4 \tan^2 \alpha} - \frac{1}{2}$$

So

$$a^2 b^2 = \tan^2 2\alpha \left[- \frac{A^4 + B^4}{4} + A^2 B^2 \left(\frac{1}{\tan^2 2\alpha} + \frac{1}{2} \right) \right]$$

$$a^2 b^2 = \tan^2 2\alpha \left[- \left(\frac{A^4}{4} - \frac{A^2 B^2}{2} + \frac{B^4}{4} \right) \right] + A^2 B^2$$

Using equation E-12, we have

$$a^2 b^2 = \frac{4 A^2 B^2 \cos^2 \phi}{(A^2 - B^2)^2} \left[- \frac{1}{4} \left(A^2 - B^2 \right)^2 \right] + A^2 B^2$$

$$= - A^2 B^2 \cos^2 \phi + A^2 B^2$$

$$a^2 b^2 = A^2 B^2 \sin^2 \phi \tag{E-16}$$

So from equations E-5, E-6 and E-16, we have

$$V^2 = \frac{a^2 b^2}{a^2 \cos^2 (\theta - \alpha) + b^2 \sin^2 (\theta - \alpha)} \tag{E-17}$$

Using equations E-12 and E-16, we have

$$a^2 + \frac{A^2 B^2 \sin^2 \phi}{a^2} = A^2 + B^2$$

$$a^4 - (A^2 + B^2)\ a^2 + A^2 B^2 \sin^2 \phi = 0$$

$$a^2 = \frac{1}{2} (A^2 + B^2) - \frac{1}{2} \left[(A^2 + B^2)^2 - 4 A^2 B^2 \sin^2 \phi \right]^{1/2} \tag{E-18}$$

$$b^2 = \frac{1}{2} (A^2 + B^2) + \frac{1}{2} \left[(A^2 + B^2)^2 - 4 A^2 B^2 \sin^2 \phi \right]^{1/2} \tag{E-19}$$

Thus equation III-8 is given as equation E-17 where a, b and α are defined by equations E-18, E-19 and E-13.

APPENDIX F

DERIVATION OF EQUATION III-11

If we assume that the correct value of V^2 in equation III-5 is

$$V^2 = \frac{1}{2} (A^2 + B^2)$$

then the possible error in V^2 is C, the amplitude of the modulation term in equation III-5. The probable error in V^2 is defined as that magnitude of the error whose probability of being exceeded is one-half. Since the error form in equation III-5 is sinusoidal, then the value of the possible error for which the probability of being exceeded is one-half occurs when the argument of the cosine is $\pi/4$. Therefore the probable error in V^2 is $C/\sqrt{2}$.

Let δ be the probable error in V. Then

$$(V + \delta)^2 = V^2 + 2 V \delta + \delta^2$$

If only first order terms in δ are kept, then the probable error in V^2 is seen to be $2 V \delta$.

$$2 V \delta = \frac{C}{\sqrt{2}}$$

or

$$\delta = \frac{C}{2\sqrt{2}\left[\frac{1}{2}\left(A^2 + B^2\right)\right]^{1/2}}$$

$$\delta = \frac{C}{2\left(A^2 + B^2\right)^{1/2}} \qquad \text{(F-1)}$$

Thus, equation III-11 is just equation F-1.

APPENDIX G

ENERGY SPECTRUM GRAPHS

The energy spectrum function for the heights of 95 km through 135 km in steps of 5 km were calculated by the Groves analysis. Graphs for the heights 95 to 115 km are shown in Chapter III. The following are the graphs for the rest of the heights.

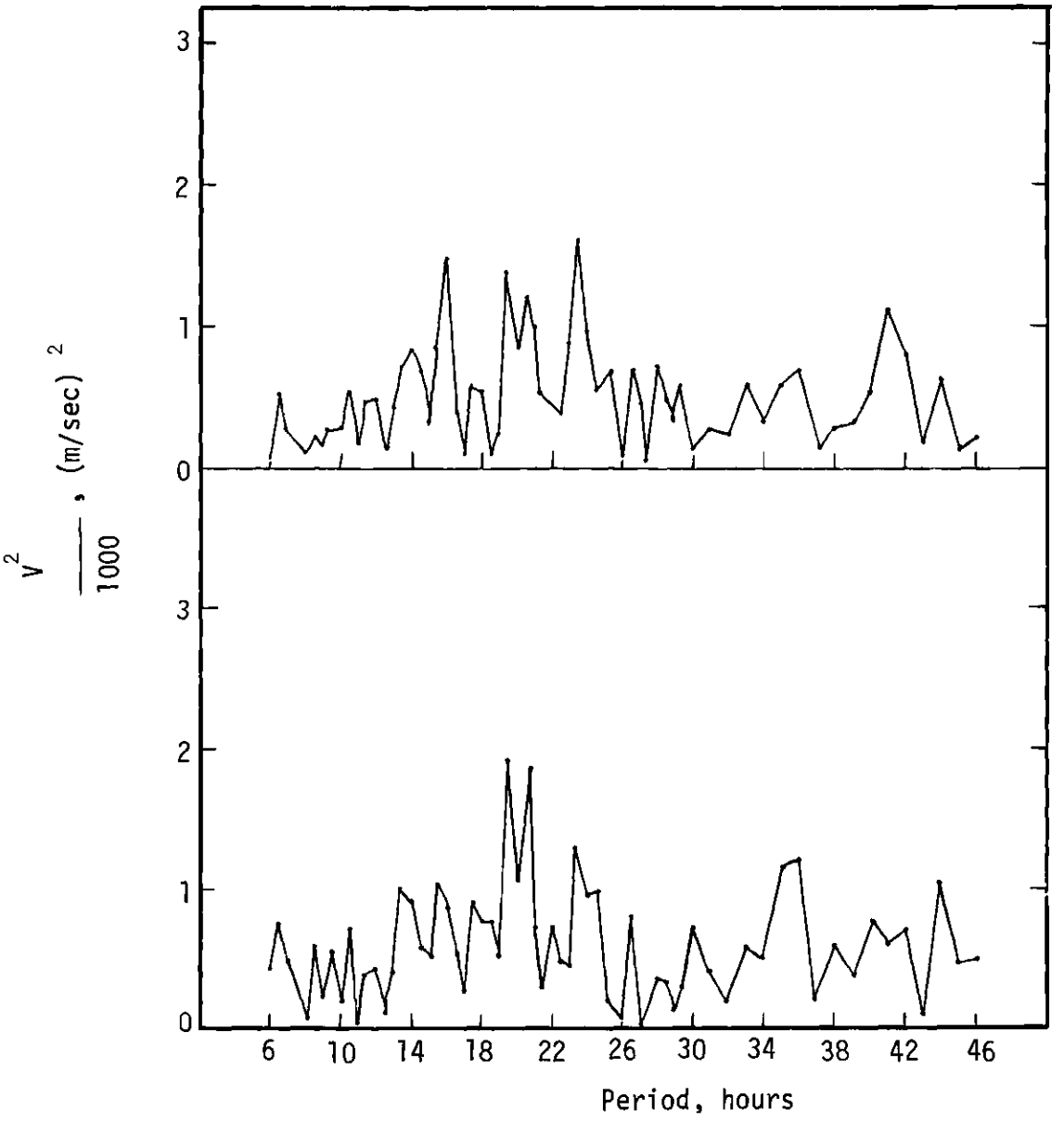

Figure 32. Energy Spectrum of Periodic Motions at 100 km (Lower) and 105 km (Upper).

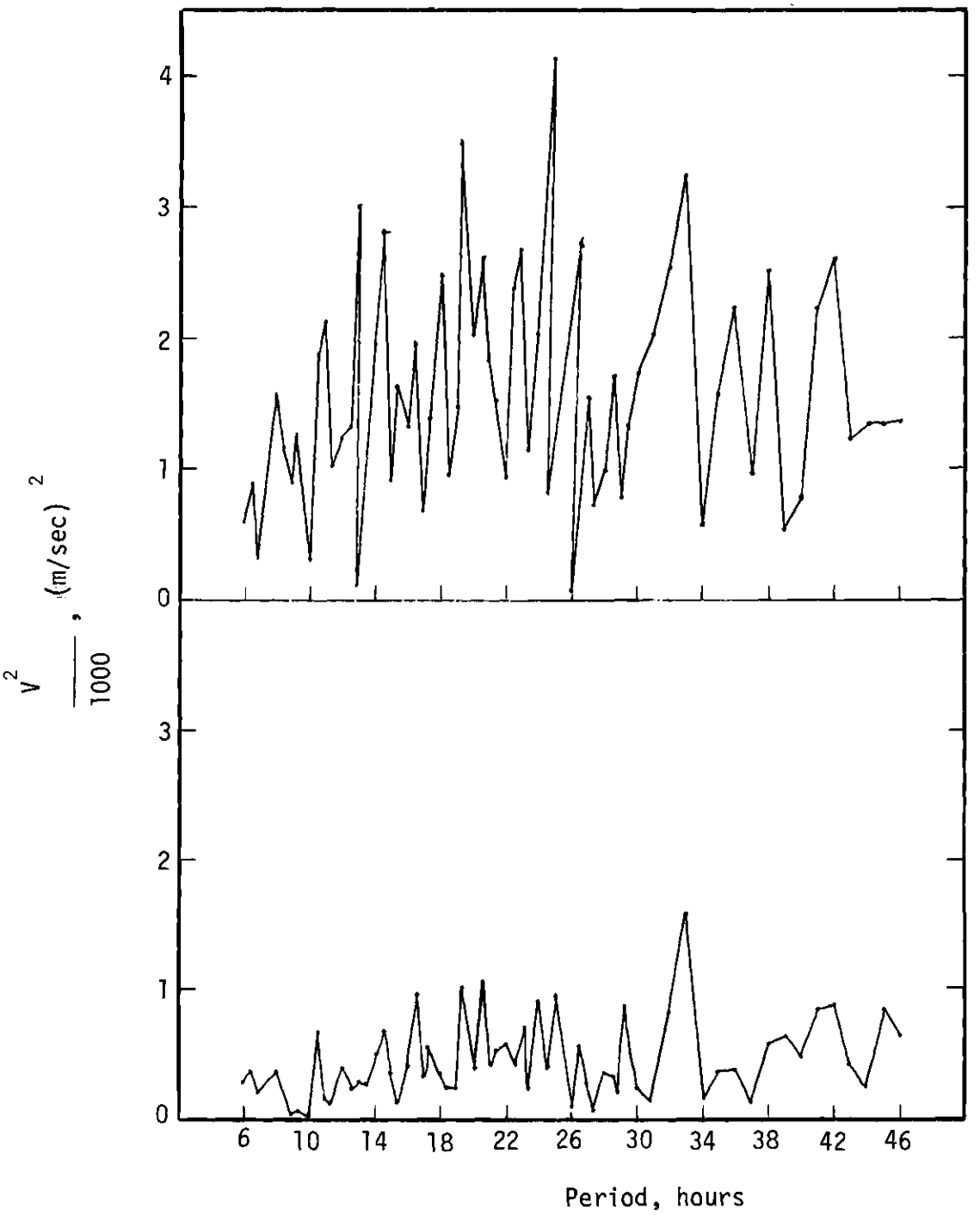

Figure 33. Energy Spectrum of Periodic Motions at 110 km (Lower) and 120 km (Upper).

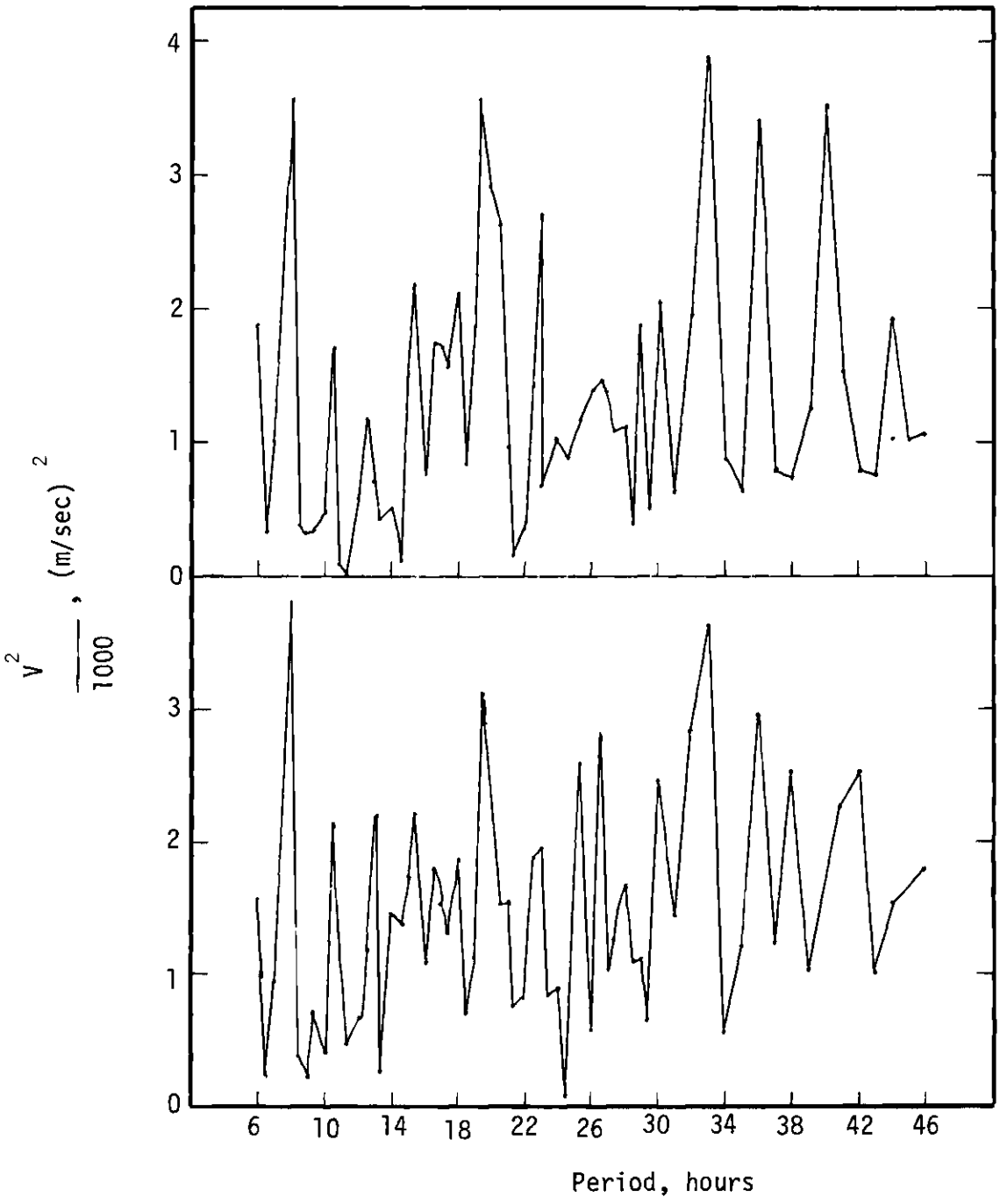

Figure 34. Energy Spectrum of Periodic Motion at 125 km (Lower) and 130 km (Upper).

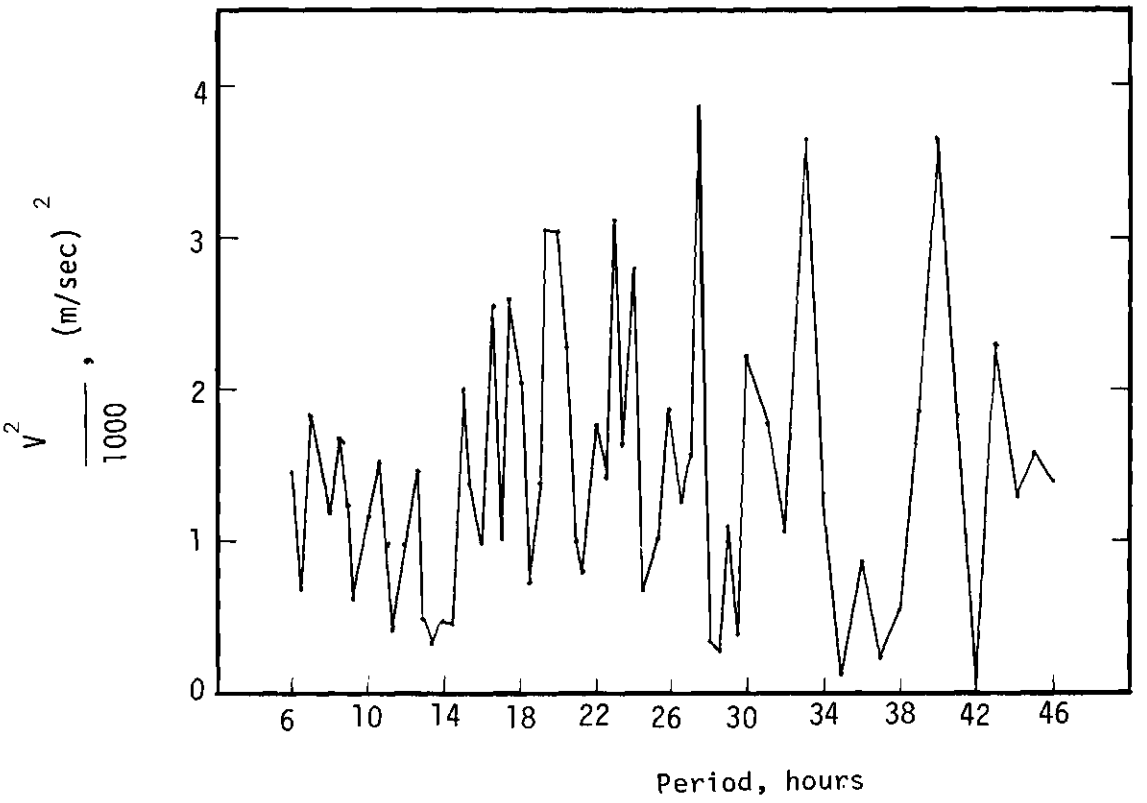

Figure 35. Energy Spectrum of Periodic Motion at 135km.

GLOSSARY OF FREQUENTLY USED SYMBOLS

Symbol	Definition	Page
a	Radius of the earth	12
C_p	Specific heat at constant pressure	13
C_v	Specific heat at constant volume	13
χ	Divergence of velocity	13
δp	Change in pressure	13
T	Change in temperature	13
F	Operator defined by equation A-35	116
f	$= \frac{\sigma}{2\ \omega}$	12
g	Acceleration of gravity	2
γ	Ratio of specific heats	13
H	Scale height of atmosphere	3
h	Equivalent depth	4
$\hat{h}$	Eigenvalue of atmosphere	4
i	$= \sqrt{-1}$	13
J	Heat added per unit mass per unit time	12
k	Wave number	37
κ	$= \frac{\gamma - 1}{\gamma}$	12
λ	Commensurable part of a day	4
M	Mean molecular weight of air	3
μ	$= \cos \theta$	12
ω	Earth's rotation rate	12
Ω	Gravitational potential	13

Glossary (Cont'd.)

Symbol	Definition	Page
$P_n^s(\theta)$	Associated Legendre Polynomials	22
p_o	Undisturbed atmospheric pressure	101
p	Actual atmospheric pressure	102
ϕ	Longitude	4
R	Universal gas constant	3
ρ_o	Undisturbed atmospheric density	101
ρ	Actual atmospheric density	102
s	Longitude wave number	4
$S^s_{\lambda,n}$	Wave type	4
σ	Frequency of atmospheric oscillation	11
t	Time	13
T_o	Undisturbed atmospheric temperature	3
T	Actual atmospheric temperature	102
θ	Latitude	12
$\Theta^s_{\lambda,n}$	Hough Functions	12
u	Southward velocity component	13
v	Eastward velocity component	13
w	Vertical velocity component	13
x	Scale height corrected altitude	12
$y_n(x)$	Defined by equation A-66	131
z	Altitude	13

BIBLIOGRAPHY*

1. Chapman, S., The lunar diurnal variation of atmospheric temperature at Batavia, 1866-1928, Proc. Roy. Soc. (London), A137, 1, 1932.

2. Groves, G. V., A theory for determining upper atmosphere winds from radio observations on meteor trails, J. Geophys. Res., 16, 344, 1959.

3. Hines, C. O., Internal gravity waves at ionspheric heights, Can. J. Phys., 38, 1441, 1960.

4. Hines, C. O., Diurnal tide in the upper atmosphere, J. Geophys. Res., 71(5), 1453, 1966.

5. Hough, S. S., On the application of harmonic analysis to the dynamical theory of tides: Part II, On the general integration of Laplace's dynamical equations, Phil. Trans, A, 191, 139, 1898.

6. Justus, C. G. and R. G. Roper, Some observations of turbulence in the 80 to 110 km region of the upper atmosphere, Symposium on Meteorological Investigation Above 70 Kilometers, in AMS Meteorological Monographs, No. 31, publication scheduled for April, 1968.

7. Justus, C. G., H. D. Edwards, and R. N. Fuller, Analysis techniques for determining mass motions in the upper atmosphere from chemical releases, Sci. Rept. AFCRL-64-187, 1964 a.

8. Justus, C. G., H. D. Edwards, and R. N. Fuller, A method employing star backgrounds for improving the accuracy of the location of clouds or objects in space, Photogrammetric Eng., 30, 594, 1964 b.

9. Kato, S., Diurnal atmospheric oscillation, 1, eigenvalues and Hough Functions, J. Geophys. Res., 71 (13), 3201, 1966.

10. Kochanski, A., Atmospheric motions from sodium cloud drifts, J. Geophys. Res., 69 (17), 3651, 1964.

11. Lamb, H., "Hydrodynamics," 5th ed. Cambridge Univ. Press, London, 1924.

12. Lindzen, R. S., On the asymmetric diurnal tide, Pure and Appl. Geophys., 62, 142, 1965.

*Abbreviations herein follow the form used by American Geophysical Union.

13. Lindzen, R. S., On the theory of the diurnal tide, Monthly Weather Rev., 94 (5) 298, 1966.

14. Lindzen, R. S., Thermally driven diurnal tide in the atmosphere, Quarterly J. of the Royal Meteorological Soc., 93 (395), 1967.

15. Pekeris, C. L., Atmospheric oscillations, Proc. Roy. Soc. (London) A158, 650, 1937.

16. Pekeris, C. L., Effect of the quadratic terms in the differential equations of atmospheric oscillations, Natl. Adv. Com. Aeronaut. Tech. Notes 2314, 1951.

17. Roper, R. G., Weapons Research Establishment, Department of Supply, Salisbury, South Australia, formerly a visiting professor at Georgia Institute of Technology, private communication.

18. Roper, R. G., and W. G. Elford, Meteor winds measured at Adelaide (35°S) 1961, NASA Tech. Publ. X-650-65-220, Goddard Space Flight Center, Greenbelt, Maryland, 1965.

19. Roper, R. G., The semidiurnal tide in the lower thermosphere, J. Geophys. Res., 71 (23), 5746, 1966.

20. Rosenberg, N. W., H. D. Edwards; and J. W. Wright, Ionospheric winds; motions into night and sporadic E correlations, Space Res., 4, 171, 1964.

21. Rosenberg, N. W. and C. G. Justus, Space and time correlations of ionospheric winds, Radio Sci., 2, 149, 1966.

22. Siebert, M., Atmospheric tides, Adv. in Geophys, 7, 105, 1961.

23. Shiren, N. S., Ultrasonic traveling - wave parametric amplification, Proc. of the IEEE, 53 (10), 1540, 1965.

24. Small, K. A. and S. T. Butler, The solar semidiurnal atmospheric oscillation, J. Geophys. Res., 66 (11), 3723, 1961.

25. Taylor, G. J., The oscillation of the atmosphere, Proc. Roy. Soc. (London) A156, 318, 1936.

26. U. S. Standard Atmosphere, U. S. Government Printing Office, 1962.

27. U. S. Standard Atmosphere Supplements, U. S. Government Printing Office, 1966.

28. Weekes, K. and M. V. Wilkes, Atmospheric osicllations and the resonance theory, Proc. Roy. Soc. (London) A192, 80, 1947.

29. Wilkes, M. V., "Oscillations of the Earth's atmosphere, "Cambridge

Univ. Press, London, 1949.

30. Woodrum, Arthur and C. G. Justus, Atmospheric tides in the height region 90 to 120 kilometers, J. Geophys, Res., 72 (2), 467, 1968.

VITA

Arthur Woodrum was born March 20, 1942 in Statesboro, Georgia. He is the youngest of four sons of Walter Grover and Elise Nessmith Woodrum. On May 1, 1964 he was married to Mary Alice Blackwell of Atlanta, Georgia.

Mr. Woodrum attended Statesboro High School in Statesboro, Georgia. He entered Georgia Institute of Technology in 1960 in the field of Physics and received the degree of Bachelor of Science in Physics in 1964. Immediately, he began graduate work in Physics at Georgia Institute of Technology and received his Master of Science degree in 1966.

While in college, Mr. Woodrum was a member of the Tau Kappa Epsilon Social Fraternity. He was also a member of Phi Eta Sigma, Tau Beta Pi, Phi Kappa Phi and Sigma Pi Sigma honoraries.

Mr. Woodrum began work as a graduate research assistant in 1964 with the Space Sciences Laboratory at Georgia Tech. He has published a paper on part of his thesis which is indicated as reference 30 in the Bibliography. He is also a member of the American Geophysical Union.